UNIVERSITY OF OTTAWA

An Optical Biosensor Towards Urinary Tract Infection Diagnosis

by

Paul Béland

A THESIS

SUBMITTED TO THE FACULTY OF GRADUATE STUDIES

IN PARTIAL FULFILMENT OF THE REQUIREMENTS FOR THE

DEGREE OF MASTER OF APPLIED SCIENCE, BIOMEDICAL ENGINEERING

GRADUATE PROGRAM IN BIOMEDICAL ENGINEERING

OTTAWA, ONTARIO

SEPTEMBER, 2015

Abstract

We explore a new laboratory technique in the field of urinalysis promising a combination of speed and selectivity in support of urinary tract infection diagnosis. Laboratory experimentation demonstrates long range surface plasmon polaritons (LRSPP) waveguides as a useful biosensor to selectively detect gram negative bacteria or gram positive bacteria in human urine. The biosensor can detect bacteria at concentration of 10^5 CFU/ml, the internationally recommended threshold for diagnostic of urinary tract infection (UTI). Using a negative control solution at bacterial concentration 1000x higher than the targeted bacteria in urine with a weak concentration of constituents, the power ratio between the negative control signals to the target bacteria signal is measured to be 5.4. Thus we report a conclusive demonstration of the LRSPP waveguide biosensor selectivity to the gram of bacteria in human urine. In addition, the biosensor may prove useful as an alternative urinalysis test method to determine the urine specific gravity, to estimate proteinuria, and to detect biofilm formation on surfaces.

Preface

The work contain in this thesis was performed with the approval of the University of Ottawa office of research ethics and integrity under file number H06-14-01, dated 23 June 2014. Laboratory culture of bacteria was mixed with human urine to simulate patient samples of urinary tract infection. The intention is to demonstrate the usefulness of long range surface plasmon polariton waveguide biosensors for the detection of urinary tract infection. No clinical trial was made at this time reducing the risk of laboratory incident.

Acknowledgements

I take this opportunity to express gratitude to Dr. P. Berini, A. Krupin, A. Olivieri, E. Lisicka-Skrzek, Dr. M Godin, A. Trottier and P. Pelletier for their help and support. I thank my wife Marie-Eve for the unceasing encouragement, support and attention. I am also grateful to my children Maude, Simon and Audrey who provide me an untarnishable source of motivation to work hard.

Table of Contents

List of Tables

List of Figures and Illustrations

Chapter One:
Optical biosensor for urinalysis

Urinalysis emerged in the 17th century from uroscopy which has a long history [1]. Hippocrates (460–355 BC) described urine as a filtrate of the humors coming from blood. Later, Galen (AD 129–200) theorized that urine represented a filtrate of the blood, not of the humors. In the middle age, Gilles de Corbeil (1165–1213), introduced a glass vessel in which a physician viewed urine, assessing color, consistency, and clarity called ¨the matula¨. The matula was in a way the first biosensor for urinalysis.

Uroscopy became a tool of uneducated practitioners and an increasing number of physicians which were diagnosing from urine alone, exaggerating the importance of urinary diagnosis. This may have led to the renunciation of uroscopy by the medical profession. On the other hand, when Galen added heat to precipitate the protein in urine, he invented the first documented laboratory technique, which led to urinalysis. Diagnostic information which could be collected from urine includes protein, glucose, blood, infection, concentration (today specific gravity), and sediments [2]. Later, Louis Pasteur (1822-1895) proved that urine was a chemically favourable medium for the germination of life using it as a broth medium [3]. In 1881, Roberts published the first observation of bacteria in fresh urine [4]. To this day, urinalysis is a diagnostic tool largely used, and in particular for the diagnosis of urinary tract infection (UTI).

1.1 Diagnosis of urinary tract infection (UTI)

Hippocrates associated urinary sediment with fever. The observed sediment may well have been due to white blood cells and bacteria from a urinary tract infection (UTI). He also describes bubbles on the surface of fresh urine as an indication of disease and it turned out that it can indicate urinary tract infection [5].

In the 19th century, Louis Pasteur demonstrated the properties of urine as a growth medium and later Robert Koch used agar to solidify the growth media [6]. At the normal incubation temperature of 37º Celsius, agar is solid and today it is the dominant constituent of culture plate for microorganism. In fact, culture of urine sample on agar plate is still today the golden standard for the diagnosis of UTI [7].

1.1.1 Urinary tract infection

The pathogenesis of urinary tract infections is described in Figure 1. Bacteria or yeast typically enter the urethra (step 1). Pathogens colonize the bladder then adhere to uroepithelial tissue (step 2). The pathogens invade the epithelial tissue (steps 3 and 4). At this point, patients can experience UTI symptoms. Pathogens can ascend the ureters and infiltrate the kidneys (steps 7 and 8) and cause a kidney infection. In urosepsis the pathogen invades the bloodstream through the one-cell-thick proximal tubule of kidney nephrons to enter the bloodstream [8].

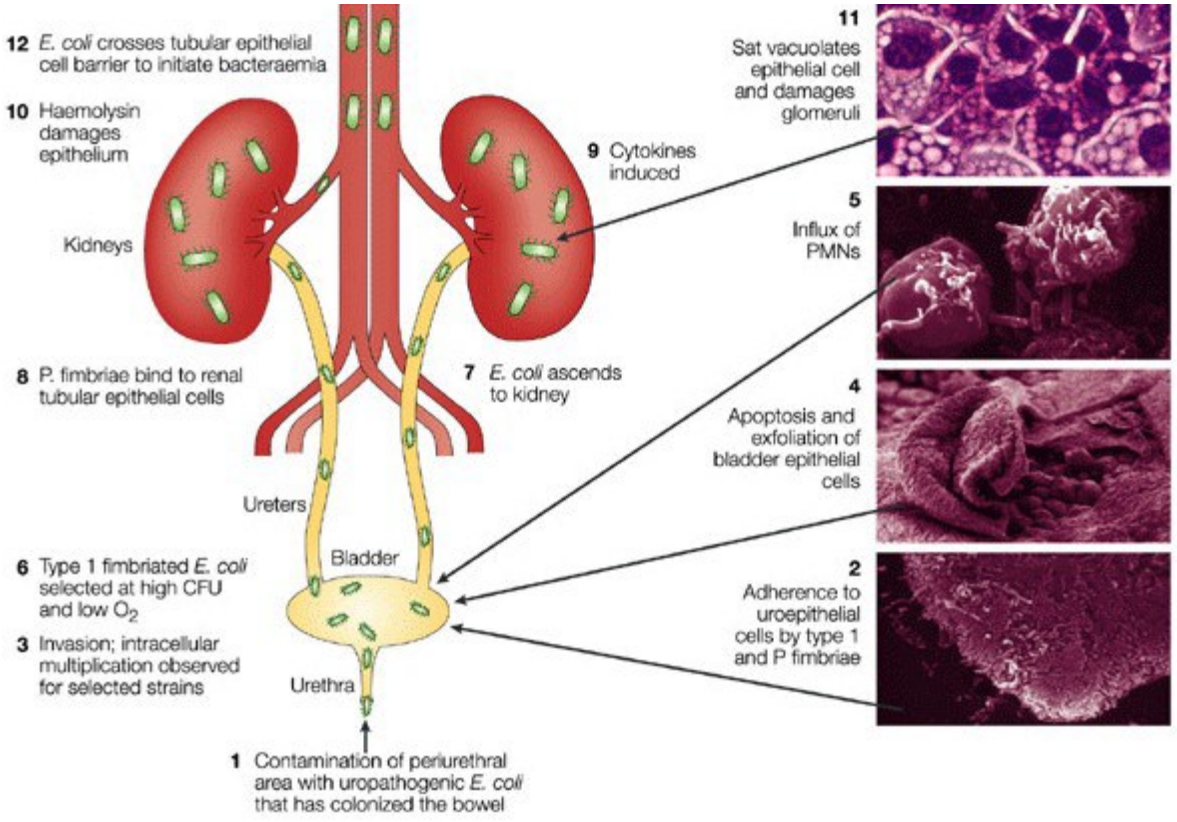

Figure 1 Pathogenisis of urinary tract infection [8]

UTI is classified as upper for an infection of the kidney or lower for an infection of the bladder as described in the Merck`s Manual [9]. It can further be categorised as complicated or uncomplicated [10], where uncomplicated refers to infected women with a structurally and functionally normal urinary tract. Urinary tract infections in men, elderly people, pregnant women, or patients who have an indwelling

catheter or an anatomic or functional abnormality are considered complicated urinary tract infections. The pathogen causing approximately 75% of UTI is the Uropathogenic Escherichia coli (UPEC) [11], a gram negative bacteria. Gram-positive species occur in 30 to 40% of complicated UTI isolates [12].

1.1.2 Clinical diagnostic of UTI

Today, numerous physicians may diagnose uncomplicated UTI only based on patient symptoms and prescribe antibiotics to rapidly contain the infection and avoid sepsis. When relying on urinalysis, indicators of UTI include dipstick or microscopy results for leukocytes, nitrites, protein, white blood cells, red blood cells, and bacteria [5]. With uncomplicated UTI, positive leukocyte esterase and nitrite tests are sufficient to recommend treatment without culture. As a result of these practices, bacteria develop resistance to the most often prescribed antibiotics [12, 13, 14].

In the case of complicated UTI, effort should be made to perform a urine culture to detect the causative organism and their antimicrobial susceptibility [15]. From the urine culture, a concentration of bacteria colony forming unit per millilitre (CFU/ml) is reported. As shown in Figure 2, the threshold for infected urine samples is a count greater than 10^5 CFU/ml.

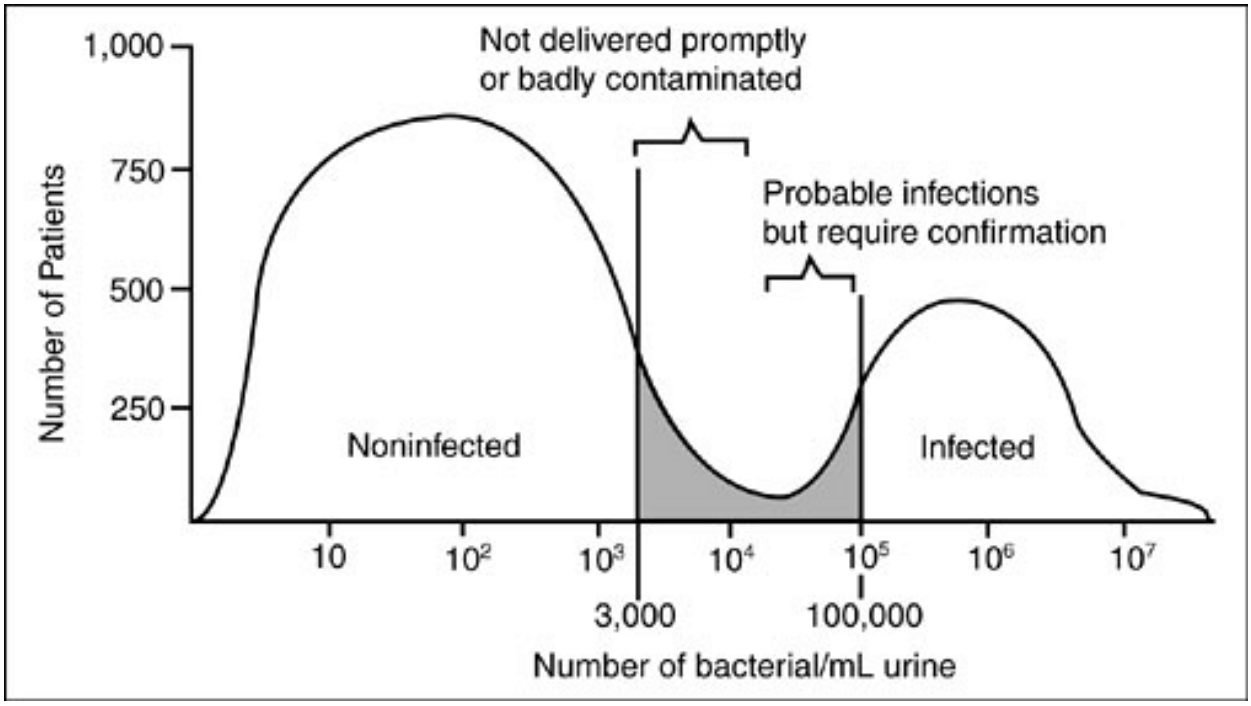

Figure 2 Distribution of bacterial count in patient urine sample indicating UTI infected and noninfected patients [16].

In clinical use today, automated systems can simultaneously analyse multiple urine samples and also perform susceptibility testing to antibiotics [17], but the culture times remain long. Alternative culture in liquid broth instead of agar does speed up the process with positive results being obtainable in 45 minutes [18] but negative results will take longer. Also, with this approach, antibiotic susceptibility testing is done as a follow up test and will therefore require more time before the most effective antibiotic can be prescribed to the patient. The task of identifying the pathogenic bacteria is part of the bacteriology field of study [19].

To improve the diagnosis of UTI we proposed to study a new technology, the label free biosensor. In broad terms, we want to understand if a label free biosensor can bring some advantages in terms of simplicity, speed, specificity, and selectivity when compared to other urinalysis techniques.

1.2 Introduction to urinalysis

As a clinical tool, urinalysis can be broken down into 3 types of analysis: physical, microscopy, or chemical. The physical analysis assesses color, clarity, odour, and specific gravity. Using a centrifuge and microscopy, one can quantify the presence of red blood cells, white blood cells, epithelial cells, bacteria,

yeast, parasites, spermatozoa, mucus, casts, urinary crystals, and urinary sediment artefacts. From chemical analysis, one can determine urine pH, presence of protein, glucose, ketones, haemoglobin, bilirubin, urobilinogen, leukocyte esterase, and nitrite [20]. The following subsection is not exhaustive but it provides details about urinalysis instruments that could be partially or totally substituted by a long range surface plasmon polariton waveguide biosensor.

1.2.1 Chemical technique: the dipstick

A standard urine test strip (or dispstick), as shown in Figure 3 comprises different chemical pads or reagents which react (change color) when immersed in, and then removed from, a urine sample. The analysis includes testing for the presence of proteins, glucose, ketones, haemoglobin, bilirubin, urobilinogen, acetone, nitrite and leucocytes as well as testing of pH and specific gravity or to test for infection by pathogen [21]. Interpretation of the results is not straightforward for diagnosis because numerous conditions result in false positives and or false negatives. For example, for UTI diagnosis, the dipstick monitors nitrites produce by bacteria. Unfortunately, not all bacteria generate nitrites from nitrates and false negative test results can be observed from the dipstick test resulting in a poor sensitivity during clinical trials.

Figure 3 Urinalysis using dipstick [22]

1.2.2 The refractometer

We denote 3 major optical instruments for urinalysis: the refractometer, the spectrophotometer, and the automated microscope. The refractometer is one of 3 techniques to measure the specific gravity (SG), the density ratio of a substance to the density of water. Urine SG can also be measured with a urinometer and reagent strips [23, 24]. When using a refractometer to measure SG, the critical angle of total reflection is measured and using Snell`s law, represented in Figure 4, the index of refraction (RI) is calculated. Three different ways of relating the index of refraction to specific gravity have been proposed in the past [25]. One relation uses the Gladstone-Dale equation: $(n-1)/\rho = \text{sum}(km)$ where n is the index of refraction, ρ is the density in g/cm^3, k is the molar refractivity in cm^3/g, and m is the mass fraction of the miscible liquid; the density of the substance is obtained. We note that with this model, SG or RI is related to the mass of constituents in solution. We should also note that large biological element in the urine will interfere with the measurement, leading to the next two subsections: microscopy and spectrophotometers.

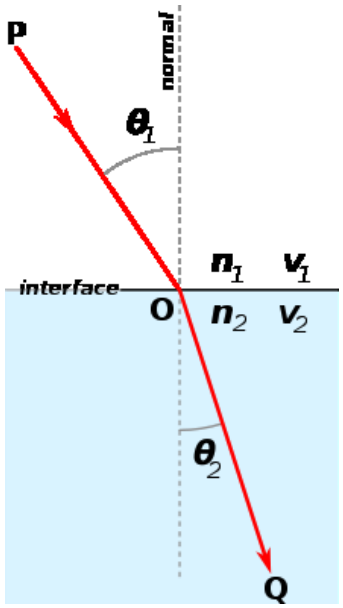

Figure 4 Pictorial representation of Snell`s law where n1 and n2 are the refractive index of medium 1 and 2, v1 and v2 are the speed of light in the respective medium. The critical angle is the angle of incidence (θ1) that provides an angle of refraction (θ2) of 90-degrees

1.2.3 The microscope and cytometer

Microscopic urinalysis is a common way to identify large urine constituents under a microscope after centrifugation. Image galleries have been constituted for the identification of red blood cells, white blood cells, epithelial cells, bacteria, yeast, parasites, spermatozoa, mucus, casts, urinary crystals, and urinary sediment artefacts. The technique may include bright field microscopy, phase contrast microscopy, polarizing microscopy, dark field microscopy, fluorescence, and interference-contrast. Many commercial systems exist including Kova, Urisystem, Count-10, Quick-prep, censlide, and R/S workstation.

Image cytometry makes use of a microscope to determine cell size, cell count and cell morphology. The hemocytometer is a specially designed glass microscope slide originally invented to count red blood cells. It is made up of a microscopic grid and chamber of known volume. A sample fluid is injected in the chamber and then by microscopic inspection the number of cells is counted. The cell concentration in the sample fluid is simply calculated. The concentration range that can be measured in this way is limited and therefore dilution may be used to extend the range [26]. Also, staining to enhance contrast or to detect specific molecules is done by labeling them with fluorochromes.

1.2.3.1 Flow cytometers for UTI diagnosis

In flow cytometry, a fluorescent label is added to the test fluid and microfluidic channels are used to flow the samples through an optical detector. With appropriate dye, the flow cytometer will count the bacteria, the red blood cell, the leukocyte and other biological elements of the urine sample. Flow cytometers have been used in clinical trials of UTI diagnosis and proved useful to reduce the number of culture requests. Identification of the bacteria from the flow cytometer is also possible [27, 28, 29, 30].

1.2.4 The spectrophotometer

A spectrophotometer is used for the measurement of transmittance or reflectance of solutions. In its simplest form it is made up of a light source, a monochromator, a fluid sample and a detector. [31]. Using a calibration procedure that measures multiple solutions with known protein concentration, it is possible to

determine the protein concentration in urine of an unknown sample. Also, the spectrophotometer is often used in laboratory to characterise the growth curve of bacteria in a liquid growth medium. Again calibration against plated culture is required but then in situ measurements of the bacterial concentration are made. Clinically it has been successfully used. A urine sample is cultured in liquid broth and identification of positive culture is obtainable in 45 minutes [18] but negative results take as long as culture on agar plate. In addition it is not a selective detection technique.

1.2.5 Bacteria culture on agar from urine samples

In medicine, the presence of bacteria in urine, also called bacteriurea, is indicative of urinary tract infection unless the urine sample was contaminated. The bacteria in urine are 0.5 to 5 micrometers in length. Most bacteria morphology is either spherical or rod shaped and some are spiral. Based on their type of membrane, they can be classified as gram negative (with an outer membrane) or gram positive (no outer membrane). A schematic representation of these 2 classes is shown in Figure 5. Bacteriuria can be detected from dipstick, from microscopy, or from bacterial culture on agar plate: the gold standard. Here we detail how the culture of bacteria is performed.

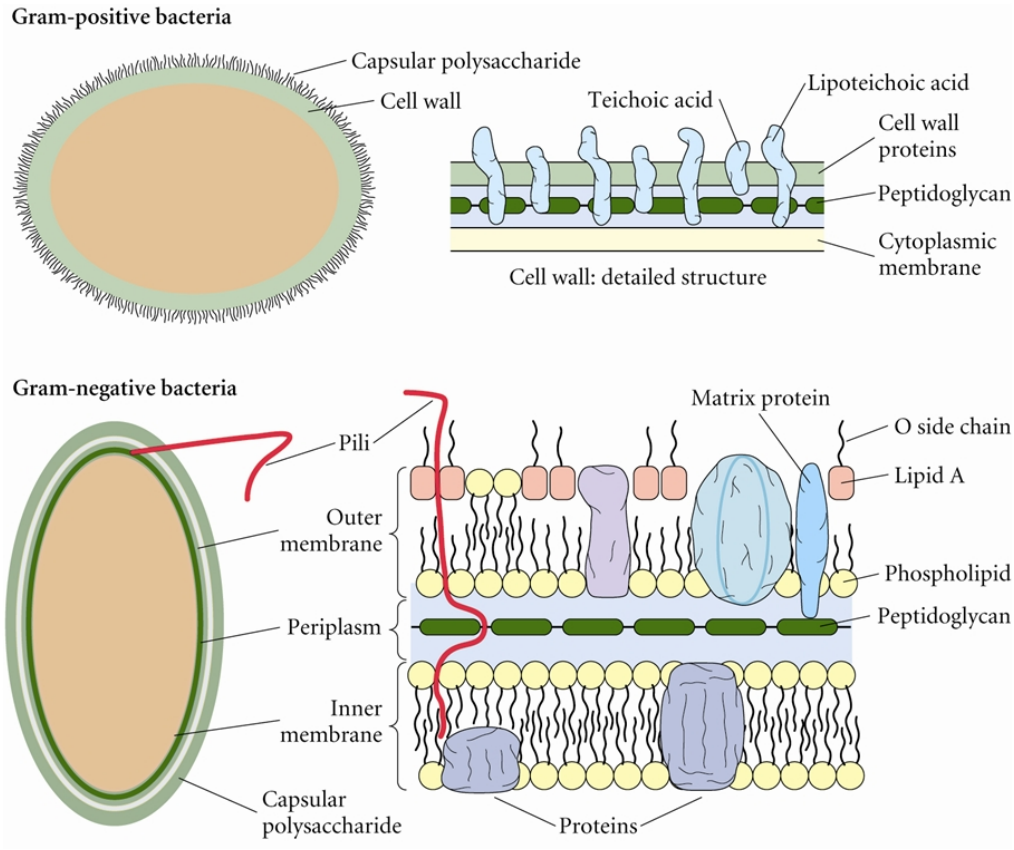

Figure 5 Antigens involved in host responses to bacteria for gram positive and gram negative bacteria [32]

We have seen in the historical review that still today, bacteria are cultured on AGAR plates in a petri dish containing the nutrients required for growth and replication. Antibiotics are sometimes used to selectively grow a specific species. But first a urine sample is collected in one of four ways:

1. Midstream clean catch: Patient voids first portion of urine, then collects urine specimen midstream and discards the latter portion
2. Catheterization: Urine collected from a catheter
3. Suprapubic aspiration: Urine collected from needle into the bladder
4. Cystoscopy: invasive procedures

The sample is processed within 2 hours of collection or refrigerated for 24 hours at 2º to 8º Celsius [33, 34]. To determine the concentration of bacteria in given urine samples, the plate count and dilution technique is commonly used [35]. In this technique, 100 µl of urine with bacteria is diluted in 900 µl of LB broth and mixed well. A sample of 100 µl is taken from this new solution and diluted again in 900 µl of LB broth.

This step is repeated 10 times. Then 100 µl from each solution is inoculated onto a 100 mm petri dish and using the inoculation loop the fluid is streaked across the complete surface. The petri dish is then incubated at 37ºC for 48 hours. A count of the colony forming units (CFU) is finally performed in each petri dish with 30 to 300 CFU therefore providing sufficient statistical evidence to report the concentration of the original samples.

Bacteria are also categorized by their morphology through inspection under a microscope. Figure 6 summarize the different morphologies. We are most interested in the baccilus morphology of the *E.Coli* and the staphylococci morphology of the *S.Epi* bacteria

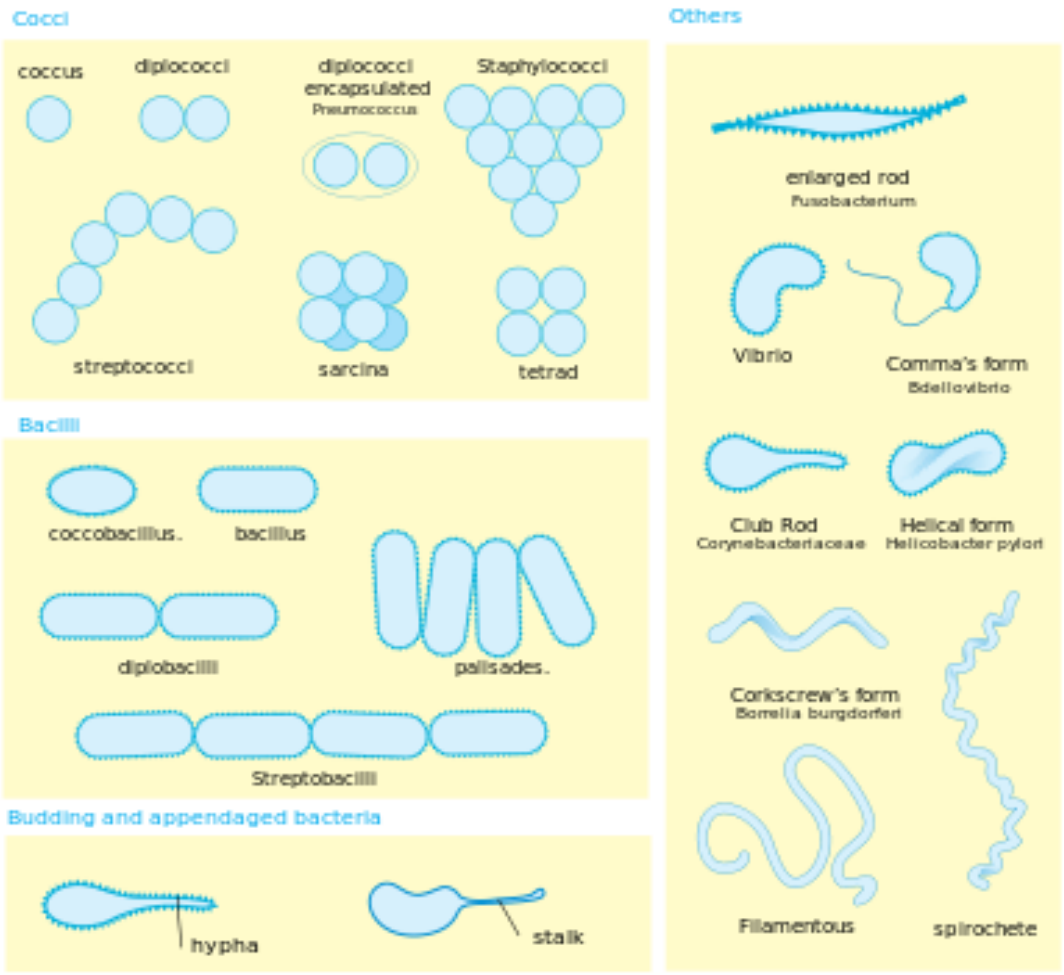

Figure 6 Bacteria morphology. E.Coli is a baccilus and S.Epi is a staphylococci morphology [36]

Another property of bacteria is their need for oxygen to grow, referred to as aerobic (need oxygen) or anaerobic (no oxygen). They can be identified by growing them in a test tube of thioglycollate broth which produces a range of oxygen concentrations from the top to the buttom of the tube as shown in Figure 7.

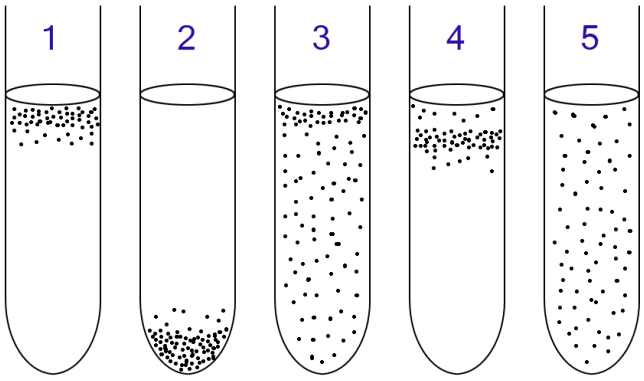

Figure 7 1: Obligate aerobes need oxygen 2: Obligate anaerobes are poisoned by oxygen 3: Facultative anaerobes can grow with or without oxygen 4: Microaerophiles need oxygen 5: Aerotolerant do not require oxygen. [37]

1.3 Label-free biosensor

A biosensor is a sensor that integrates a biological element with a physiochemical transducer. It is composed of an analyte, sample handling and preparation, a bio receptor, a transducer and the observed signal as shown in Figure 8a).

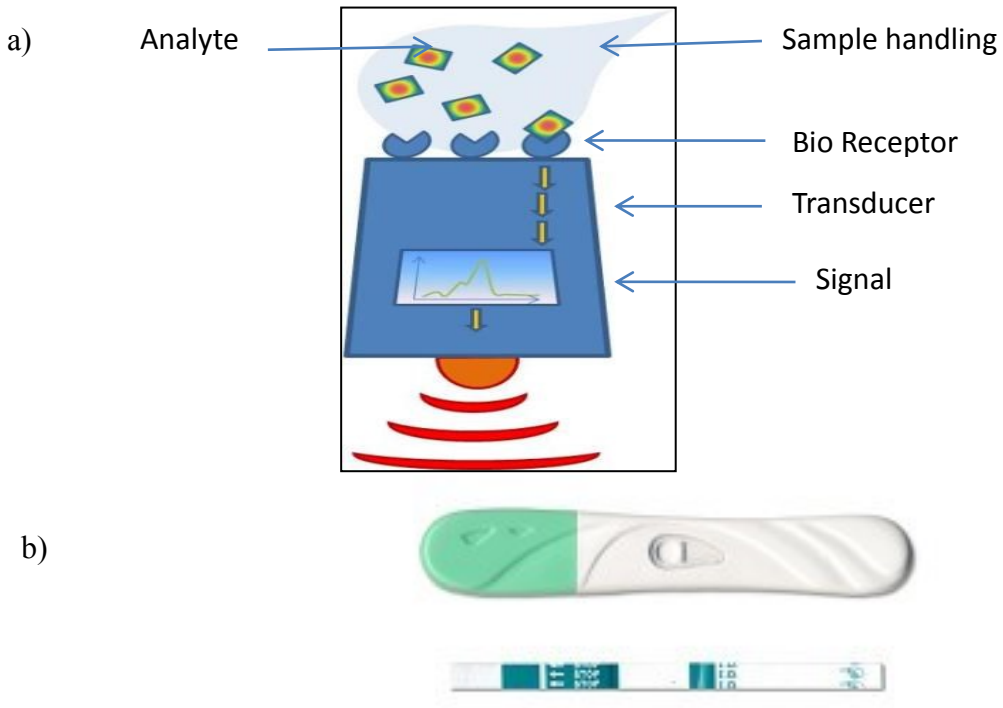

Figure 8 a) Label free biosensor block diagram b) pregnency test as an example of label free biosensor implementation[38]

Commercial examples of biosensors used includes pregnancy tests from urine samples (Figure 8.b)) which detects the hCG protein in urine, the glucose monitoring device from blood samples used by diabetes patients, the i-Stat for rapid clinical analysis of many constituents of a blood sample [39], and the Biacore instruments based on surface plasmon resonance technology [40]. The review of technology for UTI reported in [41] indicates that biosensors have the potential to address the point of care requirements of rapid pathogen identification and antimicrobial susceptibility of UTI.

The label free biosensor studied in this thesis is named the long range surface plasmon polariton (LRSPP) waveguide biosensor. It has been first demonstrated as a biosensor in 2013[42] to detect red blood cells based on type. We will further describe it in section 2.1 but first let's discuss the surface plasmon resonance (SPR) label free biosensor and its demonstrated use for urinalysis to date.

1.3.1 The surface plasmon resonance biosensor

The history and mode of operation of the surface plasmon (SPR) biosensor was described in [43]. In 1983, an SPR biosensor was demonstrated using the Kretschmann (1971) method which was suggested to excite

the surface plasmon. Much like the refractometer, the Kretschmann configuration for SPR is based on the total internal reflection (TIR) optical phenomenon. From Snell`s law the incident light will be totally reflected at angles greater than the critical angle except that some of the electromagnetic energy of the incident light penetrates a short distance (tens of nanometers) into the less optically dense medium creating an exponentially decaying evanescent wave as depicted in Figure 9.

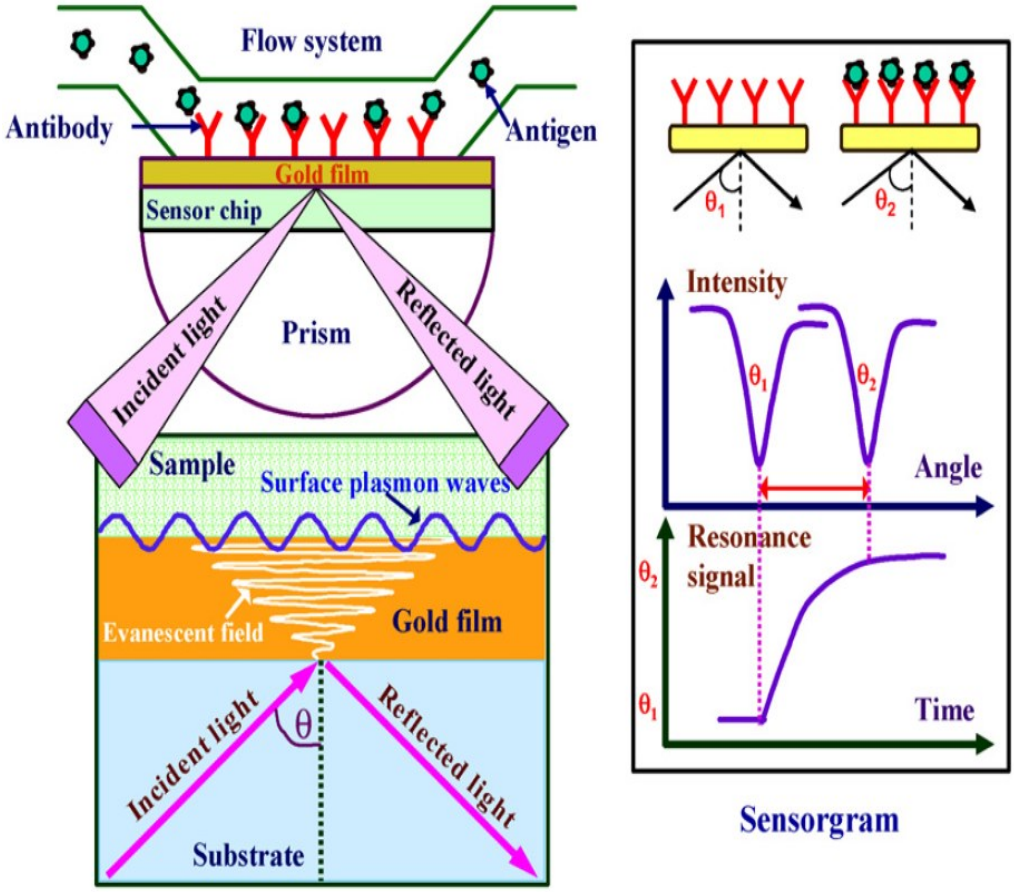

Figure 9 Kretschmann method to excite surface plasmon resonance integrated with a fluidic channel for biosensing.[44]

Resonance of the free oscillating electrons in the metal film is excited by the evanescent wave causing an attenuation of the reflected signal at a specific angle called the SPR angle which is greater than the critical angle of total reflection. The SPR angle depends on the refractive index of the material close to the metal surface. Hence when we capture molecules at the surface, the analyte and ligand association and dissociation can be observed on a sensorgram as shown in Figure 10. Note that on commercial systems, the

units for the abscissa are resonance units (RUs) where 1000 RU correspond to a 0.1 º change in the SPR angles. This 1000 RU also corresponds approximately to 1 ng/mm^2 on the surface of the detector chip [40].

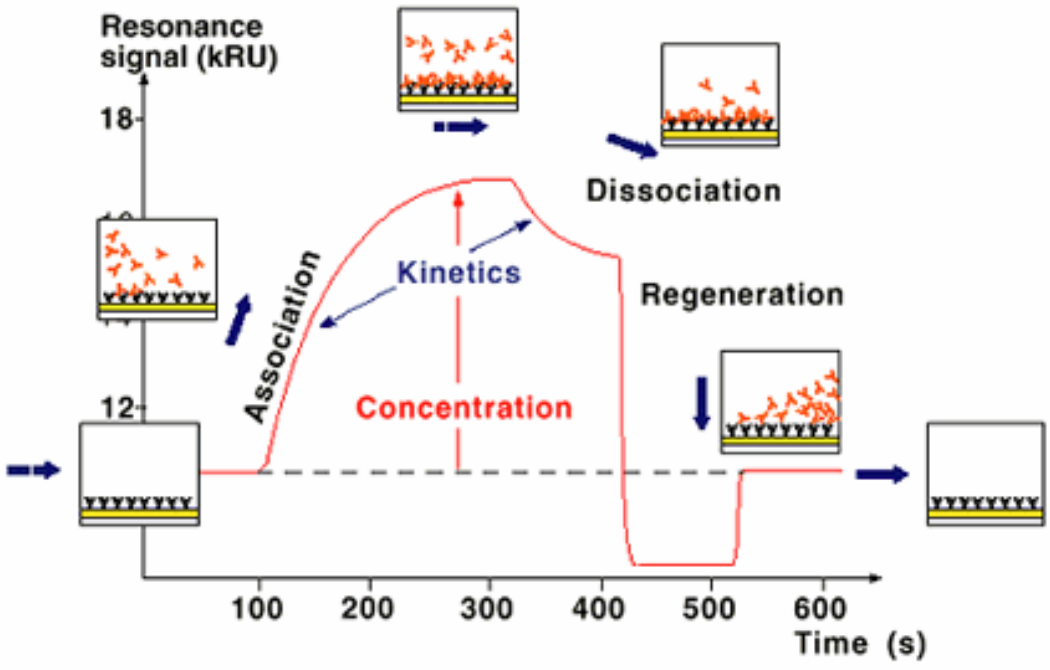

Figure 10 SPR sensorgram showing association, dissociation and regeneration. 1 kRU corresponds to a 0.1 º change of the SPR angle [45].

Using SPR and sensorgrams with different analyte and ligands leads to numerous biosensing applications, including the detection of protein, virus, health markers, and bacteria. We review here the literature on SPR biosensors for urine but first we review the detection of bacteria with a SPR biosensor.

Generally, the detection of bacteria with SPR is limited due to the depth of penetration of the evanescent field of 100 nm, compared to the size of the bacteria which is of 1-5 µm. In addition, the low contrast in refractive index of the bacterium cytoplasm and an aqueous solution also limits detection [45, 46, 47]. Yet in 2008 a successful detection was acehived by Fratamico [48] for *E.Coli*. Using a commercial SPR biosensor (Biacore) a sensitivity of 5×10^7 CFU/ml was demonstrated.

Similar results were obtained with the SpreetaTM SPR biosensor [49]. As shown in Figure 11, the sensing strategy can improve the detection limit to $1x10^3$ CFU/ml with sandwich assay, and 10^4 CFU/ml with

Protein G assay [50,51]. Many more detection experiments of bacteria with SPR were presented [52, 53, 54, 55]. An extensive review of SPR applications is provided in [47].

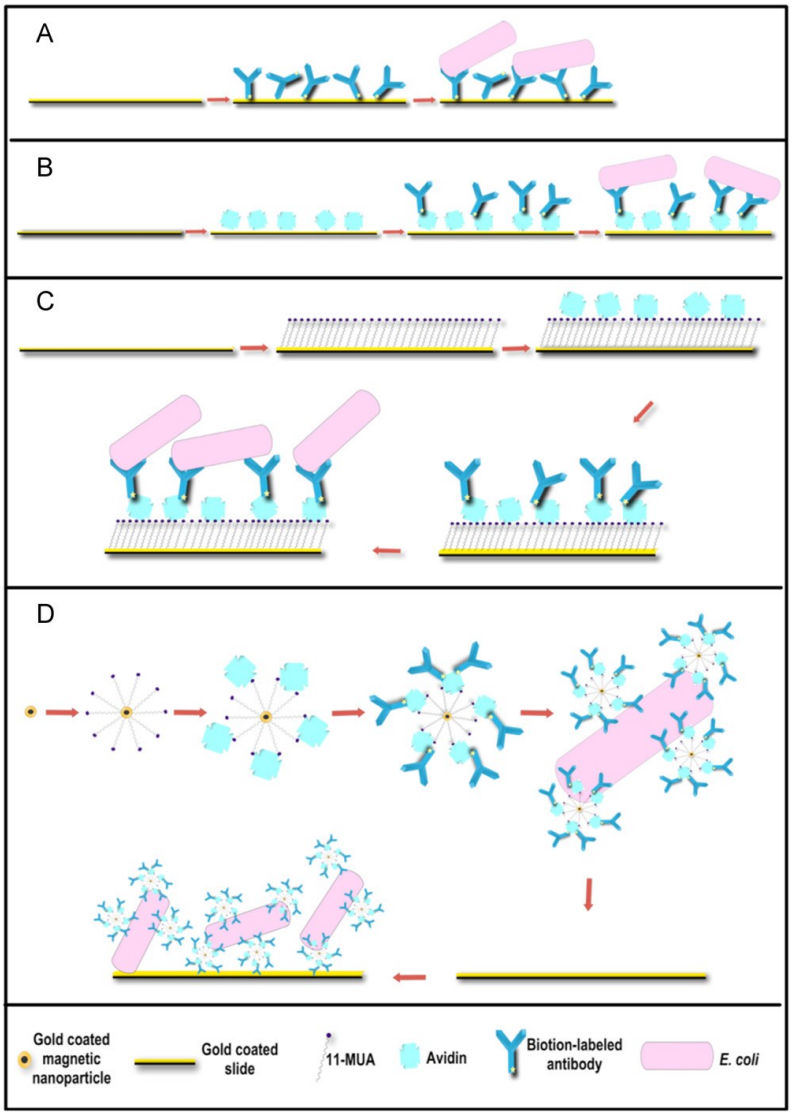

Figure 11 Schematic of sensing strategies(A) non-specific adsorption (4.8 x 10^5 CFU/ml), (B) specific adsorption (6.2 x 10^3 CFU/ml), (C) SAM formation (35 CFU/ml), and (D) using nanoparticles (3 CFU/ml). [50]

Directly using urine as the analyte for a given detection problem offers advantages for the diagnostic of disease. Disease markers in urine are numerous and we report here a number of detection problems in this area.

In [56] an SPR biosensor was used to measure the creatine and the marker for diabetes, transferrin. Considering that urine concentration changes greatly with water intake, detection of creatine is used to

correct the concentration of other urine markers. The paper reports a single biosensor to detect transferrin at the same time as creatine.

CFP-10 antigen is a marker for tuberculosis. It was detected in the clinical urine samples of 55 patients using an SPR immunosensing system [57,58]. A monoclonal antibody was immobilized on the gold surface. Also cystamine was used for blocking. The functionalisation of the biosensing device is described in a companion paper [59]. We need to consider that ¨The measurement temperature was maintained at 25±0.1 ◦C by a temperature controlling system during the entire procedure.¨[59]. Also the urine preparation included ¨pre-treated by centrifugation at 3000 rpm for 10 min to eliminate precipitates, usually large chunks of proteins. The supernatants were then diluted with PBS buffer to 0.5% by volume¨ [57].

The human growth hormone (hGH), the human luteinizing hormone (hLH), and the human follicle stimulating hormone (hFSH) were analyzed by competitive immunoassay using urine samples without dilution or sample pre-treatment. The detection limits of the SPR immunoassays were in the 250 pM to1nM range. [60, 61]

A clinical trial comparing 5 healthy patients with 5 patients with active rheumatoid arthritis (DAS28Z5.1) was performed. Urine samples were not centrifuged, filtered or pH neutralized. In conclusion, the lentiviral-based SPR method was rapid, used non-radioactive ligands, and gives reproducible results for urine samples, with no requirement for preliminary treatment [62].

Food poisoning from puffer fish is best detected in urine because TTX concentrations are 10 times higher than in blood at levels of 100 ng/ml [63]. The paper demonstrates a robust and re-generable assay for quantitative detection of TTX in urine.

Public health and environment protection is regulated by restrictions on toxic substances. Trichloro-2-pyridinol (TCP) is a urine biomarker from exposure to chlorpyrifos, an organophosphorus pesticide widely used in agricultural and urban environment. Highly sensitive detection of TCP in human urine without the need for preparation of samples was demonstrated in [64].

In summary, the main advantages of SPR over other immunoassay sensing methods (e.g. ELISA) are real-time detection: kinetics information about the reaction, quick data acquisition (10-20 min), and label-free detection (no chemical manipulation with ligand/analyte system). To date, various urinalysis detection problems have been demonstrated with applications in the area of food poisoning, environmental biomarker detection, and clinical diagnostic of diseases.

1.3.2 The long range surface plasmon polariton waveguide biosensor

As an introduction to the LRSPP biosensor, we review the theory of the light propagation at the surface of a metal stripe cladded by a dielectric. Technical implementation of a LRSPP waveguide biosensor will be given in section 2.1.

Making use of the Drude model of electrical conduction to define the electronic equation of motion, and a linear relationship between current density and electric field, the electromagnetic solution to the structure presented in Figure 12 can be obtained using the Method of Line (MoL). A solution to the propagation constant as a function of metal thickness is shown in Figure 12(c). We denote the low insertion loss obtained for the S_b mode, which is also called the LRSPP mode, for metal thickness below 100 nm. Using this mode of propagation, LRSPP biosensor was presented by Krupin in [42]. Unlike the SPR biosensor discussed above, the LRSPP waveguide biosensor uses butt-end coupling to excite the LRSPP mode. This is currently unique in the literature on plasmon based label free biosensor. It provides economic advantages for integration with fluidic and optical components needed in the mass production of biosensors.

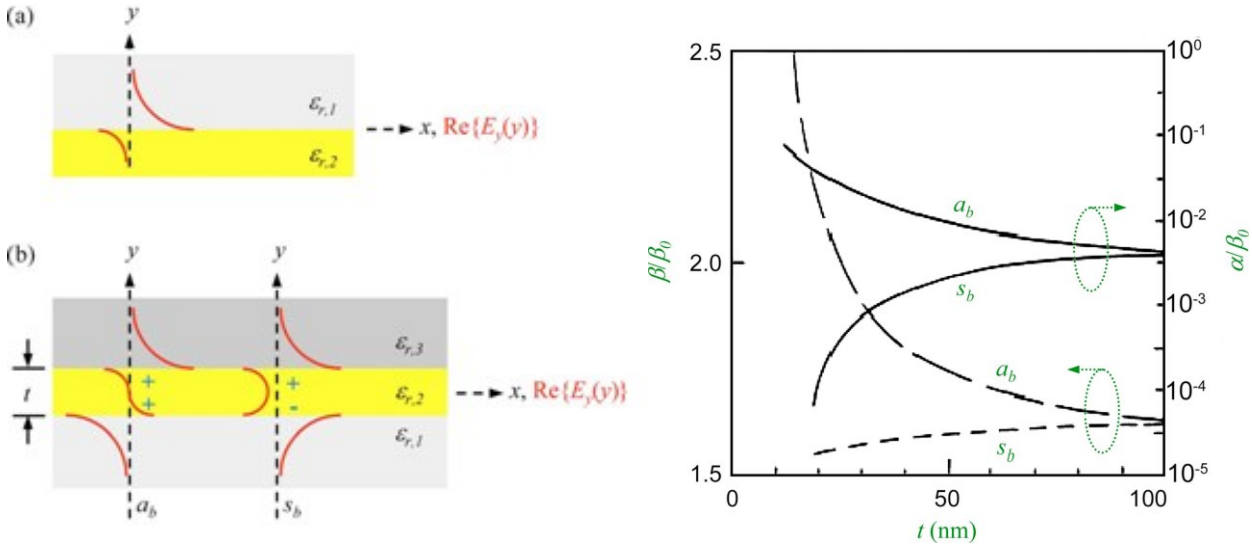

Figure 12 Representation of electromagnetic mode intensity at the metal dielectric interface. The s_b mode is referred to as the LRSPP mode. a) Single metal dielectric, b) thin metal film between 2 dielectrics, c) solution to propagation constant as a function of metal thickness for the asymmetric (a_b) and symmetric (s_b) modes [65].

In theory, all of the applications presented for SPR are also applicable to LRSPP biosensors. The major difference is in the geometry of the biosensor and the penetration depth of the electromagnetic field. For LRSPP waveguide biosensors, the penetration depth is estimated to be 2 μm which is 5 times larger than conventional SPR [42]. This is an advantage for LRSPP waveguides over SPR for the detection of bacteria which are 1 to 5 μm in diameter.

1.3.2.1 Specific Gravity measurement using a LRSPP Waveguide

We have previously seen in section 1.2.2 that many techniques exist to measure the specific gravity (SG) of urine. The LRSPP waveguide biosensor is also capable of making a SG measurement given the appropriate conversion table for a specific type of fluid. As reported in [66], the conversion table should consider the fluid temperature and its constituents. For complex fluids like urine, the conversion table between refractive index and specific gravity can be found in the CRC Handbook of Chemistry and Physics [67].

The importance of knowing the fluid constituents is better understood from the Gladston-Dale equation presented in section 1.2.2, i.e: (ρ) = (n-1)/sum(km), which indicates that the molar refractivity (k) is a characteristic of the fluid which needs to be known. For example, knowing that the molar refractivity (k) of

water is k=0.33, and measuring the RI of a water sample as n=1.33, we can compute the specific gravity from $(\rho)/(\rho w) = (n-1)/(\text{sum}(km)x(\rho w)) = 1.33\text{-}1/0.33x1 = 1$.

Another parameter to consider when using the LRSPP waveguide biosensor to measure the specific gravity is the wavelength of the laser source. The standard wavelength for refractive index measurements with an Abbe refractometer is 589 nm [67] which is obtained from a sodium yellow light. Using this wavelength, the refractive index of water is 1.333 [68]. In comparison, at 1310 nm the refractive index of water is 1.3195 according to [69] which corresponds to a difference of 0.0135.

In the literature, LRSPP waveguide biosensors have been demonstrated using a CYTOP cladding. With this arrangement, bulk sensing of fluids with a varying refractive index has been shown with PBS-Glycerol mixtures of known concentration [42]. In this laboratory-controlled environment, PBS-Glycerol solutions of known composition, i.e: known specific gravity, were measured with a refractometer (Model 2010, Metricon, Prism 200-P1) with RI ranging from 1.3282 to 1.3409 at 1310 nm. The solutions were then measured with the LRSPP waveguide biosensor. For a given waveguide this provides the calibration information required to relate the LRSPP waveguide power measurement to the SG of a PBS-Glycerol solution. Unfortunately, the exact composition of the PBS-Glycerol solutions was not published in the article. We note that the RI measurements reported correspond to a 1% dynamic range centered at the CYTOP refractive index of 1.3346 (@1310 nm). The best sensitivity for the LRSPP waveguide biosensor is reported to be $2.3x10^{-6}$ RIU at the optimum point of this range. In comparison, clinical refractometers advertise a refractive index accuracy of $2x10^{-4}$ [70] and a dynamic range of 1.4% for urine centered at a refractive index of 1.3394 (@589 nm). The CRC table of human urine reports specific gravity values from 1.000 to 1.037 which correspond to human urine RI of 1.3338 to 1.3482, or equivalently a dynamic range 1 % centered at RI=1.341 (@589nm).

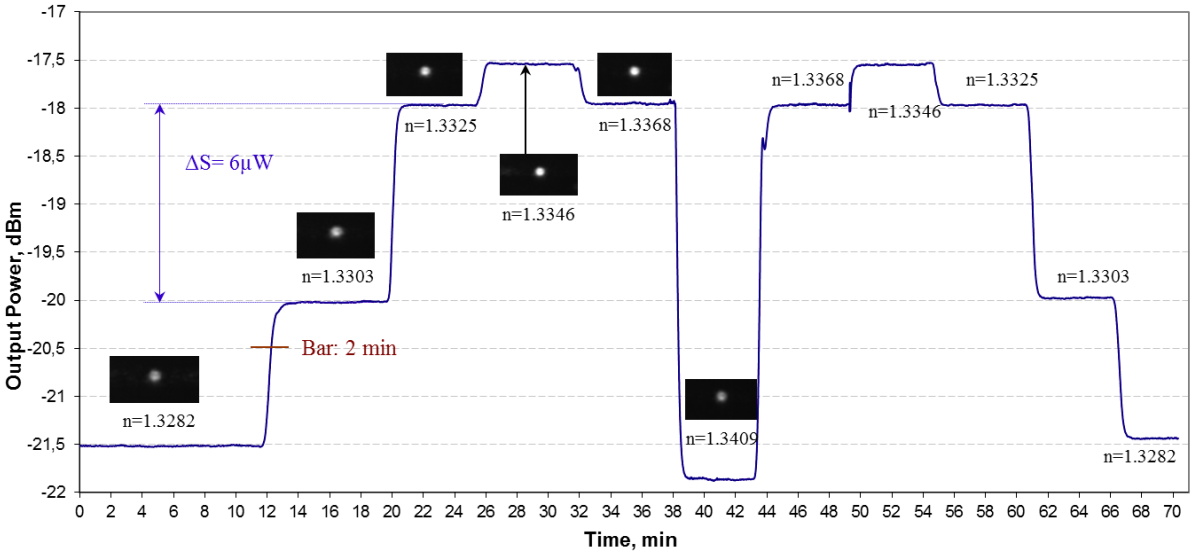

Figure 13 Bulk sensing of a LRSPP waveguide biosensor functionalised with 16-MHA [42]

From the theory of the LRSPP mode propagation [71], we compute the LRSPP mode dynamic range to be 1.3% when using a gold thickness of 30 nm on SiO2 which has a RI=1.444. When an analyte solution RI exceeds this, the LRSPP mode will not be purely bound but become radiative creating background light which can dominate the power measurement in the interrogation system. It is not known at what point the loss of mode purity will significantly degrade the refractive index measurement and therefore render the specific gravity measurement unusable.

In summary, the LRSPP waveguide has not yet been used to measure the SG of urine. The literature provides bulk sensing of PBS-Glycerol demonstrating that the measurement dynamic range of the detector is comparable to that of clinical refractometers. Operation beyond LRSPP mode cutoff seems possible [71]

1.3.2.2 Proteinuria measurement using a LRSPP Waveguide

Proteinuria is a medical condition where an excess of protein is found in the urine. Measurements can be performed using a dipstick [72]. It can also be estimated using a specific gravity measurement as discussed in section 1.3.2.1. The UK Renal association recommends that ¨proteinuria should be assessed by measurement either of the protein to creatinine or albumin to creatinine ratio, ideally on an early-morning

urine specimen¨ [73]. Proteinuria is defined as an excretion of more than 150 mg of protein per day. Normal excretion is composed of 20% protein with a low molecular weight of less than 20 kD, 40% of albumin with a molecular weight of 65 kD, and 40% of Tamm-Horsfall mucoproteins. [74].

It is feasible with the LRSPP waveguide biosensor to detect Bovine Serum Albumin which is chemically similar to human serum albumin as shown in Figure 14. The concentration of BSA used was 100 µg/ml which is low enough to avoid changing the bulk refractive index of the sensing solution (PBS-Glycerol with a RI=1.3303). Hence, protein detection with a LRSPP waveguide will manifest itself as both physisorbtion on a properly functionalised surface and as a change in RI for concentrations greater than 100 µg/ml. The detection of creatine has not yet been demonstrated on LRSPP waveguides but was demonstrated with an SPR biosensor [56].

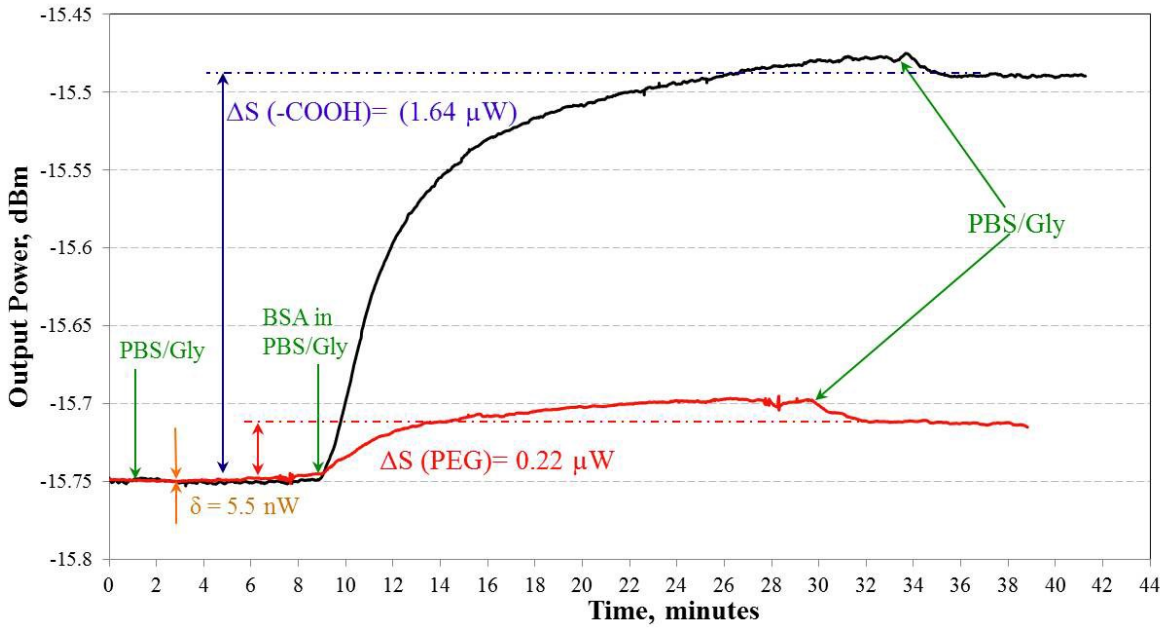

Figure 14 BSA physisorption on two surfaces: 16-MHA (carboxyl-terminated, adsorptive surface shown in blue) and PEG (non-specific adsorption preventing surface, shown in red) [42].

1.3.2.3 Bacteriuria measurement using a LRSPP Waveguide

Bacteriuria refers to the detection of bacteria in urine. As seen in section 1.3.1, the SPR biosensor has been used to detect bacteria in clean fluid and it has also been used to detect protein in urine but it has not been

demonstrated for the detection of bacteria in urine. The LRSPP waveguide biosensor has also been demonstrated for the detection of bacteria in a PBS Glycerol solution using a bacterial concentration of 10^{10} CFU/ml and using a gram negative antibody on the surface of the detector to detect *E.Coli* bacteria. [75].

To be meaningful, a bacteriuria technique needs to demonstrate a sensitivity better than 10^5 CFU/ml in order to properly diagnose UTI. This has not been shown with LRSPP waveguide biosensors. On the other hand, red blood cell detection at a sensitivity of $3x10^5$ cells/ml was demonstrated in [76].

1.4 Thesis outline

To improve the diagnosis of UTI we proposed to study a new technology, the label free LRSPP biosensor. In broad terms, we want to understand if a label free biosensor can bring some advantages in terms of simplicity, speed, specificity, and selectivity when compared to other urinalysis techniques. More specifically, we demonstrate that directly testing urine sample, a complex fluid, with a LRSPP waveguide biosensor we can selectively detect the gram of a bacteria in minutes. Clinical test to demonstrate specificity and selectivity have not been tackled in this work. On the other hand, the robustness of the detection techniques in presence of bacterial contamination, which is probable in clinical trials, was evaluated suggesting that the positive to negative ratio approach taken will translate into good specificity and selectivity for the diagnostic of UTI.

The thesis is assembled as a collection of articles submitted and supplemented with laboratory measurements.

Chapter 1 provides background knowledge about urinalysis and associated test methods, including the test for the diagnostic of the urinary tract infection. We introduce urinalysis techniques, and the label free biosensor. We also review the state of the art of SPR biosensors and the LRSPP waveguide biosensor.

Chapter 2, sub section 1 details the biosensor system developed for urinalysis. It augments the description of the test setup found in the articles with additional laboratory protocols and procedure. Sub section 2 presents measurement results submitted to Biomedical Optics Express. It demonstrates the use of

the LRSPP waveguide biosensor to selectively detect gram negative and gram positive bacteria. Sub section 3 presents additional results submitted to Photonics North where the urine contains multiple bacteria. Sub section 4 presents additional laboratory results such as cut back measurements to characterise insertion loss of the LRSPP waveguide, measurements obtained during functionalization of the waveguide surface with protein G and antibody, descriptions of the bacteria growth and count technique, visual inspections demonstrating the effectiveness of SDS as a mean to dissolve the bacteria after a test, rapid sensing of dead *vs.* live bacteria, the detection of biofilm formation on a die, the limitations of the fluidic test jig, results showing the effect of measuring beyond the LRSPP mode cut off, and the detection of organic material in a PBS-glycerol solution.

Chapter 3 concludes the thesis by summarizing the LRSPP waveguide biosensor performance for urinalysis. It describes the contributions of this work and proposes future research activities required to successfully implement the LRSPP waveguide biosensor as a urinalysis tool.

1.5 References

1. J A Armstrong, ¨Urinalysis in Western culture: A brief history,¨ Kidney International v71, pp. 384–387. (2007), http://www.nature.com/ki/journal/v71/n5/full/5002057a.html
2. W.I. White, ¨A New Look at the Role of Urinalysis in the History of Diagnostic Medicine,¨ CLIN.CHEM.v37/1,pp. 119-125 (1991).
3. J.Lister, ¨Lister Collected Paper¨, Oxford University Press (1909) vol. 2, 175-178 (1909), http://www.victorianweb.org/science/health/depaolo.html
4. W. Roberts ¨On the occurrence of micro-organisms in fresh urine¨. Br Med J 1881;ii:623-5 (1881).
5. Simerville JA, Maxted WC, Pahira JJ. ¨Urinalysis: a comprehensive review.¨ Am Fam Physician 2005; 71: 1153–1162. (2005).
6. Web Reference: http://medicalmicrobiologyinfo.blogspot.ca/2010/09/bacterial-culture-media.html
7. G. Schmiemann, E. Kniehl, K. Gebhardt, M. Matejczyk, E. Hummers-Pradier ¨The Diagnosis of Urinary Tract Infection: A Systematic Review,¨ Dtsch Arztebl Int 107(21): 361–7 (2010).
8. J. B. Kaper, J. P. Nataro, and H. L. T. Mobley, ¨Pathogenic Escherichia coli,¨ Nature Reviews Microbiology, vol. 2, no. 2, pp. 123–140, (2004).
9. Web Reference: http://www.merckmanuals.com/home/kidney_and_urinary_tract_disorders/urinary_tract_infections_uti/overview_of_urinary_tract_infections.html
10. T. M. Hooton and W. E. Stamm, ¨Diagnosis and treatment of uncomplicated urinary tract infection,¨ Infect. Dis. Clin. North Am., vol. 11, no. 3, pp. 551–581, (1997).
11. B. Foxman, ¨The epidemiology of urinary tract infection,¨ Nat Rev Urol, vol. 7, no. 12, pp. 653–660, (2010).

12. F. M. E. Wagenlehner and K. G. Naber, ¨New drugs for Gram-positive uropathogens,¨ International Journal of Antimicrobial Agents, vol. 24, Supplement 1, no. 0, pp. 39–43, (2004).
13. G. Kahlmeter, ¨Prevalence and antimicrobial susceptibility of pathogens in uncomplicated cystitis in Europe. The ECO/SENS study,¨International Journal of Antimicrobial Agents, 22 (2003).
14. D. Prakash and R.S. Saxena, ¨Distribution and antimicrobial susceptibility pattern of bacterial pathogens causing urinary tract infection in urban community of Meerut city, India¨, ISRN Microbiology, Article ID 749629, 13 pages (2013).
15. G. Schmiemann, E. Kniehl, K. Gebhardt, M.M. Matejczyk, E. Hummers-Pradier ¨The Diagnosis of Urinary Tract Infection A Systematic Review,¨ Dtsch Arztebl Int vol. 107, no 21, pp. 361–7 (2010).
16. W. Brumfitt, A.Percival, ¨Pathogenesis and laboratory diagnosis of nontuberculous urinary tract infection: a review.¨ J Clin Pathol; vol. 17, p. 482 (1964).
17. P. Kerfoot , D. McGhie, E. Cahill and T.A. Fountain, ¨Mechanised batch screening method for the detection of bacteriuria,¨.J Clin Pathol vol.3; no. 36, pp. 1318-9 (1983).
18. L. Rici ¨L'automazione delle urinocolture nuovi percorsi diagnostici ed organizzativi,¨ SIMPIOS, Grado, 7-9 April (2008).
19. N.R. Krieg , ¨Bergey's Manual of Systematic Bacteriology,¨ vol. 1. The Williams & Wilkins Co., Baltimore, 964 pp, (1984)
20. S. Strasinger, M. Schaub Di Lorenzo ¨Urinalysis and body fluids,¨ F.A. Davis company, sixth edition (2014).
21. R. James MD, ¨Urine Dipstick Testing:Everything You Need to Know¨ Emergency medecie news, vol. 29 – no. 6, pp: 3-51, (2007)
22. Web Reference: http://www.beaumont.ie/kidneycentre-forpatients-aguidetokidneydisease-dia
23. K.J. Stuempfle; D.G. Drury ¨Comparison of 3 Methods to Assess Urine Specific Gravity in Collegiate Wrestlers,¨ Journal of Athletic Training vol. 38, no. 4, pp. 315–319 (2003).
24. A.E. Burkhardt, K.G. Johnston, C.E. Waszak, C.E. Jackson, and S.R. Shafer ¨A Reagent Strip for Measuring the Specific Gravity of Urine,¨ Clinical Chemistry, vol. 28, no. 10, (1982).
25. R.D. Allen ¨A new equation relating index of refraction and specific gravity,¨ Am Mineralogist, pp247-255, (1956).
26. Web Reference: http://en.wikipedia.org/wiki/Cytometry
27. M.A. Broeren, S. Bahceci, H.L. Vader, N.L. Arents "Screening for urinary tract infection with the Sysmex UF-1000i urine flow cytometer," J Clin Microbiol vol. 49**,** pp. 1025–1029 (2011)
28. M. Marschal, M. Wienke, S. Hoering, I.B. Autenrieth, J.-S. Frick, "Evaluation of 3 different rapid automated systems for diagnosis of urinary tract infection," Diagnostic Microbiology and Infectious Disease vol. 72**,** pp. 125–130, (2012).
29. J. Wang, Y. Zhang, D. Xu, W. Shao, and Y. Lu, "Evaluation of the Sysmex UF-1000i for the Diagnosis of Urinary Tract Infection," AJCP, vol. 133, no. 4, pp. 577–582, (2010).
30. M.A. Van Dilla, R.G. Langlois, D. Pinkel, et al. ¨Bacterial characterization by flow cytometry,¨ Science vol. 220, pp. 620-622, (1983).
31. R.C. LI, D.E. NIX, and J.J. SCHENTAG, ¨New Turbidimetric Assay for Quantitation of Viable Bacterial Densities,¨ Antimicrobial agents and chemotherapy, vol 37, no.2, pp. 371-374 (1993).
32. Web Reference: http://www.ppdictionary.com/bacteria/gpbac/bacteria_comparison.jpg
33. NCCLS. ¨Urinalysis and Collection, Transportation, and Preservation of Urine Specimens;¨ Approved Guideline. GP-16A2, No. 19. 2nd ed. (2001).
34. G. Mandell et al, ¨Principles and Practices of Infectious Diseases¨. 7th ed. Philadelphia, Pa: Churchill-Livingstone; (2009).
35. G.R.W Burton,¨Microbiology for the Health Sciences,¨ Fourth ed., J.B. Lippincott Company, (1992).

36. Web reference: http://en.wikipedia.org/wiki/Bacterial_cellular_morphologies
37. Web reference: http://en.wikipedia.org/wiki/Anaerobic_organism
38. J. Tokas, R. Begum, S. Jain, and H. Yadav, ¨Biosensor (General principles and applications),¨ http:// http://www.pitt.edu/~super4/36011-37001/36421.ppt
39. K.A. Erickson,and P. Wilding, "Evaluation of a novel point-of-care system,the i-STAT portable clinical analyzer¨. Clin. Chem. Vol. 39, pp. 283–287, (1993).
40. Web reference: http://ctcb.bio.ed.ac.uk/CTCB/SPR_-_BIAcore_T200.html
41. K.E. Mach, P.K. Wong, J.C. Liao, ¨Biosensor diagnosis of urinary tract infections: a path to better treatment?,¨ Trends in Pharmacological Sciences, vol 32, no. 6, pp. 330-336, (2011), http://dx.doi.org/10.1016/j.tips.2011.03.001.
42. O. Krupin, H. Asiri, C. Wang, R.N. Tait, and P. Berini, "Biosensing using straight long-range surface plasmon waveguides," OPTICS EXPRESS , vol. 21, no. 1, pp. 698-709, (2013).
43. B. Liedberg, C. Nylander and I. LundstrÖm, ¨Biosensing with surface Plasmon resonance- how it all started. Biosensors and Bioelectronics.¨ Biosensors & Bioelectronics vol. 10, pp. i-ix (1995).
44. D.R. Shankaran, V. Gobi, and N. Miura, ¨Recent advancements in surface plasmon resonance immunosensors for detection of small molecules of biomedical, food and environmental interest,¨ Sensors and Actuators B. 121 ed., pp. 158–177, (2007).
45. D. Wei,¨Development of a surface plasmon resonance biosensor for the identificaition of campylobacter Jejuni,¨. Auburn alabama: Graduate Faculty of Auburn University (2006).
46. E.A. Perkins, D.J. Squirrell, ¨Development of instrumentation to allow the detection of microorganisms using light scattering in combination with surface plasmon resonance `` Biosensors & Bioelectronics, pp. 853–859, (2000).
47. I. Abdulhalim, M. Zourob, A. Lakhtakia ¨Surface Plasmon Resonance for Biosensing: AMini-Review,¨ Electromagnetics, vol. 28, pp. 214–242, (2008).
48. P. M. Fratamico, T. R. Strobaugh, M. B. Medina, and A. G. Gehring, "Detection of Escherichia coli O157:H7 using a surface plasmon resonance biosensor," Biotechnol. Techn. vol. 12, pp. 571-576 (1998).
49. C.A. Meeusen, E.C. Alocilja, and W. Osburn, ¨Detection of E. coli O157:H7 Using a Surface Plasmon Resonance Biosensor.¨ ASAE Meeting Paper No: 01-7030. St. Joseph, Mich. ASAE. (2001).
50. Ö. Torun, İ. H. Boyac, E. Temür, and U. Tamer, ¨Comparison of sensing strategies in SPR biosensor for rapid and sensitive enumeration of bacteria,¨ Biosens. Bioelectr. vol. 37, pp. 53-60, (2012).
51. A. Subramanian, J. Irudayaraj, T. Ryan, ¨A mixed self-assembled monolayer based surface plasmon immunosensor for detection of E. coli O157:H7.¨ Biosens. Bioelectron. vol. 21, pp. 998-1006 (2006).
52. K.H. Seo, R.E. Brackett, N.F. Hartman, and D.P. Campbell, ¨Development of a rapid response biosensor for detection of Salmonella typhimurium,¨ J. Food Prot. vol. 62, no. 5, pp. 431-437 (1999).
53. G.C.A.M Bokken, R.J. Corbee, F. van Knapen, and A.A. Bergwerff, ¨Immunochemical detection of Salmonella group B, D and E using an optical surface plasmon resonance biosensor.¨ FEMS Microbiology Letters, vol. 222, pp. 75-82 (2003).
54. P. Leonard, S. Hearty, J. Quinn, and R. O'Kennedy, ¨A generic approach for the detection of whole Listeria monocytogenes cells in contaminated samples using surface plasmon resonance.¨ Biosensors and Bioelectronics. vol. 19, pp. 1331-1335 (2004).
55. M. Vala, S. Etheridge, J. Roach, and J. Homola, "Long-range surface plasmons for sensitive detection of bacterial analytes," Sens. Act. B 139, pp. 59-63 (2009).
56. K. Nakamoto, N. Sekioka, R. Kurita and O. Niwa ¨On-chip surface plasmon resonance measurementof disease marker protein and small metabolite combined with immune and enzymatic reactions,¨

Twelfth International Conference on Miniaturized Systems for Chemistry and Life Sciences, San Diego, California, USA, pp. 471-473, (2008).
57. S.C. Hong, J. Leea, ¨Clinical immunosensing of tuberculosis CFP-10 in patient urine by surface plasmon resonance spectroscopy,¨ Sensors and Actuators B 160, pp. 1434-1438, (2011)
58. S.D. Lawn, A.D. Kerkhoff, M.Vogt, R.Wood, ¨Diagnostic accuracy of a low cost, urine antigen, point of care screening assay for HIV-associated pulmonary tuberculosis before antiretroviral therapy: a descriptive study¨. The Lancet Infectious disease, vol 12, pp. 201-209, (2012).
59. S. Hong, H. Chen, J. Lee, H. Park, Y. Kim, H. Shin, et al. ¨Ultrasensitive immunosensing of tuberculosis CFP-10 based on SPR,¨ Sens. Actuators B: Chem. 156, pp. 271–275, (2011)
60. J. Trevino,A. Calle, J.M. Rodríguez-Fraded, M. Melladod, L.M. Lechuga, ¨Single- and multi-analyte determination of gonadotropic hormones in urine bySurface Plasmon Resonance immunoassay¨ Analytica Chimica Acta 647, pp. 202–209, (2009).
61. L. G. Carrascosa1, J. Treviño1, A. Calle2 and L. M. Lechuga1 ¨Real-time SPR biosensing for early clinical diagnostics,¨ IBERSENSOR 2008 ,6º Congreso Iberoamericano de Sensores 24-26 de Novembro de 2008, São Paulo, Brasil, (2008)
62. B. Vega, A. Calle, A. Sanchez, L.M. Lechuga, A.M.Ortiz, G. Armelles, J.M. Rodriguez-frade, M. Mellado, ¨Real-time detection of the chemokine CXCL12 in urine samples bysurface plasmon resonance¨ Talanta 109, pp. 209–215, (2013).
63. A.D. Taylor, H. Vaisochero, J. Deeds, S. DeGrasse, and S. Jiang ¨Tetrodotoxin Detection by a Surface Plasmon Resonance Sensor in PufferfishMatrices and Urine¨ Hindawi Publishing Corporation, Journal of Sensors, Article ID 601704, 10 pages (2011).
64. E. Mauriz, A. Calle, J. J. Manclús, A. Montoya, L.M. Lechuga ¨On-line determination of 3,5,6-trichloro-2-pyridinol in human urine samples by surface plasmon resonance immunosensing, ¨ Anal Bioanal Chem, vol. 387, pp. 2757–2765, (2007).
65. P. Berini, ¨Long-range surface plasmon polaritons`¨, Advances in Optics and Photonics, pp. 484–588 (2009).
66. J.W. George, ¨The Usefulness and Limitations of Hand-held Refractometers in Veterinary Laboratory Medicine: An Historical and Technical Review,¨ Veterinary Clinical Pathology, vol. 30, no. 4, pp 201-210, (2001).
67. CRC Handbooks of Chemistry and Physics, CRC Press Inc. 60th Edition (1980)
68. A.H. Harvy, J. Gallagher and J.M.H. Levelt Sengers ¨Revised formulation for the refractive index of water and steam as a function of wavelength, temperature and density`` J. Phys. Chem Ref. Data vol. 27, pp. 761–74, (1998).
69. K. Chang-Bong, B.S. Chin, ¨Measurement of the refractive index of liquids at 1.3 and 1.5 micron using a fibre optic Fresnel ratio meter ¨ Meas. Sci. Technol. vol. 15, pp. 1683–1686, (2004).
70. ¨Instruction manual for Reichert TS-METER Total Solids Refractometer¨ Model 1310400A, www.reichert.com, (2003)
71. I. Breukelaar, R. Charbonneau, and P. Berini, ¨Long-range surface plasmon-polariton mode cutoff and radiation in embedded strip waveguides,¨ J. Appl. Phys. vol. 100, pp. 43–104 (2006).
72. Web Reference http://en.wikipedia.org/wiki/Proteinuria
73. Web Reference http://www.renal.org/docs/default-source/guidelines-resources/Detection_Monitoring_and_Care_of_Patients_with_CKD_-_Final_Version_28_February_2011.pdf?sfvrsn=0
74. Web Reference: http://www.aafp.org/afp/2000/0915/p1333.html
75. A. Khan, O. Krupin, E. Lisicka-Skrzek and P. Berini ¨Sensing of bacteria immobilised under static conditions using longrange surface plasmon waveguides in Cytop,¨ Proc. of SPIE vol. 8007, (2011).

76. O. Krupin, C. Wang, P. Berini, ¨Selective capture of human red blood cells based on blood group using long-range surface plasmon waveguides,¨ Biosensors and Bioelectronics vol. 53, pp. 117–122, (2014).

Chapter Two:
A sensor for the selective detection of bacteria

2.1 The long range surface plasmon waveguide as a biosensor

A LRSPP waveguide biosensor is obtained by measuring and analyzing the optical response of the LRSPP waveguide stimulated by a fluid containing a target pathogen. A sensorgram which relates the injection of the test fluid containing analyte with the optical response over time provides a visual picture of the interaction within the biosensing area of the biosensor. The biosensing area, which is effectively the surface of the etched Au line guiding the LRSPP optical mode, is functionalised with antibody (the bio-receptor) to provide selective adsorption of the target pathogen and to prevent nonspecific adsorption of other constituents from the urine.

A picture of the complete measurement system is shown in Figure 15. We divide this system in 5 sub-systems: the LRSPP device and jig assembly sub-system, the optical interrogation and detection sub-system, the chemical microfluidic injection sub-system, the mechanical alignment and anti-vibration sub-system, and the data acquisition and analysis sub-system. The complete system was assembled from commercial components and integrated to form the LRSPP waveguide biosensor system. A description of the system can be found in section 2.2 of the Paper submitted to Biomedical Optics Express. In the following subsection we provide the system specifications of each component as a baseline to achieve the performance we obtained.

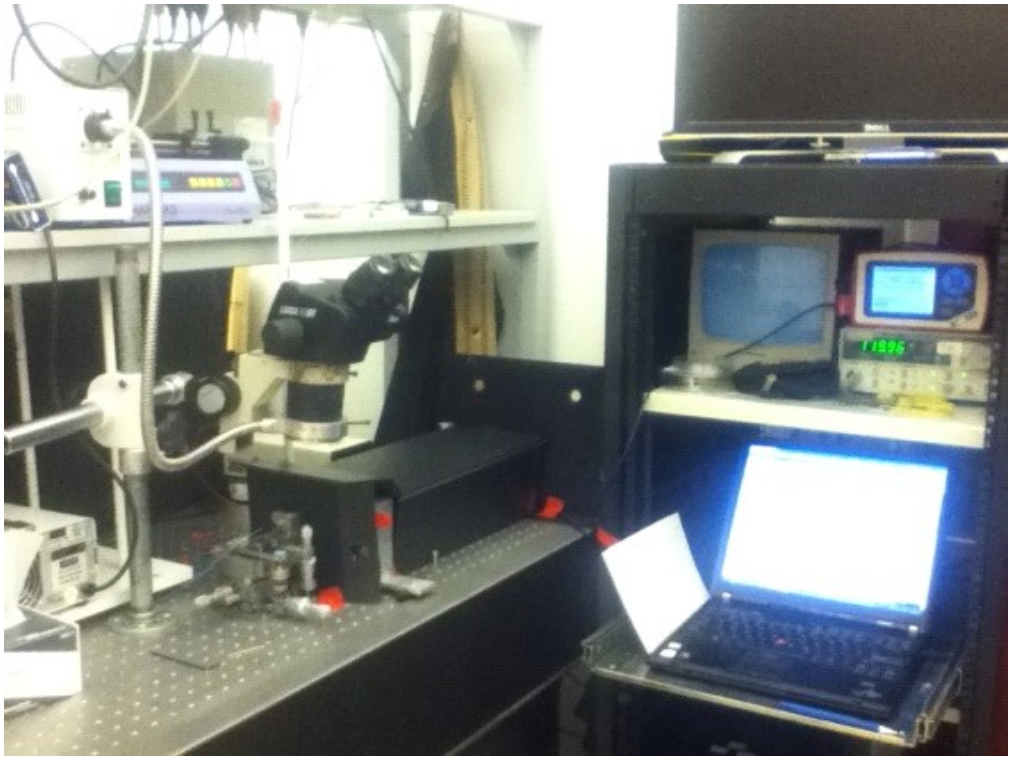

Figure 15 Picture of the LRSPP waveguide biosensor system

2.1.1 Preparation of the LRSPP device and jig assembly sub-system

The biosensor in a jig assembly is shown in Figure 16. The jig was manually assembled in the laboratory.

The following subsection describes the fabrication steps required to obtain a complete jig assembly.

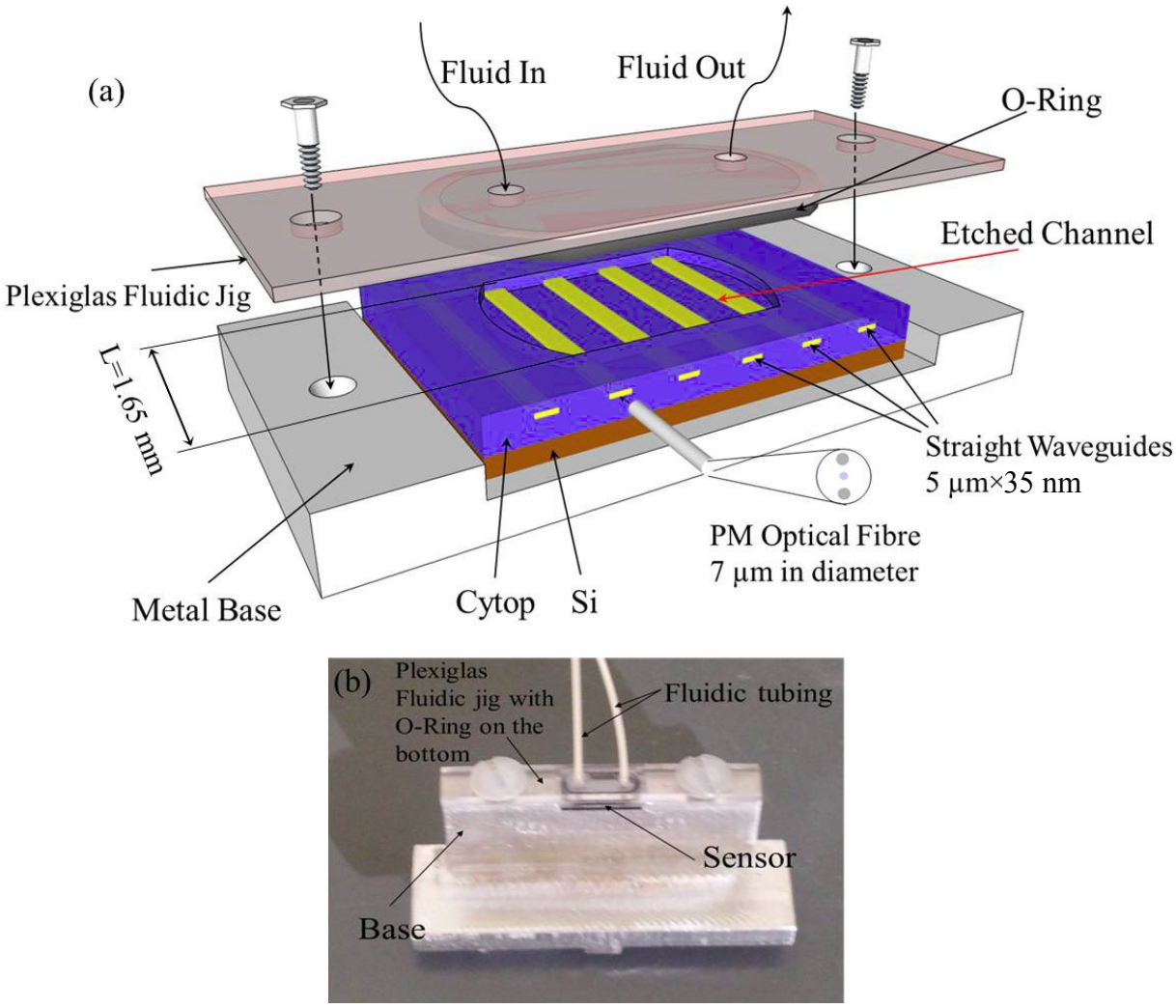

Figure 16 Sensing device with integrated fluidics: a) schematic of the device placed on the metal base with a Plexiglas jig on top; the volume of the fluidic cell is 20 µL; b) image of the device with fluidics fixed on the metal base. [©2013 Optical Society of America; adapted from [1]].

2.1.1.1 Jig top cover fabrication steps

First a Plexiglas piece was machined with a track of the size of the selected O-ring (Apple Rubber Products inc. part number R00161-020-75VTB, 161 x 020 Fluorocarbon). The fluidic tubing (IDEX health and Science, Tub Peek Nat 510 µm x 255 µm x 1.5m) is cut to a 50 cm length and inserted in the appropriate hole. Krazy Glue was applied to the top side along the edge of the tubing, causing it to flow into the plexiglass hole by capillary action ensuring a strong bond. A 1 hour curing was applied. The Silicone glue (GE Silicone I, 100% Silicone Rubber) was placed in the track of the O-ring and the O-ring put in place using tweezers. The top cover assembly was immediately assembled on a jig with a dummy die in order to

apply pressure on the O-ring while the silicone glue cured for 24 hours. The next day, an X-acto knife was used to remove the excess glue from the inside edge of the O-ring. A gage 22 needle was glued with Krazy Glue at the end of the fluidic outlet tubing. Finally, a leak test was performed to ensure that we can pull fluid through the system without the formation of air bubbles or leakage of the fluid.

2.1.1.2 Surface Cleaning and Regeneration at the Au surface and at the antibody level

To ensure the cleanliness of the waveguide facets for efficient optical input and output coupling, a fresh sensor die was cleaned by ultra-sonication (FB-11201, Fisher Scientific) in heptane for 5 min to remove any possible debris formed during dicing of the wafer. The sensor die was then left immersed in two sequential acetone baths for 5 and 30 min, respectively, to completely remove the dicing photoresist. After a thorough washing in IPA and drying with nitrogen gas (N_2), the sensor die was placed in a digital UV ozone system (PSD-UV-4, Novascan) to remove any possible organic matter from the Au surface. The die was then washed intensely with IPA and distilled/de-ionized water (DDI H_2O), followed by Nitrogen (N_2) drying. Cleaned sensor die assembled in the test jig were all primed with DDI H_2O before assembly onto the test system.

Upon completion of experimental runs, the Au surface of the sensor die was discarded or fully regenerated. The regeneration process starts by flowing 2 ml of SDS then 2 ml of DDI H_20. The die is removed from the jig and deposited in a vial of SDS for periods of 24 to 96 hours to dissolve the lipopolysaccharide membrane of the bacteria. The die is further cleaned by rinsing and depositing in a vial with Acetone, IPA and DDI H_2O to remove debris. Nitrogen gas (N_2) is used to dry the surface and a microscope inspection provides necessary quality control step. The regenerated surface of a sensor die is finally placed in a UV/ozone chamber before starting a new experimental run. Measurement of the optical insertion loss with a RI-controlled fluid after cleaning was used as a quality measure before re-using a die in a new experimental run.

2.1.1.3 Surface functionalization with protein and antibody

Once inserted into the test system, the surface of a Au stripe was functionalized by injecting GProt solution for 20 min at a rate of 20 µl/min. Following this step, and for a gram negative selective surface, Gneg was injected for 10 min at a rate of 20 µl/min followed by stop flow for 80 min which results in the deposition of a monolayer of gram negative antibody. For the gram positive selective surface, GPos was injected for 10 min at a rate of 20 µl/min followed by stop flow for 80 min which results in the deposition of a monolayer of gram positive antibody. In both cases, we complete the functionalization by injecting BSA for 5 min at a rate of 20 µl/min. This functionalization approach was selected as our simple non-specific binding strategy because BSA blocks possible adsorption sites and leaves a monolayer of antibody to bind with the target. A flat sensorgram (<0.10 dB variation) response from BSA deposition is required for a valid surface functionalization.

2.1.2 The optical interrogation and detection sub-system

The light source was a PM-fiber pigtailed laser diode (NLK1B5GAAA, NEL) in a laser mount (LDM-4980, ILX) controlled by current and temperature controller (LDX3220, ILX) delivering 14.5 dBm of output power at a free-space optical wavelength of 1310 nm with a set current of 120 mA and a set temperature of 30º C. A set current of 50 mA (delivering 11.1 dBm) is sometime used. The optical PM fiber (PMJ-3S3A-1300-7/125-1-1-1, OZ Optics Ltd.) used to excite a sensor was 0.5 m long, cleaved and fixed into a fiber holder. A 25× optical lens (25/0.50, Melles Griot) was used to focus the output light onto an optical sensor (S144C, Thorlabs) connected to a power meter (PM100, Thorlabs). An optical aperture was used during alignment of the laser beam and to reduce the power detected at the sensor due to background light. An optical beam splitter (BSW29, Thorlabs) was used to split the output beam in order to provide an image of the mode on an IR camera (Micronviewer 7290A, electrophysics). Without a sensor in the set-up, the detected power was typically 7.9 dBm. Thus, we estimate the loss through the cleaved optical fiber, lens, aperture and beam splitter to be 6.6 dB, of which 5 dB comes from the beam splitter at the set angle. The

typical insertion loss of a 3.8 mm long cladded waveguide was measured to be 27 dB. Thus the maximum output power that we can obtain with a LRSPP waveguide biosensor in the set-up is about -19.1 dBm, providing more than 11 dB of dynamic range on the power detector (rated for -30 dBm at 1310 nm).

In our experimental arrangement, and when operating above LRSPP cutoff, the biosensing region is defined by the area of the Au stripe exposed in the fluidic channel, shown in Fig. 1(a) [8]. On die C53B1310 the sensing area is 5 μm wide by 1.6 mm long. The probing depth of LRSPPs is about 2 μm [1], which is about 5× larger than conventional SPR.

2.1.3 The chemical fluid injection sub-system

A bacteriological control area is delimited by all components of the fluidic circuit. A closed fluid circuit starts from an input syringe, followed by a 50 cm long segment of Pico tubing (IDEX 550 μm outer dia., 250 μm inner dia.), inserted into the syringe end. The other end of the input tubing was glued to a hole in a Plexiglas cover bearing an O-ring to seal the fluidic channel of the test device. A similar segment of output tubing was glued to another hole in the cover and returns from the cover to the stainless steel needle at the end of the output syringe. A hermetically-sealed connection is obtained by gluing the tubing inside the needle and wrapping it with tape. The output syringe completes the fluidic circuit. The piston of the output syringe is fixed into a syringe pump to precisely control the rate of flow. The syringe pump (PicoPlus, Harvard Apparatus) and associated syringes where located on a shelf 30 cm above the optical setup. Injection of fluid was normally done by pulling during experimental runs, and pushing to prime the line or clear an air bubble from the fluid circuit.

2.1.4 The mechanical alignment and anti-vibration sub-system

The mechanical sub-system was integrated from commercial components. Two multi-axis positioning stages were used to align the laser beam, one out of a polarized fiber and one out of the test device providing precise alignment accuracy and stability. For the fiber-to-waveguide alignment, a 6-axis stage was used to manipulate the fiber holder with the fiber. For test device alignment, a 3-axis stage to manipulate the fluidic

jig assembly was used. Alignment was performed just before time zero and all of the positioner actuators were fixed for the duration of the experiment.

2.1.4.1 End-fire coupling LRSPP Waveguide biosensor

End-fire coupling, also referred to as butt-coupling, refers to the means of excitation of the LRSPP waveguide mode on the Au strip line embedded in CYTOP. Excitation of the LRSPP mode is obtained from the precise alignment of a vertically polarized optical fiber with the edge of the device as shown in Figure 17 [6]. Index matching fluid can be used to minimise the insertion loss through the air gap at the interface. On the other hand, an index matching fluid will evaporate over time and can eventually cause a variation of the insertion loss in the setup. More precise alignment is necessary when not using index matching fluid but long term stability is then obtained. Consideration must also be given to the polarisation of the light inside the optical fibre. Figure 17 [6] shows the LRSPP output at various excitation polarisation angles indicating that the best coupling is obtained for 0º of polarisation (or a transverse magnetic incident mode). In addition to polarisation alignment, precise alignment in azimuth, elevation, lateral motion (X), vertical motion (Y) and proximity (Z) must be obtained to minimize the coupling loss at the interface and obtain long term stability of the optical signal at the detector. Vibration at this interface will cause fluctuation of the detected signal therefore reducing the sensitivity of the detectable signal.

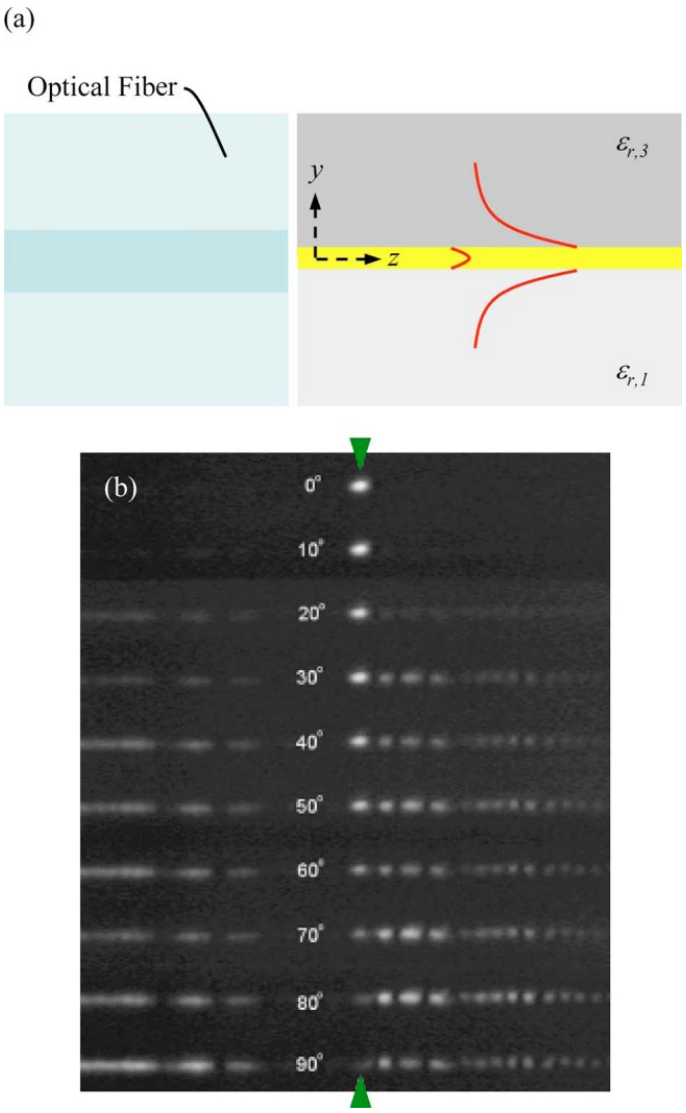

Figure 17 a) Optical fiber butt coupled to the input of the metal stripe exciting the LRSPP waveguide mode (the mode transverse magnetic field intensity is sketched in red). b) Images of output mode as a function of the angles of incident polarisation, 0° (TM polarization) [6] © 2000 Optical Society of America.

From a practical perspective, alignment of the laser beam is first performed through a polariser and the orientation of the optical fiber changed to maximize the power with the polariser set at 0º and then fine tuning by rotating the polariser at 90º and minimising the detected optical power. Then, the silicon die is inserted in the test system and the polarizer is removed. We precisely align the beam perpendicular to the die in elevation and azimuth. For that purpose, the aperture located after the 25x objective is mostly closed. The laser beam out of the fiber is aligned through the silicon portion of the die in azimuth, elevation,

horizontal motion, vertical motion and proximity to the die until we get the maximum power at the power detector. This process ensures the fiber azimuth and elevation is perpendicular to the dye surface. Finally, one cladded waveguide from the die is aligned in horizontal, vertical and proximity into the laser beam. The purity of the detected mode on the IR camera is used to fine tune the position of the die into the laser beam coming from the fiber. The output lens and other optical components are all fixed as they were previously aligned with the laser.

2.1.5 The data acquisition and analysis sub-system

A personal computer is interfaced to other electronic components for control and data acquisition. The list of equipment used is summarized in section 2.2, subsection 2.8. Of the equipment listed, only the infrared camera and the optical power detector are interfaced to the laptop for data capture. Pictures and video from the IR camera are recorded to report on the quality of the optical mode at the output of the LRSPP waveguide biosensor. The power detector samples 100 times per second and the average of those sampled is stored in a text files for future analysis and creation of the sensorgram.

2.2 Paper submitted to Biomedical Optics Express

My Contribution: The paper in this section was published by Biomedical Optics Express. I performed all laboratory measurements and wrote the first draft of the paper. The functionalization protocol used came from O. Krupin. Dr. Berini directed the work and edited the paper.

Preamble: The selective detection of gram positive and gram negative bacteria in urine using the LRSPP waveguide biosensor is demonstrated and discussed to determine its usability for the diagnostic of urinary tract infection. The publication also reports comparative measurement of urine refractive index between a precision refractometer and the LRSPP waveguide biosensor. Hence our experimentation reveals that the LRSPP waveguide biosensor is capable of clinical measurement like specific gravity and bacteriuria.

Selective detection of bacteria in urine with a long-range surface plasmon waveguide biosensor

Paul Béland[1], Oleksiy Krupin[2], and Pierre Berini[3,4,5,*]

[1] *Dept. of Biomedical Engineering, University of Ottawa, 161 Louis Pasteur, Ottawa, K1N 6N5, Canada*
[2] *Dept. of Biological and Chemical Engineering, University of Ottawa, 161 Louis Pasteur, Ottawa, K1N 6N5, Canada*
[3] *School of Electrical Engineering and Computer Science, University of Ottawa, 800 King Edward Avenue, Ottawa, K1N 6N5, Canada*
[4] *Dept. of Physics, University of Ottawa, 150 Louis Pasteur, Ottawa, K1N 6N5, Canada*
[5] *Centre for Research in Photonics, University of Ottawa, 800 King Edward Avenue, Ottawa, K1N 6N5, Canada*
[*] *berini@eecs.uottawa.ca*

Abstract: Experimentation demonstrates long-range surface plasmon polariton waveguides as a useful biosensor to selectively detect gram negative or gram positive bacteria in human urine having a low concentration of constituents. The biosensor can detect bacteria at concentrations of 10^5 CFU/ml, the internationally recommended threshold for diagnostic of urinary tract infection. Using a negative control urine solution of bacterial concentration 1000× higher than the targeted bacteria, we obtain a ratio of 5.4 for the positive to negative signals.

OCIS codes: (170.0170) Medical optics and biotechnology; (170.7230) Urology; (280.1415) Biological sensing and sensors; (240.6680) Surface plasmons; (130.3120) Integrated optics devices; (230.7390) Waveguides, planar; (250.5403) Plasmonics.

References and links

1. G. Schmiemann, E. Kniehl, K. Gebhardt, M. Matejczyk, E. Hummers-Pradier "The Diagnosis of Urinary Tract Infection: A Systematic Review," Dtsch. Arztebl. Int. **107**, 361–367 (2010).
2. J. A. Simerville, W. C. Maxted, and J. J. Pahira, "Urinalysis: a comprehensive review," Am. Fam. Physician **71**, 1153–1162 (2005).
3. M. A. Broeren, S. Bahceci, H. L. Vader, N. L. Arents "Screening for urinary tract infection with the Sysmex UF-1000i urine flow cytometer," J. Clin. Microbiol. **49,** 1025–1029 (2011).
4. M. Marschal, M. Wienke, S. Hoering, I. B. Autenrieth, J.-S. Frick, "Evaluation of 3 different rapid automated systems for diagnosis of urinary tract infection," Diagn. Microbiol. Infect. Dis. **72,** 125–130 (2012).
5. J. Wang, Y. Zhang, D. Xu, W. Shao, and Y. Lu, "Evaluation of the Sysmex UF-1000i for the Diagnosis of Urinary Tract Infection," Am. J. Clin. Pathol. **133**, 577–582 (2010).
6. M. A. Van Dilla, R. G. Langlois, D. Pinkel, *et al.* "Bacterial characterization by flow cytometry," Science **220,** 620-622 (1983).
7. B. Liedberg, C. Nylander, and I. Lundstrom, "Surface plasmon resonance for gas detection and biosensing," Sens. Act. **4**, 299–304 (1983).
8. M. Vala, S. Etheridge, J. Roach, and J. Homola, "Long-range surface plasmons for sensitive detection of bacterial analytes," Sens. Act. B **139**, 59-63 (2009).
9. V. Chabot, Y. Miron, M. Grandbois, and P. G. Charette, "Long range surface plasmon resonance for increased sensitivity in living cell biosensing through greater probing depth," Sens. Act. B **174**, 94-101 (2012).
10. P. Berini, "Long-range surface plasmon polaritons," Adv. Opt. Phot. **1**, 484–588 (2009).
11. Ö. Torun, İ. H. Boyac, E. Temür, and U. Tamer, "Comparison of sensing strategies in SPR biosensor for rapid and sensitive enumeration of bacteria," Biosens. Bioelectr. **37**, 53-60 (2012).
12. P. M. Fratamico, T. R. Strobaugh, M. B. Medina, and A. G. Gehring, "Detection of *Escherichia coli* O157:H7 using a surface plasmon resonance biosensor," Biotechnol. Techn. **12,** 571-576 (1998).
13. J. Trevino, A. Calle, J. M. Rodríguez-Fraded, M. Melladod, L. M. Lechuga, "Single- and multi-analyte determination of gonadotropic hormones in urine by Surface Plasmon Resonance immunoassay," Anal. Chim. Acta **647**, 202–209 (2009).
14. W. R. Wong, O. Krupin, S. D. Sekaran, F. R. M. Adikan, and P. Berini, "Serological Diagnosis of Dengue Infection in Blood Plasma Using Long-Range Surface Plasmon Waveguides," Anal. Chem. **86**, 1735−1743 (2014).
15. C. Chiu, E. Lisicka-Skrzek, R. N. Tait, and P. Berini, "Fabrication of Surface Plasmon Waveguides and Devices in Cytop with Integrated Microfluidic Channels," J. Vac. Sci. Technol. B **28**, 729−735 (2010).
16. S. Hassan, M. Khodami, R. N. Tait, and P. Berini, "Fabrication of long-range surface plasmon-polariton Bragg gratings with microfluidic channels in Cytop claddings," Microelectr. Eng. **135**, 38–44 (2015).
17. O. Krupin, H. Asiri, C. Wang, R. N. Tait, and P. Berini, "Biosensing using straight long-range surface plasmon waveguides," Opt. Express **21**, 698-709 (2013).

18. ethics@uottawa.ca, Bureau d'éthique et d'intégrité à la recherche, 75 Laurier Avenue East, Université d`Ottawa, K1N 6N5, numéro dossier H06-14-01, 23 juin 2014 (personal communication, 2014).

19. I. Breukelaar, R. Charbonneau, and P. Berini, "Long-range surface plasmon-polariton mode cutoff and radiation in embedded strip waveguides," J. Appl. Phys. **100**, 43–104 (2006).

20. D. F. Putnam "Composition and concentrative properties of human urine," Prepared by McDonnell Douglas Astronautics company – western division, Huntington Beach, Calif. 92647, Contractor Report NASA CR-1802, (1971).

21. W. R. Wong, O. Krupin, F. R, M. Adikan, and P. Berini, "Optimization of long-range surface plasmon waveguides for attenuation-based biosensing," J. Lightwave Technol. (in press).

22. X. Su and J. Zhang, "Comparison of surface plasmon resonance spectroscopy and quartz crystal microbalance for human IgE quantification," Sens. Act. B, **100**, 309-319 (2004).

23. R. F. Dutra, R. K. Mendes, V. Lins da Silva, and L. T. Kubota, "Surface plasmon resonance immunosensor for human cardiac troponin T based on self-assembled monolayer," J. Pharm. Biomed. Anal **43**, 1744–1750 (2007).

1. Introduction

The gold standard for the diagnosis of Urinary Tract Infection (UTI) is the detection of pathogen along with the presence of clinical symptoms. The best detection and identification of the pathogen remains the culturing of patient urine sample [1]. This technique provides very good selectivity of the pathogen and superior sensitivity but requires 24 to 48 hours in a microbiology laboratory environment. Nitrite dipsticks provide results in less than one hour but cannot detect organisms which are unable to reduce nitrate to nitrite [2]. In addition, dipsticks have poor sensitivity especially with diluted urine or low colony count samples. In the labeled biosensing category, flow cytometry is a family of automated systems providing results in less than one minute for detection levels below 10^5 CFU/ml [27-29]. Selectivity in flow cytometry can be obtained by double staining with fluorescent dyes [30]. However, fluorescence detection requires labeling by well-trained personnel, which can add several hours to perform the detection. Here we investigate the ability of a label-free long-range surface plasmon polariton (LRSPP) waveguide biosensor to detect and identify bacteria as gram positive or gram negative species in human urine samples. Experimental results demonstrate the performance of the sensor, from which we define a protocol supporting the diagnostic of UTI.

Label-free biosensors such as surface plasmon resonance (SPR) [7], LRSPP resonance [8,9] and LRSPP waveguides [10] can provide detection of bacteria in clean fluids [8,11,12]. They are capable of detection selectivity similar to enzyme-linked immunosorbent assay (ELISA). Thus, they have the potential, in principle, to improve clinical diagnosis [13,14] of many diseases if conclusive detection in complex human fluids such as blood serum and urine can be achieved. We demonstrate here that this is possible using a simple non-specific binding mitigation strategy and by careful comparison with negative controls.

Here we use a surface functionalized with antibody to selectively capture target bacteria on the LRSPP waveguide. Test devices are manufactured in a wafer-based fabrication process [15,16] and are interrogated by a laser-based test system [17]. Injecting the content of syringes in the fluidic channel of the test device, the biosensing area is exposed to attachment chemistries then antibodies to functionalize the surface in preparation for a test. The test fluid containing the target or control bacteria is then injected. If present at a high enough concentration, the target bacteria is selectively adsorbed by the antibody, disrupting the LRSPP mode propagation. By measuring and analyzing the optical response of the waveguide with a power detector and an infrared camera, we establish the presence of the target bacteria.

2. Materials and methods

2.1 Chemical and biochemical reagents:

Our labeling convention to identify solutions prepared is to use an acronym with a date in the format: AAAAmmdd, where AAAA is the biochemical acronym; mm is the month and dd is the day of creation. A complete list of the labeled solutions and preparation protocols used in experimentation can be found in Table 3 of Appendix A. Unless stated differently, all chemicals were acquired from Sigma-Aldrich. Chemicals used includes: distilled deionized water (DIH2O) from a Barnstead™ Nanopure™ system D11931. Phosphate buffered saline (PBS, 0.01 M, pH 7.4), sodium dodecyl sulfate (SDS)(71725-50G), 2-isopropanol semiconductor grade (IPA), acetone HPLC grade ≥ 99.9%, heptane, glycerol (electrophoresis grade), LB broth (Lennox), PBS Glycerol (PBSG) solutions were filtered through Millex-GP filters (PES membrane 0.22 μm). Labeled fluids Gprot (P4689-1MG): protein G (50 μg/ml) dissolved in PBSG0715 and used to functionalize the bare gold surface of a waveguide. Labeled fluids GNeg (AB41202): gram negative antibody (50 μg/ml) in PBSG0715 buffer solutions. Labeled fluids GPos (AB20344): gram positive antibodies (50 μg/ml) diluted in PBS. Labeled fluids BSA (A0281-250): bovine serum albumin (100 μg/ml) dissolved in PBSG. Labeled fluids Urine: A human urine sample was collected from the donor on the day of experimentation [18]. All urine samples were centrifuged at 3000 rpm for 7 min and the supernatant filtered through Millex-GP filters. Labeled fluids EColi: *Escherichia coli XL1 Blue* were donated by the Canadian Blood Services (CBS). Labeled fluid SEPI: *Staphylococcus epidermidis ATCC 12228* bacteria were donated by the CBS. Inoculation of bacteria into LB Broth was done aseptically (CAREG laboratory of uOttawa). Weekly cultures of the bacteria were grown in 10 ml vials and incubated at 37º C.

The cultured bacteria were centrifuged at 3000 RPM for 7 min and the supernatant removed with a syringe and replaced with a PBS, PBSG or urine test solution as required by the specific experiment.

2.3 Biosensor fabrication:

The biosensors were fabricated by cladding a Au stripe, 5 µm wide and 35 nm thick, with top and bottom CYTOP layers, each 8 µm thick, on a 4-inch Si wafer. Au evaporation and lift-off were used to define the Au features using an optical lithography technique. The top CYTOP cladding was etched down to the Au stripe surface to form a large fluidic channel of sensing length L = 1.65 mm. The Au stripe is on a CYTOP pedestal of height ~ 400 nm created by over-etching the fluidic channels. A thick layer of photoresist was deposited onto the wafer before it was sent for dicing into ~300 dies per wafer. The detailed fabrication process of the sensors was described in previous work [15,16]. A microscope image under 50× magnification of a portion of a die after experimentation is shown in Fig. 1(a). The sensor dies utilized originated from wafer 4D1-A reticule C53B1310, and were 3.8 mm long by 6.4 mm wide. Each die had several straight uniform Au waveguides, 5 µm wide and 35 nm thick, of which stripes 9 and 13 were mostly used for sensing experiments as they are located in the centre of the fluidic channels. Stripe 10 was also used for sensing experiments, as a failed (unresolved) step-in-width grating which is mostly uniform and centrally located within the fluidic channel. Stripes 1, 3 and 21 are fully cladded and were used for alignment trials and waveguide quality checks.

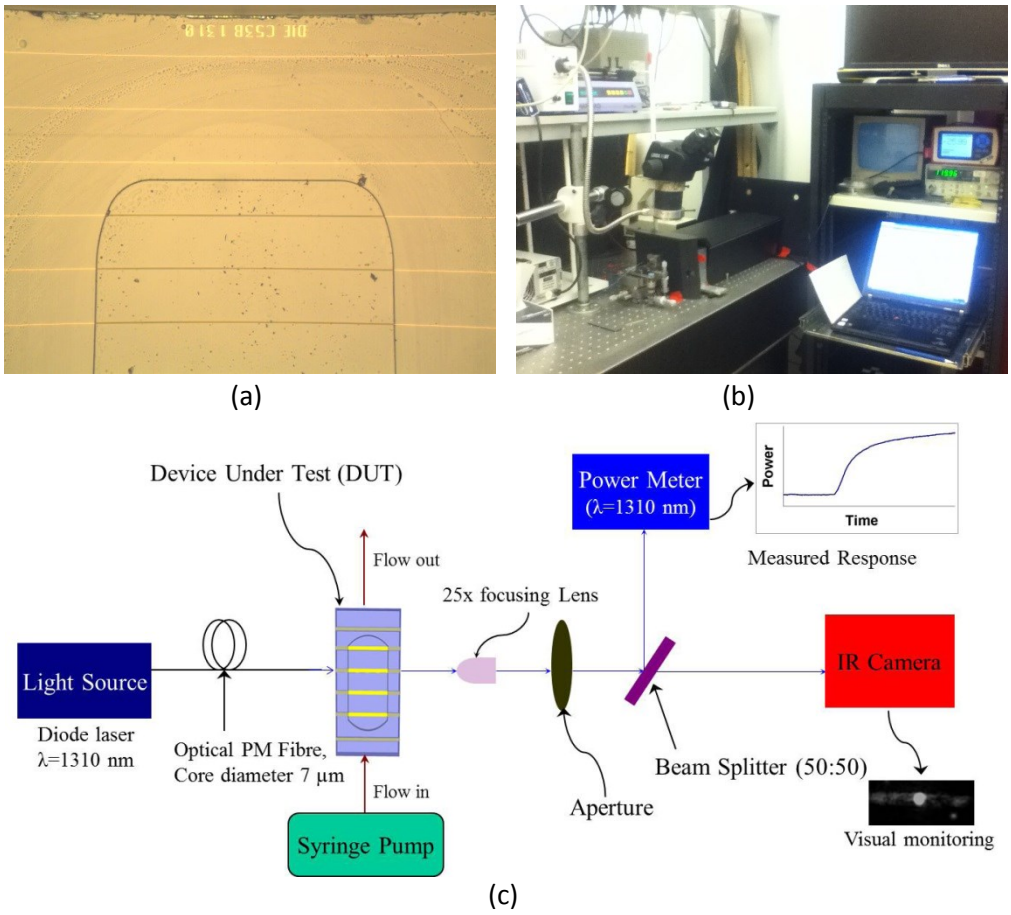

Fig. 1 (a) Microscope image at 50× magnification of the top portion of die C53B1310 after use. (b) Photograph of the interrogation system. (c) Block diagram of the LRSPP waveguide biosensor interrogation system [©2013 Optical Society of America; adapted from [17].

2.4 Die cleaning process:

To ensure the cleanliness of the waveguide facets for efficient optical input and output coupling, a fresh sensor die was cleaned by ultra-sonication (FB-11201, Fisher Scientific) in heptane for 5 min to remove any possible debris formed during dicing of the wafer. The sensor die was then left immersed in two sequential acetone baths for 5 and 30 min, respectively, to completely remove the dicing photoresist. After a thorough washing in IPA and drying with nitrogen gas (N_2), the sensor die was placed in a digital UV ozone system (PSD-UV-4, Novascan) to remove any possible organic matter from the Au surface. The die was then washed intensely with IPA and distilled/de-ionized water (DDI H_2O), followed by Nitrogen (N_2) drying. Cleaned sensor die assembled in the test jig were all primed with DDI H_2O before assembly onto the test system.

2.5 Surface functionalization process:

Once inserted into the test system, the surface of a Au stripe was functionalized by injecting GProt solution for 20 min at a rate of 20 µL/min. Following this step, and for a gram negative selective surface, Gneg was injected for 10 min at a rate of 20 µL/min followed by stop flow for 80 min which results in the formation of a monolayer of gram negative antibody. For a gram positive selective surface, GPos was injected for 10 min at a rate of 20 µL/min followed by stop flow for 80 min which results in the formation of a monolayer of gram positive antibody. In both cases, we complete the functionalization by injecting BSA for 5 min at a rate of 20 µL/min. BSA injection was selected as a simple non-specific binding mitigation strategy, as BSA would block open adsorption sites without interfering with the monolayer of antibody. Generally however, a flat sensorgram response was observed during BSA injection, indicating low vulnerability to non-specific binding and valid surface functionalization.

Upon completion of experimental runs, which could last up to 36 hrs (2160 min), the Au surface of the sensor die was discarded or fully regenerated. The regeneration process starts by flowing 2 ml of SDS then 2 ml of DIH20. The die is then removed from the jig and deposited in a vial of SDS for periods of 24 to 96 hours to dissolve the lipopolysaccharide membrane of the bacteria. The die is further cleaned by rinsing and depositing in vials with Acetone, IPA and DIH2O to remove debris. Nitrogen gas (N_2) is used to dry the surface and a microscope inspection provides necessary quality control. The regenerated surface of a sensor die is then placed in a UV/ozone chamber before starting a new experimental run. Measurement of the optical insertion loss with a RI-controlled fluid after cleaning was used as a quality measure before re-using a die in a new experimental run.

2.7 Mechanical test system:

A block diagram of the test system is shown in Fig. 1(b). It was integrated from commercial components. A bacteriological control area is delimited by all components of the fluidic circuit. A closed fluid circuit starts from an input syringe, followed by a 50 cm long segment of Pico tubing (IDEX 550 µm outer dia., 250 µm inner dia.), inserted into the syringe end. The other end of the input tubing was glued to a hole in a Plexiglas cover bearing an o-ring to seal the fluidic channel of the test device. A similar segment of output tubing was glued to another hole in the cover and returns from the cover to the stainless steel needle at the end of the output syringe. A hermetically-sealed connection is obtained by gluing the tubing inside the needle and wrapping it with tape. The output syringe completes the fluidic circuit. The piston of the output syringe is fixed into a syringe pump to precisely control the rate of flow. The syringe pump (PicoPlus, Harvard Apparatus) and associated syringes where located on a shelf 30 cm above the optical setup. Injection of fluid was normally done by pulling during experimental runs, and pushing to prime the line or clear an air bubble from the fluidic circuit.

Two multi-axis positioning stages were used to align the laser beam, one out of a polarized fiber and one out of the test device, providing precise alignment accuracy and stability. For the fiber-to-waveguide alignment, a 6-axis stage was used to manipulate the fiber holder and fiber. For test device alignment, a 3-axis stage to manipulate the fluidic jig assembly was used. Alignment was performed just before time zero and all of the positioner actuators were fixed for the duration of the experiment.

2.8 Optical test system:

All Optical components were fixed onto an anti-vibration table. The light source was a PM-fiber pigtailed laser diode (NLK1B5GAAA, NEL) in a laser mount (LDM-4980, ILX) controlled by current and temperature controller (LDX3220, ILX) delivering 14.5 dBm of output power at a free-space optical wavelength of 1310 nm with a set current of 120 mA and a set temperature of 30º C. A set current of 50 mA (delivering 11.1 dBm) is sometime used. The optical PM fiber (PMJ-3S3A-1300-7/125-1-1-1, OZ Optics Ltd.) used to excite a sensor was 0.5 m long, cleaved and fixed into a fiber holder. A 25× optical lens (25/0.50, Melles Griot) was used to focus the output light onto an optical sensor (S144C, Thorlabs) connected to a power meter (PM100, Thorlabs). An optical aperture was used during alignment of the laser beam and to reduce the power detected at the sensor due to background light. An optical beam splitter (BSW29, Thorlabs) was used to split the output beam in order to provide an image of the mode on an IR camera (Micronviewer 7290A, electrophysics). Without a sensor in the set-up, the detected power was typically 7.9 dBm. Thus, we estimate the loss through the cleaved optical fiber, lens, aperture and beam splitter to be 6.6 dB, of which 5 dB comes from the beam splitter at the set angle. The typical insertion loss of a 3.8 mm long cladded waveguide was measured to be 27 dB. Thus the maximum output power that we can obtain with a LRSPP waveguide biosensor in the set-up is about -19.1 dBm, providing more than 11 dB of dynamic range on the power detector (rated for -30 dBm at 1310 nm).

In our experimental arrangement, and when operating above LRSPP cutoff, the biosensing region is defined by the area of the Au stripe exposed in the fluidic channel, shown in Fig. 1(a). On die C53B1310 the sensing area is 5 µm wide by 1.6 mm long. The probing depth of LRSPPs is about 2 µm [17], which is about 5× larger than conventional SPR.

3. Bulk sensing of urine with an LRSPP waveguide

The response of LRSPP waveguide biosensors due to directly injecting human urine is shown in Fig. 2. A bare Au surface was used in Fig. 2(a) whereas a gram negative antibody on protein G surface was used in Fig. 2(b). These two surface functionalizations could be used for different urinalysis experimentation (as will be shown later). Four water-based solutions, namely PBSG0715, Urine0820A, Urine0820B and water, of varying refractive index (RI), were injected in sequence. Considering

LRSPP mode cutoff and radiation [19], we expect a reduction in output power as the difference between the RI of CYTOP and that of the solution increases, because the RI asymmetry between the top and bottom claddings of the waveguide increases. The images of the output mode, shown as insets to Fig. 2, confirm excitation of the LRSPP mode for all solutions except pure water (DIH2O) which has a RI 15.1 mRIU below that of CYTOP. With a large RI asymmetry in the top (test fluid) and bottom (CYTOP) claddings, the LRSPP mode becomes cut-off, and propagation occurs in the form of radiative modes that leak into the higher RI cladding. but that may still exhibit localization near the metal stripe [19]. The output observed for the case of DIH2O consists essentially of background optical energy with the LRSPP not being evident. Note that on the IR camera, the output is magnified by 25× and is limited in diameter by the aperture.

The RI of each test solution used was measured at 1310 nm using a refractometer (Model 2010, Metricon, Prism 200-P1). The RI of urine varies depending on the concentration of its constituents. The major constituents of urine are water (H_2O), Urea (H_2NCONH_2), chloride (Cl^-), sodium (Na^+) and potassium (K^+), and it has been shown that the RI of urine varies linearly with the solute weight fraction [20]. Fig. 2(a) confirms that urine of lower constituent concentration (Urine0820B, RI = 1.32798) generates a lower output power than urine of higher constituent concentration (Urine0820A, RI = 1.32991). Both urines have a RI that is lower than that of CYTOP (1.3346), so the higher-index solution brings the waveguide closer to symmetry thus reducing its insertion loss and producing a higher output power [21].

We sometimes note in Fig. 2(b) a slope or binding curve at the transition between 2 fluids. With more careful observation, we note that PBSG and urine may interact if we don`t separate their injection with DIH2O or urine in low concentration. It is unclear at this time which urine constituent causes the interaction but always separating the injection of both solutions with DIH2O seems to reduce the effect and provides repeatable absolute power levels and faster settling to a stable response. Even if all fluids were filtered with a 0.2 μm syringe filters, we suspect that Urine0820A still includes large particles causing sudden variations of power. Unlike other experimentation, the test urines Urine0820A and Urine0820B were not centrifuged before filtering.

In Fig. 2(a) we note a 0.2 dB drop in output power for PBSG0715 at 45 min compared to the level at 20 min. We think that proteins contained in urine may have adsorbed on the bare Au surface. This is not seen in Fig. 2(b) probably because the gold surface was already functionalized with protein G and a gram negative antibody.

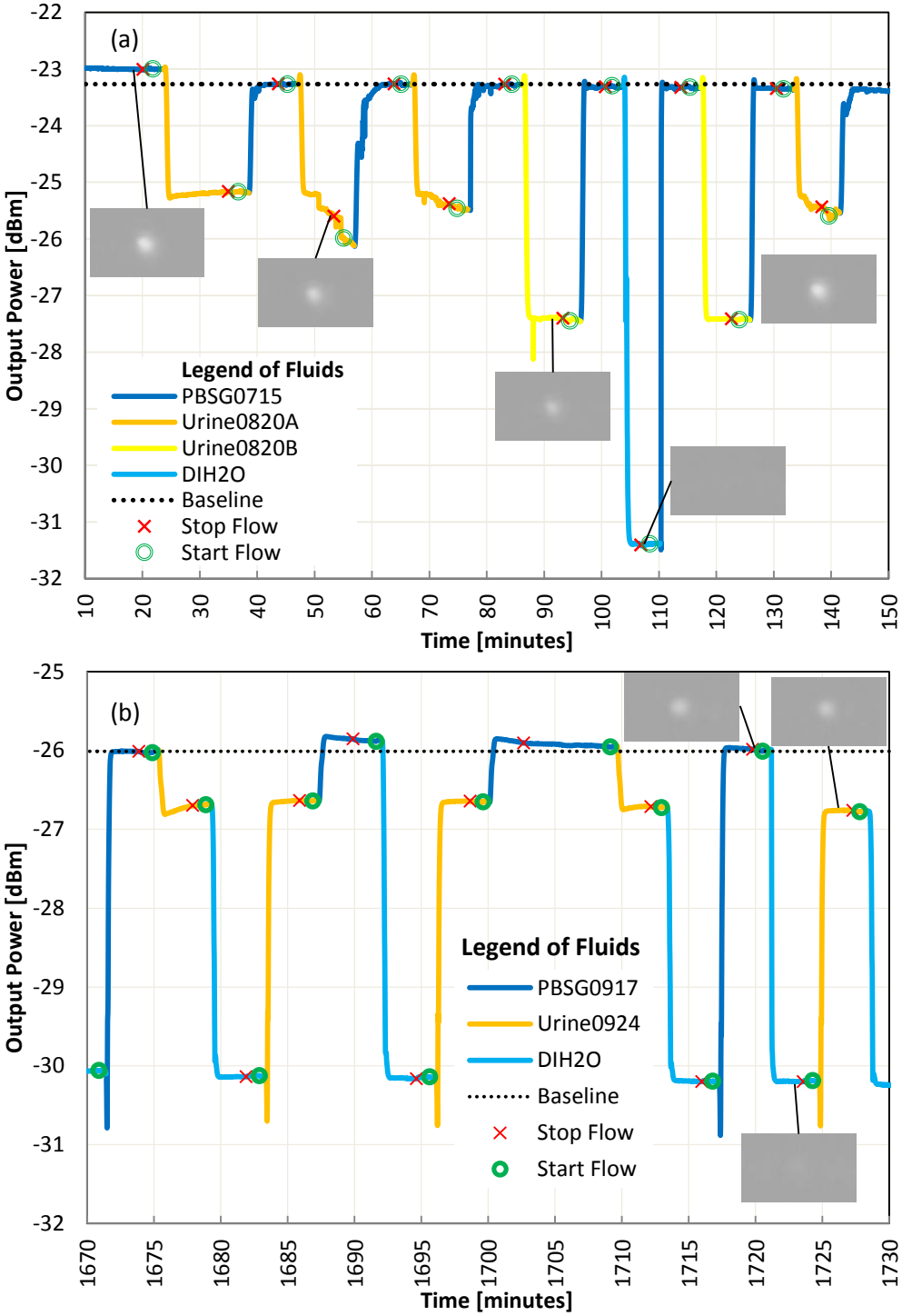

Fig. 2. (a) Bulk sensing of high concentration and low concentration urine, flow rate = 20 µl/min, laser power = 14.5 dBm, Die C53B1310 first cleaned on 07 Aug 2014. No functionalization (bare Au surface). (b) Use of DIH2O to separate urine from PBSG, flow = 80 µl/min, laser power = 11.1 dBm, Die C53B1310 first cleaned on 23 sept 2015. Surface functionalized with gram negative antibody on protein G.

The urine RI at 1310 nm is close enough to the RI of CYTOP for the waveguide to support a bound LRSPP mode of propagation, thus enabling biosensing applications in urine. Care must be taken in analyzing results when the RI of the sample becomes close to that of water because the detected power is no longer dominated by the LRSPP mode. In such cases, the sensitivity is reduced but the output remains related to biological material on the sensing area due to the propagation of radiative modes. Bulk sensing could be used to monitor the aggregate concentration of constituents in urine after proper calibration.

4. Selective bacteria detection

4.1 Gram negative bacteria detection

In order to demonstrate the selective detection of gram negative bacteria in urine, we prepared test solutions with freshly grown gram positive and gram negative bacteria. The first experiment was conducted in a clean PBSG solution and the second experiment was conducted in a urine solution. A PBS solution with heat killed bacteria was also used.

In Fig. 3(a) we demonstrate the selective detection of gram negative bacteria in PBSG. A sensor die was first functionalized with protein G and gram negative antibody as previously described (not shown in the response). A BSA solution was first injected for 5 min to confirm the quality of the Au surface functionalization (no adsorption is observed). The solution containing gram positive bacteria was then injected as a negative control. To ensure contact between bacteria and the functionalized surface, we stop the flow to allow the bacteria to sink onto the biosensing area. Re-starting the flow returns the signal to within 0.09 μW of the baseline signal (*i.e.*, Pt(292) - Pt(309) = 0.09 μW, where Pt stands for power at the observed time t in parentheses). We then inject the solution with gram negative bacteria and stop the flow again. This time the power drops by 1.18 μW (Pt(309) - Pt(336) = 1.18 μW) indicating adsorption of the bacteria by the antibody on the waveguide surface. Defining a positive-to-negative ratio (P/N) as the ratio of the difference of these powers, we obtain P/N = 13.1. A threshold of $P/N \geq 2$ could be used as a decision threshold for the selective detection of the bacteria. In addition, we show that by flowing 0.5% SDS solution for 15 min, the antibody-antigen link is broken [22, 23], the bacteria are washed away from the biosensing area, and the baseline is recovered (in this case to within 0.05 μW).

In Fig. 3(b) we injected heat killed gram negative bacteria in a PBS solution (HKECO1001). The large signal change between the PBSG0917 (RI = 1.3285) and the HKECO1001 (RI = 1.3235) signal is mainly caused by a bulk change in RI between the solutions. At time 145 min, we note a small perturbation (0.2 dB) in signal as the heat killed bacteria fall onto the biosensing area. A fluidic limitation is observed after 160 min in Fig. 3(b): After approximately 10 min without flow, our stable signal becomes noisy; we speculate that, even if we had been injecting a bacteria-free solution for 5 min, some bacteria from the tubing have back-flowed onto the biosensing area. Regardless of the cause, we avoid stopping the flow for more than 10 min in subsequent experimentation. We observe recovery of the signal to essentially the baseline level at 240 min after removing the air bubbles.

UTI diagnostic by culture provides a count of living colony. With LRSPP waveguide biosensors, it is interesting to note differences in signals when using live or dead bacteria. In Fig. 3(b) with heat killed bacteria little adsorption was observed as indicated by recovery of the signal power after exposing the waveguide to heat killed bacteria. In the following experimental sequence (not shown), heat killed bacteria in urine were injected and adsorbtion was observed by a drop of power of 0.44 μW. We suspect that duration of the stop flow, which was 5 min with PBS and 6 min with urine, is a control parameter that needs to be adjusted based on the concentration of constituents in the fluid because it affects the fluid density. Changes in the density of the fluid will affect the buoyancy of a given bacteria directly affecting the time required for a bacteria to contact the surface. Consideration of the kinetics of the antibody antigen adsorption may also be necessary in selecting the duration of the stop flow. Finally, we also note that with heat killed bacteria the signal is stable once a clean fluid replaces the solution with bacteria, as observed in Fig. 3(b) at 149 min. In

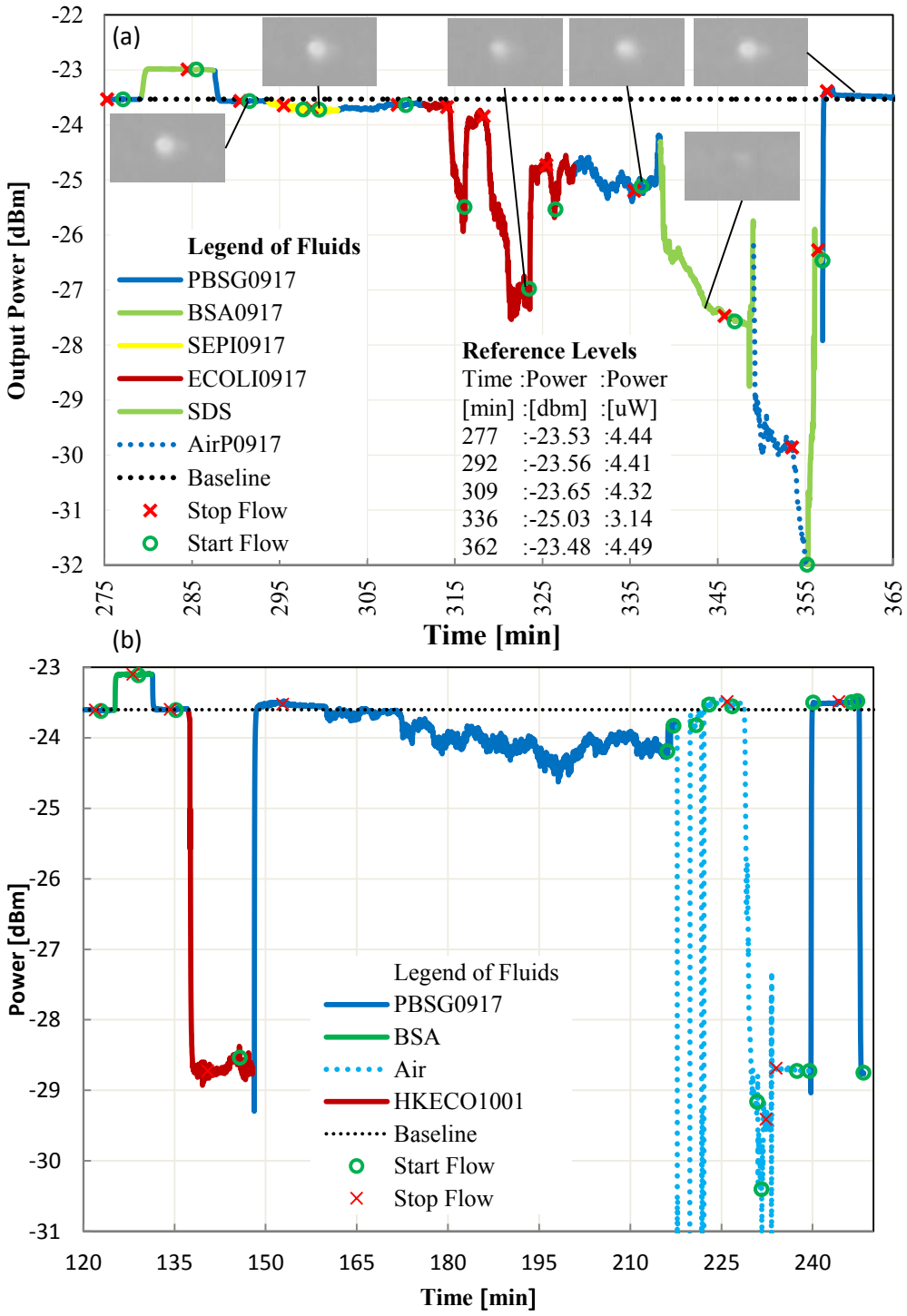

Fig. 3. (a) Live *E.coli* detection in PBSG, flow = 20 µl/min, laser power = 14.5 dBm, gram negative antibody surface, bacteria growth time of 4.3 hours in LB Broth. (b) Dead *E.coli* detection in PBSG, flow = 20 µl/min, laser power = 14.5 dBm, gram negative antibody surface.

contrast, to live bacteria in Fig. 3(a), at 330 min a noisy signal is observed. Further study of this difference may prove useful to identify live *vs* dead bacteria.

In Fig. 4, the sensor die was also functionalized with protein G and gram negative antibody. We repeat the same experimentation protocol as in Fig. 3(a) but now in urine solutions. We obtain a P/N ratio of [Pt(1480)-Pt(1525)]/[Pt(1480)-Pt(1498)] = 7.5 confirming the selective detection of gram negative bacteria in urine. We also observe in Fig. 4 from 1535 to 1595 min a very noisy signal, which may be caused in part by back-flow of material onto the waveguide surface; but it is not impossible that live bacteria also contribute to the noise. Subsequent cleaning with SDS recovers the signal to the baseline level.

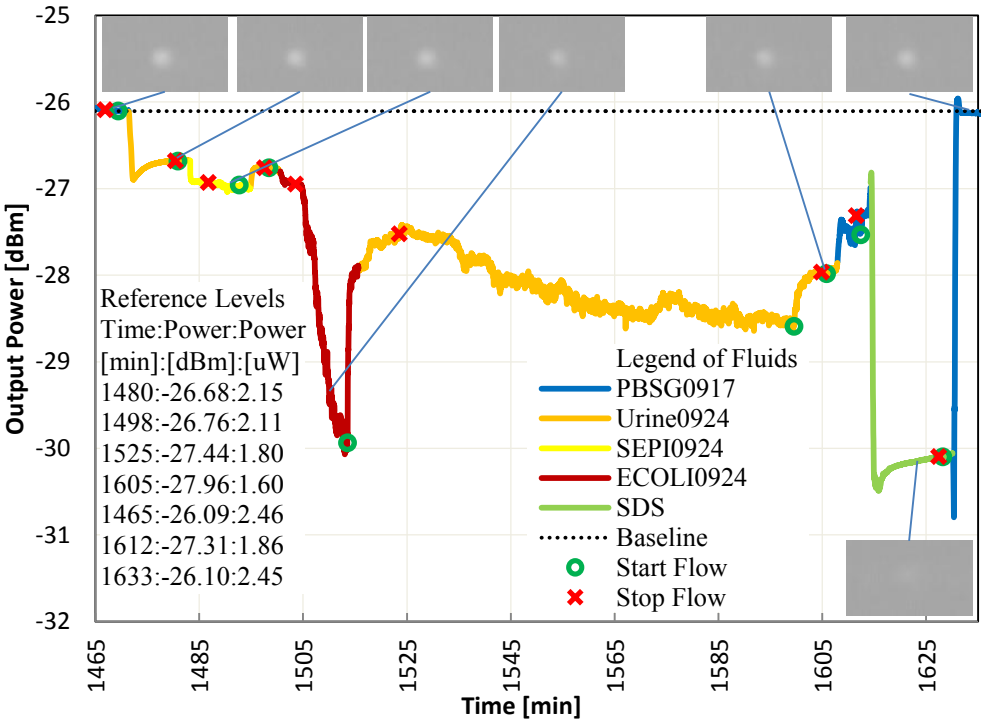

Fig. 4. Live *E.coli* detection in urine, flow = 20 µl/min, laser power = 11.1 dBm, gram negative antibody surface, bacteria growth time of 4.3 hrs in LB broth.

4.2 Gram positive bacteria detection

In order to demonstrate the detection of gram positive bacteria in urine, a sensor die was functionalized with protein G then gram positive antibody. We injected solutions with freshly grown gram negative (negative control) then gram positive bacteria in urine. Fig. 5(a) reports the results of the first experiment and Fig. 5(b) of 1 repeat of the same experiment on the following day. The high concentration of bacteria in the negative control solution causes large signal fluctuations in Fig. 5(a) during the stop flow. The signal then stabilizes at 558 min after re-starting the flow. We note that most of the signal power is recovered. The small change in power observed before and after the negative control is attributed to nonspecific binding. The gram positive bacteria solution causes a large signal change with no recovery when we re-start the flow at 578 min. Similar observations can be made relative to the repeated experiment in Fig. 5(b), where additionally the inadvertent injection of air bubbles had to be managed during the experiment. Calculating the P/N ratio for both experiments, we obtain P/N = [Pt(564)-Pt(588)]/[Pt(564)-Pt(547)] = 3.1 for Fig. 5(a) and P/N = [Pt(1229)-Pt(1246)]/[Pt(1204)- Pt(1220)] = 4.8 for Fig. 5(b). This confirms the selectivity of gram positive bacteria in urine.

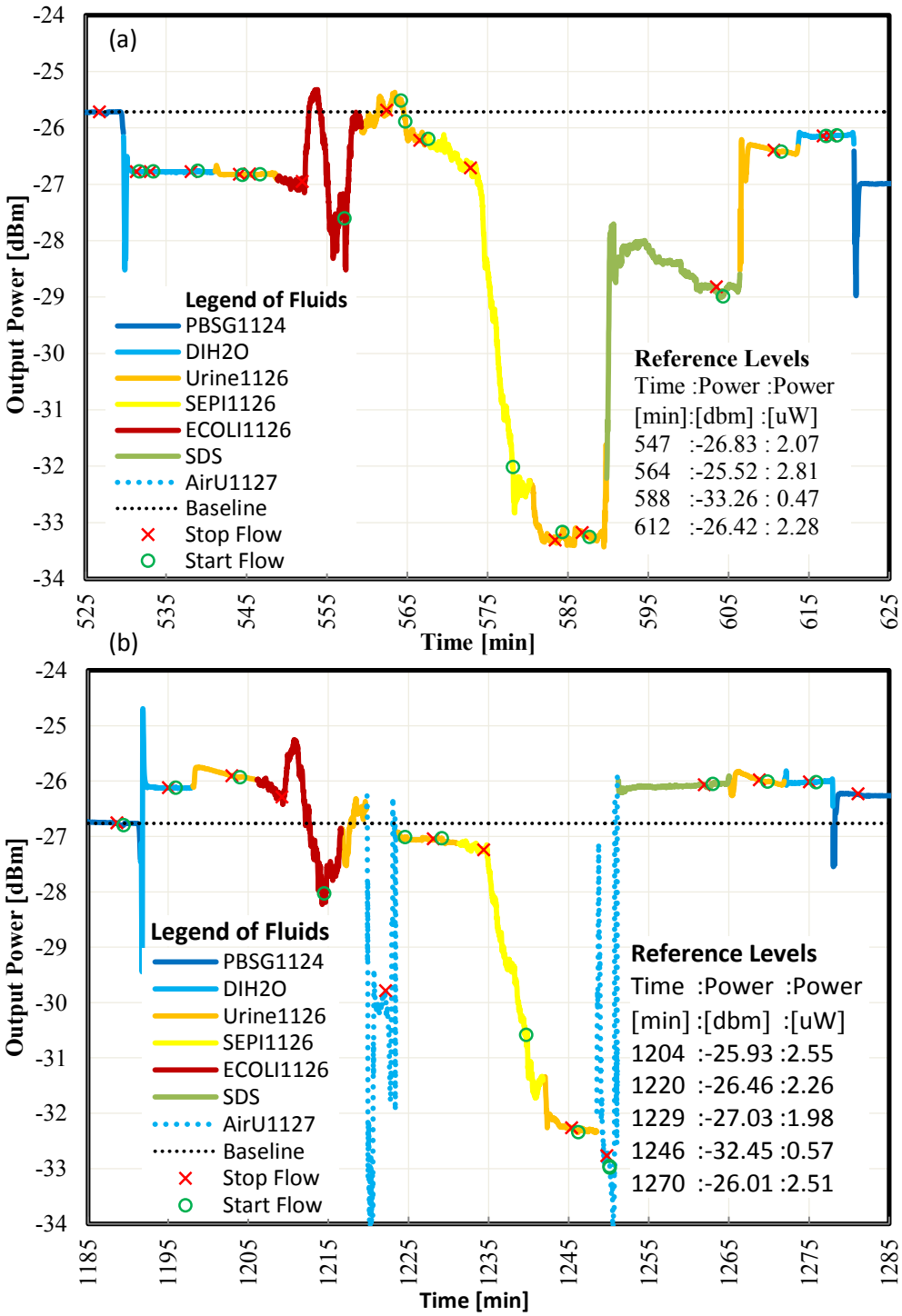

Fig. 5. (a) Live *S.epi* detection in urine, flow = 20 µl/min, laser power = 14.5 dBm, gram positive antibody surface. (b) Repeat of live *S.epi* detection in urine, flow = 20 µl/min, laser power = 14.5 dBm, gram positive antibody surface.

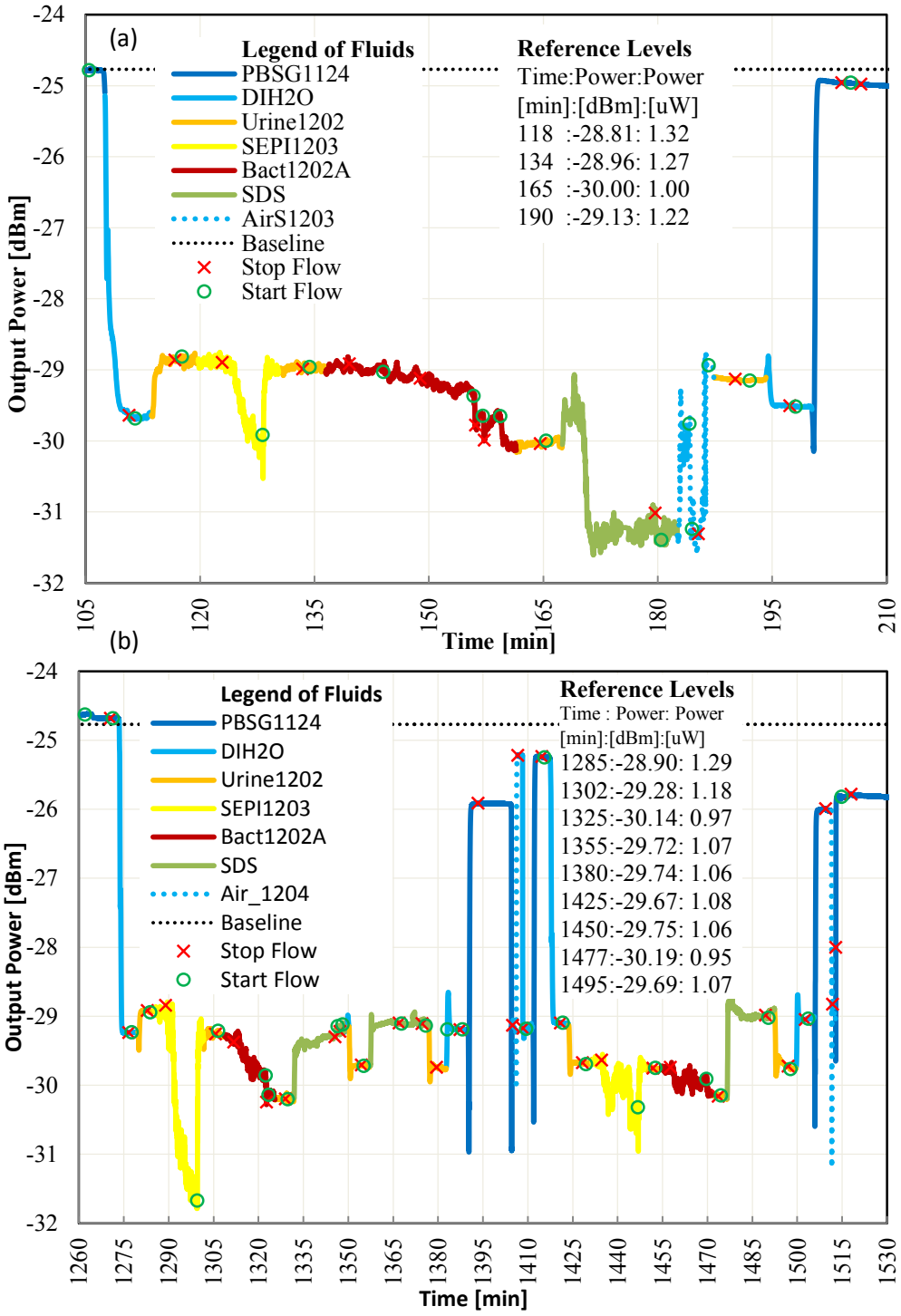

Fig. 6. a) Live gram negative bacteria detection with contamination in urine, flow = 20 µl/min, laser power = 14.5 dBm, gram negative antibody surface. b) Repeat of live gram negative bacteria detection in the presence of contamination in urine, flow = 20 µl/min, laser power = 14.5 dBm, gram negative antibody surface.

In Fig. 5(b) at 1270 and 1275 min, the same output power is measured for Urine1126 and DIH2O. From the images of the outputs on the IR camera (not shown), we noted a visible LRSPP mode for Urine1126 which was not present for DIH2O. In both images significant background radiation was present.

4.3 Gram negative bacteria detection: low bacterial concentration with contamination

In the experiments reported in Fig. 6, the device was functionalized with a gram negative antibody, and the concentration of gram positive bacteria in our negative control solution was 1000× larger than the concentration of the target gram negative bacteria in

our positive solution. Despite this, and despite the low RI of the urine used (RI = 1.32276) which is below the RI of PBSG (RI = 1.32351), we still obtain P/N = [Pt(134)-Pt(165)]/[Pt(118)-Pt(134)] = 5.4 for the first experiment (Fig. 6(a)), and P/N = [Pt(1305)-Pt(1325)]/[Pt(1305)-Pt(1285)] = 1.9 and P/N = [Pt(1450)-Pt(1477)]/[Pt(1425)-Pt(1450)] = 5.5 for the first and second repeats, respectively (Fig. 6(b)). After the experiments, a plate culture of the target gram negative bacteria (Bact1202A) revealed the presence of contaminating bacteria with lower concentration then the target.

We note that in the first repeat (Fig. 6(b)), recovery after SDS flow was good but not excellent, as a drop of 0.1μW at 190 min relative to 118 min, and a drop of 0.27μW at 1355 min relative to 1285 min, is observed. This suggests that more nonspecific binding occurred during the second repeat. In our protocol, the die surface was immersed in PBSG1124 overnight unlike the test repeat reported in Fig. 5 where the die surface was immersed in SDS overnight. A repeat of the SDS clean at min 1360 of Fig. 6(b) didn't improve the recovery of the signal power. To better clean the surface, we intentionally pushed air into the system for a few seconds improving the signal amplitude slightly (Fig. 6(b), Pt(1405) and Pt(1514)). We speculate that the surface tension of a fluid following air is effective in removing some non-specifically bound material from the biosensing area. In the second repeat, the P/N ratio improved compared to the first repeat mainly due to very little non-specific binding (Pt(1425) - Pt(1450) = 0.02 μW).

4.4: Selective bacteria detection: Summary of results

A summary of the P/N ratios demonstrating selective detection of bacteria is collected in Table 1. All of our experiments, except for the one listed in the penultimate row, produced a P/N ratio greater than 2.

Table 1. Summary of P/N ratio demonstrating selective detection of bacteria

Experimental Figure; Sequence	Test Fluid	Negative Control		Detected Bacteria		P/N
	Label	Label	Growth time [hrs]	Label	Growth time [hrs]	
Fig. 3(a);1	PBSG0917	SEPI0917	4.3	ECOLI0917	4.3	13.1
Fig. 4;1	Urine0924	SEPI0924	4.3	ECOLI0924	4.3	7.5
Fig. 5(a);1	Urine1126	ECOLI1126	7.0	SEPI1126	18	3.1
Fig. 5(b);2	Urine1126	ECOLI1126	7.0	SEPI1126	18	4.8
Fig. 6(a);1	Urine1202	SEPI1203	17	Bact1202A	5.0	5.4
Fig. 6(b);2	Urine1202	SEPI1203	17	Bact1202A	5.0	1.9
Fig. 6(b);3	Urine1202	SEPI1203	17	Bact1202A	5.0	5.5

After completing the detection experiments, samples of test fluids with bacteria were plated using Fischer Scientific Trypticase™ Soy Agar plates (B21185). Using a dilution and plate count technique, the concentration of bacteria was estimated and is reported in Table 2. From these bacterial concentration measurements, we can approximate the sensitivity of the LRSPP waveguide biosensor. In our experimentation, the SEPI0917 test solution had the lowest bacterial concentration. This solution was grown for 4.3 hrs and caused a signal power change of 0.7μW when injected and flow stopped from 295 to 298 min of Fig. 3(a). From the SEPI1117 and SEPI1126 concentration measurements of Table 2, we estimate that 24 bacterial generations are produced in 12 hrs (or 30 min per generation). We can therefore extrapolate the concentration at 4.3 hrs of growth to 3×10^4 CFU/ml. Thus, this biosensor is capable of detecting bacterial concentrations below 1×10^5 CFU/ml, which is the internationally recognized threshold for the diagnostic of UTI. Further optimization of the test protocol and sensor design is required to estimate selectivity and sensitivity of this diagnostic approach using infected patient urine.

Table 2. Count of bacteria concentration

Label	Bacteria		Colony count		CFU / ml
	Gram	Growth time [hrs]	Dilution	Plate count	
SEPI1117	positive	6	1:1000	232	2×10^5
SEPI1126	positive	18	1:10000000000	300	3×10^{12}
Bact1202A	negative	5	1:10000	210	2×10^6
EColi1117	negative	6	1:100000000	171	2×10^{10}

5. Conclusion

Our experiments demonstrate that LRSPP waveguides can selectively detect gram negative or gram positive bacteria in human urine. A first approximation of the sensitivity of the biosensor indicates that it is relevant to the diagnostic of UTI with a detection

threshold less than 10^5 CFU/ml. In addition, the direct use of human urine in the detector greatly simplifies its future use at the point-of-care. We also expect that the test time after sample urine collection from a patient would be minutes considering that ready-to-test dies and their functionalization can be prepared ahead of time.

A clinical urine collection protocol to optimize specificity and sensitivity of a UTI diagnostic test using this technology seems feasible. Currently, the collection of urine one hour after drinking one liter of water helped to demonstrate the robustness of the biosensor with a low concentration of urine constituents, but this could also reduce the quantity of bacteria in the sample of an infected patient. Mid-stream urine is normally collected for UTI testing to reduce the risk of contamination. In Fig. 6 trials, a P/N ratio greater than 2 was observed for all, except in 1 case (P/N = 1.9). The experiments reported in Fig. 6 are particularly promising in that a P/N ratio of 5 is obtained even when 2 types of bacteria are present in the test solution and a negative control at 1000× greater concentration was used. It is unknown whether large urine constituents such as leukocytes, fungi or blood cells will interfere with the detection, but considering that they typically flow away from the biosensing zone, and that control over the test protocol can be exercised, we are hopeful that this will not be a serious issue.

Acknowledgments

We are grateful to Canadian Blood Services (Sandra Ramirez) for donating two bacteria strains: *Escherichia coli* (*E.coli*) XL1 Blue and *Staphylococcus epidermidis* (*S.epi*) ATCC 12228.

Appendix A

Table 3. List of Fluids; labeling: AAAAmmdd where ¨mm¨ is the month and ¨dd¨ is the day of creation.

Fluid label	Part Number	Origin	Description	Refr. Index
Bact1202A	XL1 blue with contamination	CBS	*E.coli* bacteria grown for 5 hrs and transferred to Urine1202. Note that the culture was contaminated before incubation with an unknown bacteria measured to have a lower concentration then *E.coli* and probably a gram positive species.	1.32276
BSA0917	A0281-250 mg	Sigma-Aldrich	Albumin from bovine serum (100 µg/ml). 2 mg of bovine serum albumin was dissolved in 2 ml of PBS and stored in one vial of 2 ml (1 mg/ml) at 4º C. On the day of use, 100 µl from the BSA vial is diluted in 900 µl of PBSG0917 resulting in a 100 µg/ml solution for use in the experiments.	N/A
BSA1202	A0281-250 mg	Sigma-Aldrich	Albumin from Bovine Serum (100 µg/ml). This batch mixed from 100 µl of PBS with 900 µl of PBSG1124. Same protocol as BSA0917.	N/A
DIH2O	D11931	Barnstead	Ultra pure water, 18.2 MΩ-cm, < 1CFU/ml, < 1µM/ml (theoretical RI = 1.3206)	1.31977
ECOLI0917	XL1 blue	CBS	E.coli bacteria grown for 4.3 hrs then transferred to PBSG0917.	1.32854
ECOLI0924	XL1 blue	CBS	*E.coli* bacteria grown for 4.3 hrs then transferred to Urine0924.	N/A
ECOLI1117	XL1 blue	CBS	*E.coli* bacteria grown for 6 hrs, then transferred to Urine1120 and concentration measured with plate culture.	N/A
ECOLI1126	XL1 blue	CBS	*E.coli* bacteria grown for 7 hrs then transferred to Urine1126.	N/A
GNeg	AB41202	ABCAM	50 µg/ml of gram negative antibody in solution of PBSG0715. 100 µl of gram negative antibody was diluted in 3900 µl of PBSG0715 and stored in 10 vials of 0.4 ml (50 µg/ml) at 4º C.	N/A
GPos	AB20344	ABCAM	50 µg/ml of gram positive antibody in solution of PBSG0917. 0.5 ml of gram positive antibodies was diluted in 0.5 ml of PBS and stored in 2 vial of 0.5 ml (50 µg/ml) at 4º C.	N/A
GProt0715	P4689-1MG	Sigma-Aldrich	1 mg of protein G (immunoglobulin-binding protein expressed in group C and G Streptococcal bacteria) was dissolved in 4 ml of PBSG0715 solution and stored in 4 vials of 1 ml (0.25 mg/ml) by freezing at -20º C. On the day of use, a protein G vial was thawed and 200 µL diluted in 800 µL of filtered PBSG solution resulting in a 50 µg/ml solution used to functionalize the bare gold surface of a waveguide with a monolayer of protein G.	N/A
HKECOL1001	XL1 blue	CBS	*E.coli* bacteria grown for 7 hrs in LB broth, transferred to PBS solution, then heat killed in oven at 80º C for 60 min.	N/A
HKECOL1008	XL1 blue	CBS	HKECOL1001 bacteria transferred to Urine1008 by spinning at 3000 RPM for 7 min.	N/A
LB Broth	L3022	Sigma-Aldrich	Mix one pouch in 500 ml of DIH2O.	N/A
PBS	P-5368	Sigma-Aldrich	Mix one pouch in 1L DIH2O ml (theoretical RI = 1.3329).	1.32351

PBSG0715	49767-250 ml	Sigma-Aldrich	66.66 g of glycerol in 500 ml of PBS.	1.33425
PBSG0917	49767-250 ml	Sigma-Aldrich	33.33 g of glycerol in 500 ml of PBS.	1.32854
PBSG1124	49767-250 ml	Sigma-Aldrich	PBSG0917 sterilized in a microwave oven for 20 min. Final concentration: approximately 10 g/100 ml.	1.33152
SDS	71725-50G	Sigma-Aldrich	5 g of sodium dodecyl sulfate in 1L of DIH2O.	N/A
SEPI0917	ATCC 12228	CBS	*S.epi* bacteria grown for 4.3 hrs then transferred to PBSG0917.	1.32854
SEPI0924	ATCC 12228	CBS	*S.epi* bacteria grown for 4.3 hrs then transferred to Urine0924.	N/A
SEPI1117	ATCC 12228	CBS	*S.epi* bacteria grown for 6 hrs then concentration measured with plate culture.	N/A
SEPI1126	ATCC 12228	CBS	*S.epi* bacteria grown for 18 hrs then transferred to Urine1126.	N/A
SEPI1203	ATCC 12228	CBS	*S.epi* bacteria grown for 17 hrs then transferred to Urine1202.	1.32276
Urine0820A	Human	anon.	First urine of the day collected on 20 Aug. 2014. Donor collected urine in the morning after fasting for 12 hrs .	1.32991
Urine0820B	Human	anon.	2nd urine of the day collected on 20 Aug. 2014. Urine collected after drinking 1L of water and waiting one hour.	1.32798
Urine0924	Human	anon.	2nd urine of the day collected on 24 Sep. 2014 (as above).	N/A
Urine1126	Human	anon.	2nd urine of the day collected on 26 Nov. 2014 (as above).	N/A
Urine1202	Human	anon.	2nd urine of the day collected on 2 Dec. 2014 (as above).	1.32276

2.3 Paper submitted to Photonics North

My Contribution: The paper in this section was submitted to Photonics North. . I performed all laboratory measurements and wrote the first draft of the paper. The functionalization protocol used came from O. Krupin. Dr. Berini directed the work and edited the paper.

Preamble: The selective detection of gram negative bacteria in the presence of gram positive bacteria in urine using the LRSPP waveguide biosensor is demonstrated and discussed. The urine sample emulates that of a patient diagnosed with urinary tract infection but with a contaminated urine sample typical of a patient not taking a mid-stream urine sample. It demonstrates the robustness of the LRSPP waveguide label free biosensor for future clinical uses.

Selective Detection of Bacteria in Urine with a LRSPP Waveguide Biosensor

Paul Béland
Department of Biomedical Engineering
University of Ottawa, Ottawa, Canada

Pierre Berini
School of Electrical Engineering and Computer Science,
Department of Physics, and
Centre for Research in Photonics
University of Ottawa, Ottawa, Canada

Oleksiy Krupin
Dept. of Biological and Chemical Engineering Science
University of Ottawa, Ottawa, Canada

***Abstract*— Laboratory experimentation demonstrates long range surface plasmon polaritons (LRSPP) waveguides as a useful biosensor to selectively detect gram negative bacteria in human urine. The biosensor can detect bacteria at concentrations of 10^5 CFU/ml, the internationally recommended threshold for diagnostic of urinary tract infection (UTI). Using a negative control solution at bacterial concentration 1000× higher than the targeted bacteria in urine with a weak concentration of constituents, the power ratio between the negative control signal to the target bacteria signal is measured to be 6.7 on the first test and 2.5 for a lower bacterial concentration after regenerating the surface with SDS. Hence we report a conclusive demonstration of the LRSPP waveguide biosensor selectivity to the gram of bacteria in human urine.**

Keywords—surface plasmon polaritons; urine; biosensor; bacteria

The gold standard for the diagnosis of Urinal tract infection (UTI) is the detection of pathogen in presence of clinical symptoms. The best detection and identification of the pathogen remains the culture of patient urine [1]. This technique provides very good selectivity of the pathogen and superior sensitivity but requires 24 to 48 hours in a microbiology laboratory environment. Label-free biosensors such as Long Range Surface Plasmon Polaritons (LRSPPs) [2] can provide detection of bacteria in clean fluids. These label-free biosensors can detect the presence or absence of pathogen in a fluid of interest. A surface functionalization with antibody ensures selective adsorption of the pathogen within the LRSPP waveguide active biosensing area.

In order to demonstrate the selective detection of gram negative bacteria in urine, we prepared test solution with freshly grown bacteria. Replacing the culture medium with human urine we created test solutions equivalent to a UTI infected patient. The sensor die consisted of straight Au stripes embedded in Cytop with an etched microfluidic channel [3,4], functionalized with protein G and gram negative antibody. Figure 1 reports the detected optical power when injecting 3 test fluids: a high concentration of gram negative bacteria, a high concentration of gram positive bacteria and a low concentration of gram negative bacteria. Defining a positive-to-negative ratio (P/N) as the ratio of the difference of power before and after injection of the test fluid we obtain a P/N of Pt(151)-Pt(135)/Pt(191)-Pt(174) = 6.7 for a high concentration of bacteria in the test fluid (>10^{10} CFU/ml). At a concentration of 2×10^6 CFU/ml, the ratio was P/N = 2.5.

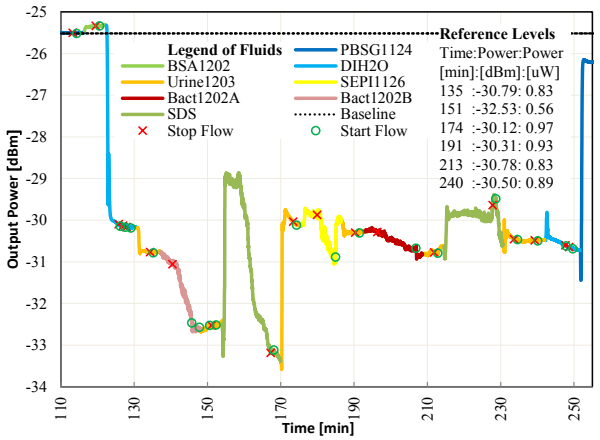

Figure 1. Gram negative bacteria detection in urine, laser power = 14.5 dBm, flow rate = 20µL/min, device functionalization: Protein G and gram negative antibody. SEPI1126 concentration: 10^{12}CFU/ml, Bact1202A concentration: 10^{10}, CFU/ml, Bact1202B concentration: 10^6, CFU/ml, P/N = 2.5

A threshold of P/N ≥ 2 confirms selective detection of the bacteria. In addition, we postulate that by flowing 0.5% SDS solution for 15 minutes, the antibody antigen link can be broken and the bacteria can be washed away from the active biosensing area therefore recovering the baseline signal. Here the baseline was not fully recovered which is indicative of some nonspecific binding occurring in the experiment.

References

[1] G. Schmiemann, E. Kniehl, K. Gebhardt, M. M. Matejczyk, E. Hummers-Pradier "The Diagnosis of Urinary Tract Infection: A Systematic Review," Dtsch Arztebl Int., Vol. 107, 361–367, 2010

[2] M. Vala, S. Etheridge, J. Roach, and J. Homola, "Long Range plasmons for detection of bacterial analytes," Sens. Actuators B, Vol. 139, 59-63, 2009.

[3] C. Chiu, E. Lisicka-Skrzek, R. N. Tait, P, Berini, "Fabrication of surface plasmon waveguides and devices in Cytop with integrated microfluidic channels," J. Vac. Sci. Technol. B, Vol. 28, pp. 729-735, 2010.

[4] O. Krupin *et al.*, “Biosensing using straight long-range surface plasmon waveguides, ” Opt.Express, Vol. 21, pp.698-709, 2013
.

2.4 Supplementary measurements

In the following subsections, we report laboratory measurement substantiating various aspect of the LRSPP waveguide biosensor including:

1. cut back measurement, used to characterise the insertion loss of the cladded waveguide,
2. sensorgram of LRSPP waveguide biosensor during surface functionalization,
3. growth of bacteria and measurement of their concentrations,
4. evidence of SDS dissolving bacteria membrane,
5. rapid sensing of dead vs live bacteria,
6. unexpected formation of biofilm on the surface of biosensors,
7. fluidic consideration such as fluid dead volume and trapping of air bubbles,
8. drift due to organic material in PBSG fluid.

2.4.1 Cut Back Measurement of Wafer 4D1-A

The insertion loss of a waveguide as a function of length can be determined by measuring waveguides of varying length using what is known as the cut back measurement [1]. The wafer 4D1-A includes LRSPP cladded waveguide die of 2.00 mm, 3.01 mm, 3.79 mm, and 4.77 mm. Using the setup shown in Figure 15, we performed mechanical alignment as described in section 2.1.4, and then measured the insertion loss of the 4 dies listed above. The results are reported in Figure 18. A linear regression allows us to establish the insertion loss as a function of length for wafer 4D1-A to be 6.8 dB/mm. In Figure 2b) of [2], the normalised attenuation of the LRSPP mode for a 35 nm thick and 5 um wide waveguide is plotted as 1.6×10^{-4}. Multiplying by the phase constant $\beta_0 = 2 \bullet \pi / 1310$ nm and converting to dB we obtain a theoretical attenuation of -6.4 dB/mm. Also in appendix A of, [3], the theoretical estimation of MPA for a 35 nm thick LRSPP waveguide is given has -7.0 dB/mm.

The coupling loss between the optical fiber and die is extrapolated to be 1.3 dB when using certified refractive index matching fluid from Cargilles, Series AA, 1.4560 [4] at the fiber and device interface .

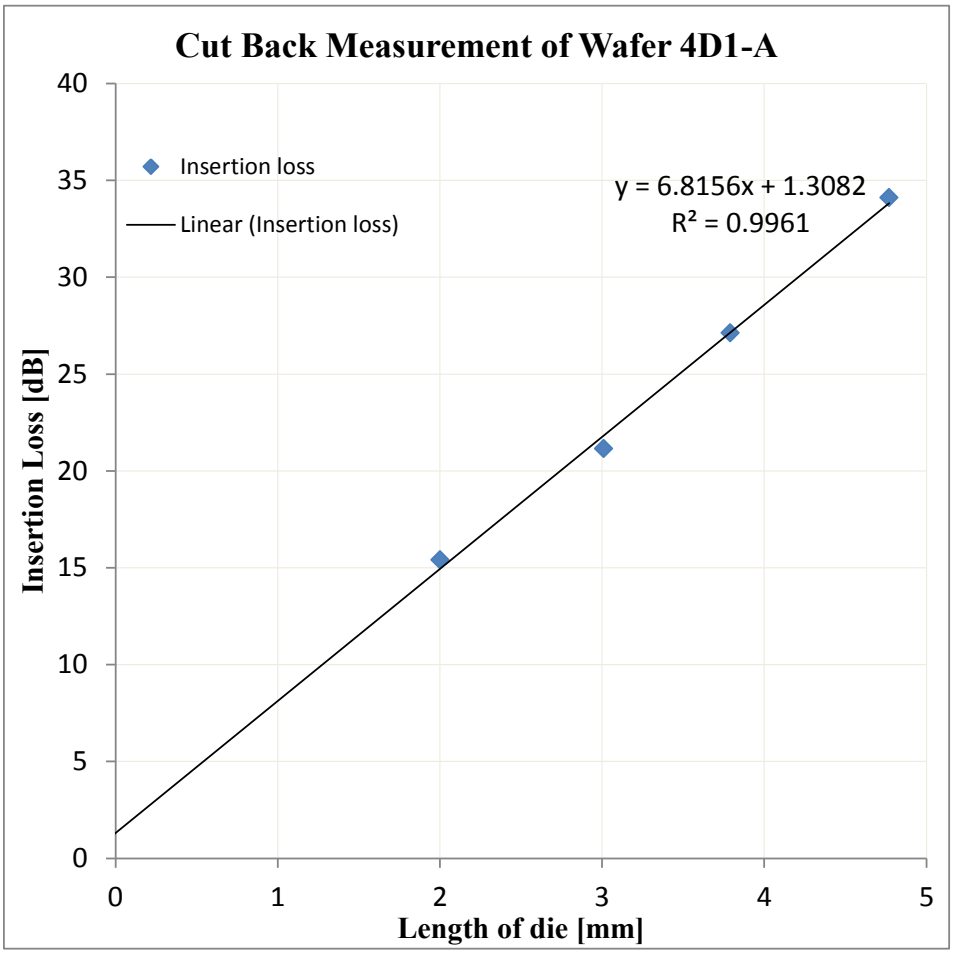

Figure 18 Mode power attenuation (MPA) measurement. Interpolated to be 6.8 dB/mm for wafer 4D1-A, using index matching fluid between the optical fiber and devices.

2.4.2 Biosensing area surface functionalization

After assembling a newly cleaned die in the test jig by closing the top cover, a syringe filled with DIH2O was used to prime the system by pushing 0.5 ml of DIH2O. The syringe pump was then started and a sequence of fluid circulated inside the jig to functionalize its surface.

In Figure 19 we present a sensorgram corresponding to the functionalization sequence. We avoid injecting PBSG solution before the Gprot. Instead, we perform mechanical alignments during the injection of Gprot. This avoids unintentional deposition of impurities that may be present in the PBSG solution from being deposited on the waveguide as reported in section 2.4.9. It also accelerates the functionalization of the die which takes a total of 130 minutes. Functionalization in less than one hour may be possible by reducing the antibody exposure time.

We note that the output power level change after deposition of the antibody is of the order of 0.2 dB because the RI of the solutions used during this process are very close to the RI of CYTOP which reduces the sensitivity of the biosensor [5,6]. Having the protein G dissolved in a PBSG solution with RI close to CYTOP facilitates the initial mechanical alignment. It provides the lowest insertion loss for the waveguide and hence an output power much larger than the background noise.

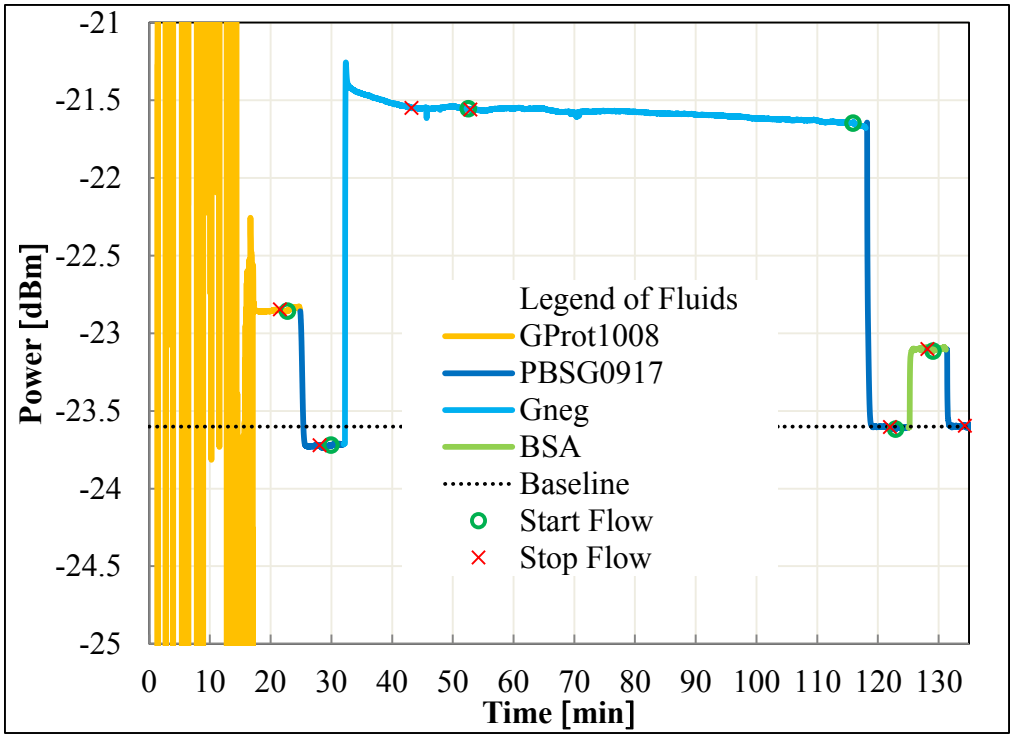

Figure 19 Faster functionalization of die with Protein G, Gram Negative antibody and BSA.

Error! Not a valid bookmark self-reference. lists the gram negative and the gram positive antibodies that were selected and successfully functionalised on LRSPP waveguide biosensor. For each antibody, we summarize the manufacturer provided data on reactivity with bacteria. We also list the prevalence of known bacteria causing UTI as per [7].

Table 4. List of bacteria reacting with the selected antibody [7]

	Gram Negative Antibody	**Gram Positive Antibody**
Part number	AB41202 (Sigma-Aldrich)	AB20344 (Sigma-Aldrich)
Reacts with:	lipopolysacchharide	lipoteichoic acid (LTA)
Immunogen	Escherichia coli O:111 B4 J5	Listeria monocytogenes
Manufacturer tested antigen (Bacteria)	E. aerogenes, S. marcescens, P. mirabilis, P. vulgaris, A. calcoaceticus, Ps. Aeruginosa	Listeria monocytogenes, Streptococcus pneumoniae, Staphylococcus aureus, Staphylococcus epidermidis, Enterococcus faecium, Bacillus cereus, Bacillus subtilis and group B Streptococcus
Bacteria causing UTI (prevalence)	Escherichia coli (70 %) Klebsiella Pneumonia (7 %) Klebsiella oxytoca (? %) Proteus mirabilis (? %)	Enterrococcus Species (6 %) group B Streptococcus (? %) Staphylococcus saprophyticus(?) Viridans streptococcus (? %)
Tested on a LRSPP sensor	**Escherichia coli (***E.Coli***)** XL1	**Staphylococcus epidermidis** (*S.Epi*)

2.4.3 Growth of bacteria and plate count technique

As discussed in [8], we emulated urine samples of patients suffering from UTI. Two bacteria strains were used: Escherichia coli (E.coli) XL1 Blue and Staphylococcus epidermidis (S.epi) ATCC 12228CRS as shown in Figure 20. The culture of the bacteria was performed at the CAREG laboratory of the university of Ottawa using aseptic inoculation techniques. First, the bacteria are thawed from -80 ºC and an inoculation loop sterilized by a flame is used to transfer a

portion of the bacteria into 10 ml of LB Broth as shown in Figure 21. The broth is then placed into an incubator at 37 ºC for varying time periods to obtain varying concentrations of bacteria.

Upon completion of the growth cycles, the bacteria are stored at 4 ºC inhibiting further growth. A 1 ml sample is put aside for future analysis of the concentration using a plate count technique. Another 1 ml sample is also put aside after the bacteria have been centrifugated and transferred to te urine analyte. To perform the concentration measurmment, ten 1 ml vial are filled with 900 µL of PBS. A 100 µL of the sample to be evaluated is diluted in the first vial with 900 µL of PBS. This first vial is shaked and 100 µL is taken from it and placed in the second vial with 900 µL of PBS. This is repeated for the 10 vial. As shown in Figure 22, 100 µL from each vial is transferred to 10 agar plate and steaked with a sterilised inoculation loop. The plates are then incubated into an oven for 48 hours. Finally, we identify the plate with 30 to 300 colony as shown in Figure 23 and each colomny to established the concentration in CFU/ml of bacteria in the original vial. Contamination are detected at this point if more then one type of colony is observed on the agar plate.

Figure 20 ***Escherichia coli (E.coli) XL1 Blue and Staphylococcus epidermidis (S.epi) ATCC 12228*****CRS in vial.**

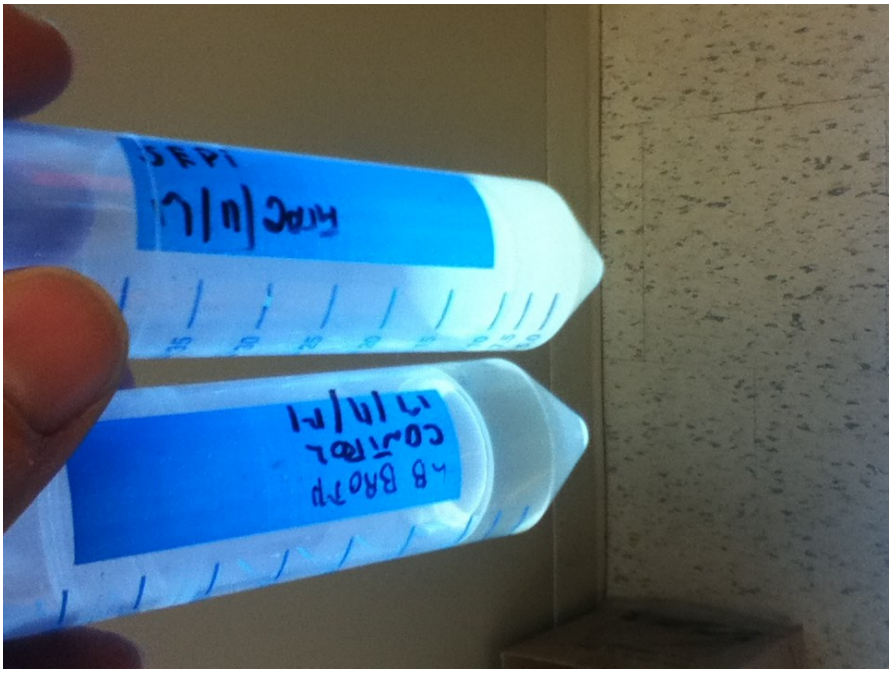

Figure 21 LB broth after inoculation with ***S.Epi.*** **Control vial is also shown.**

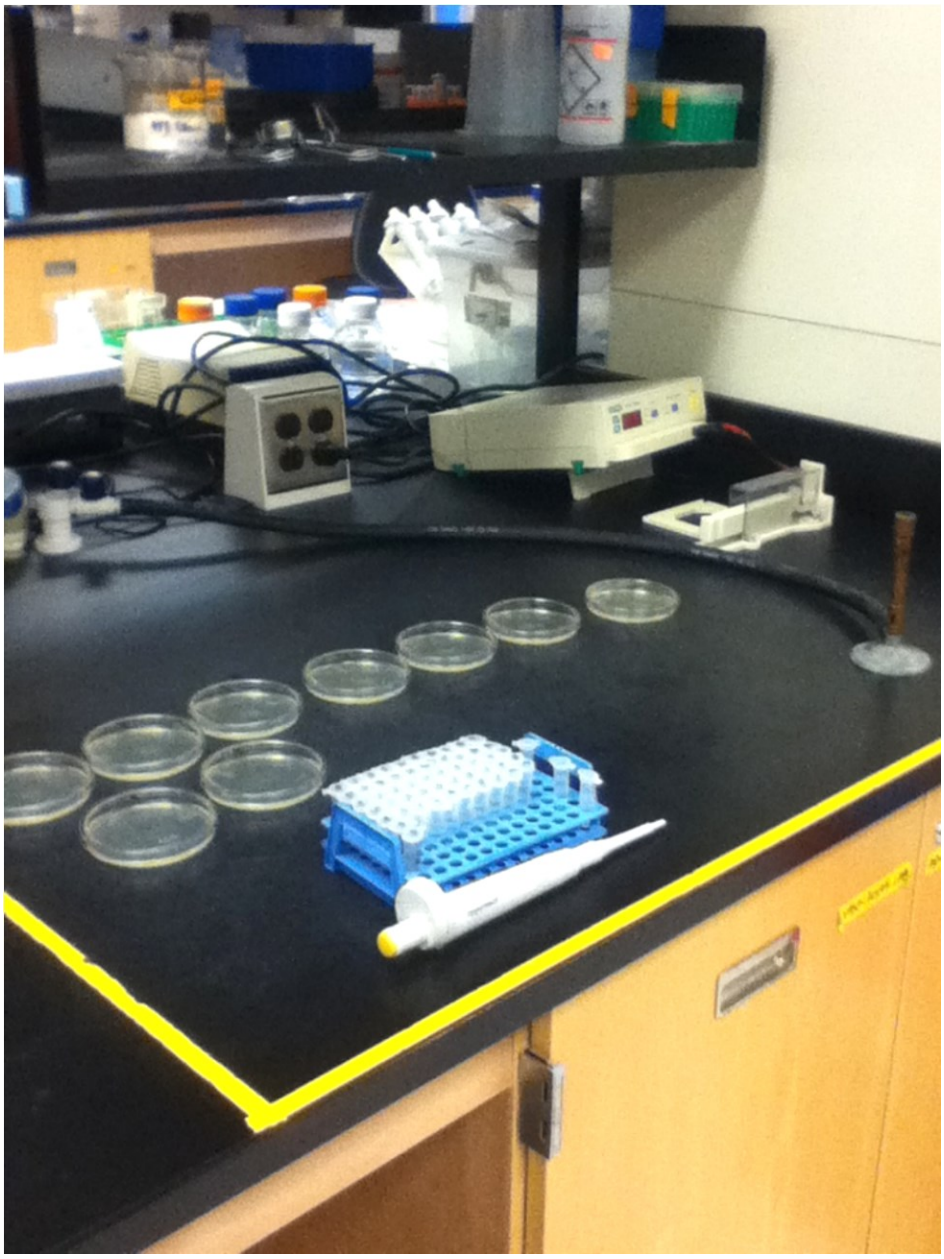

Figure 22 Measurement of Bacteria concentration using 10 agar plate.

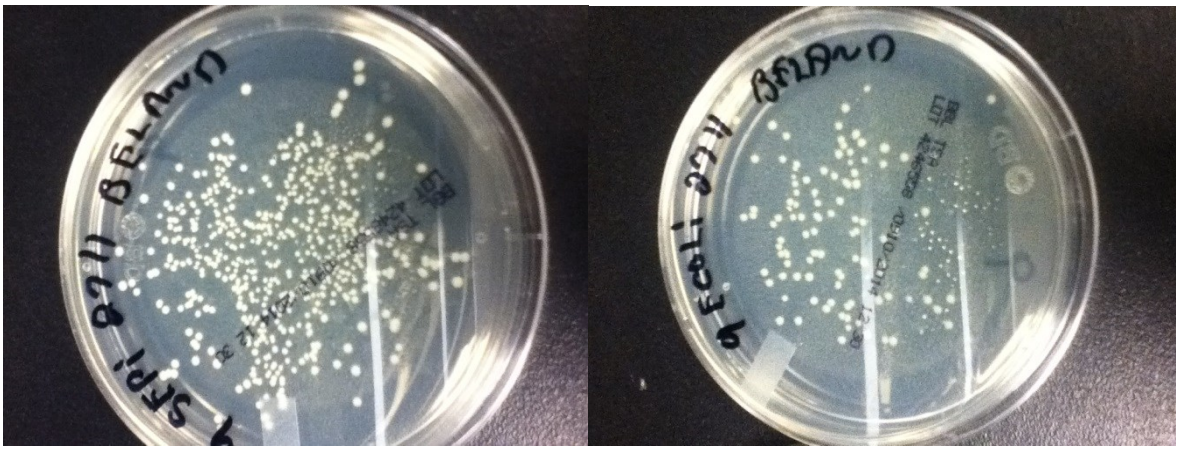

Figure 23 Agar plate after growth of *S.Epi* and *E.Coli* bacteria

2.4.4 SDS dissolves bacteria membrane

In Figure 24, we report 2 visual inspections of the same die (C53B1310) before and after exposure to SDS in a vial. Originally, the die surface was simply cleaned with acetone, IPA and DIH20. No UV ozone exposure was used. At the end of a biosensing experiment we observed bacteria on the die as sown in Figure 24 a). The bacteria seen could not be washed away using IPA or DIH2O. To remove the bacteria, the die was placed in a vial of SDS for 4 days. Figure 24 b) reports the visual inspection after SDS has completely dissolved the membrane of the bacteria. Unlike the surface regeneration technique which consists in flowing SDS for 15 min to break the antibody antigen bond, exposure to SDS will dissolve the membrane of bacteria when exposed for more than 30 min. Note that here, the bacteria were not intentionally injected but were the consequence of a failed experiment where the PBSG0715 solution may have been contaminated with bacteria.

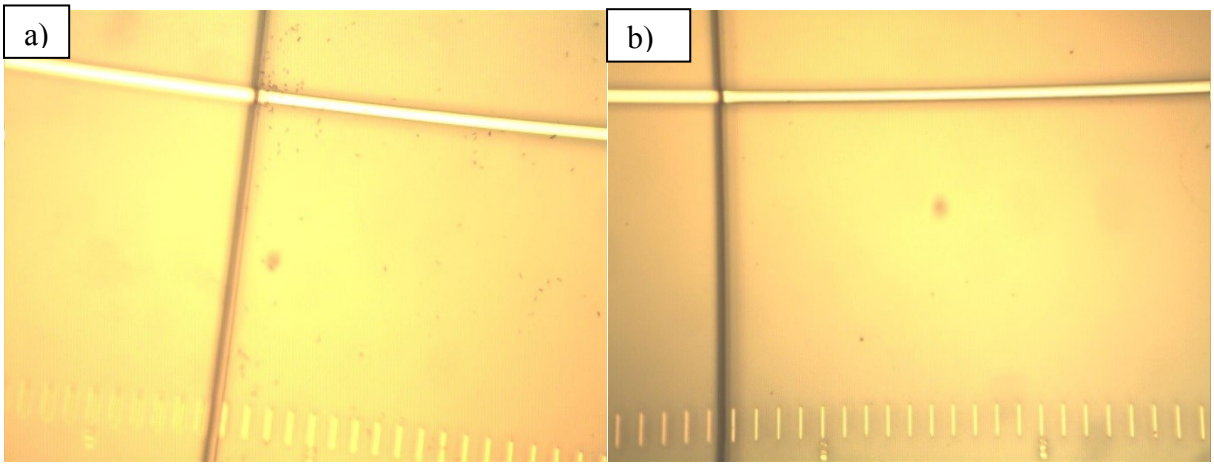

Figure 24 Visual inspection of C53B1310 Die, a) with bacteria, b) without bacteria after 4 days exposure to SDS in a vial.

2.4.5 Rapid Sensing of dead vs live bacteria

In this section we compare the signal characteristic between dead and live bacteria. Two biosensing experiments were performed in urine, one using freshly grown E-coli, and the other one using heat-killed E-Coli as shown in Figure 25 and Figure 26 respectively. A similar experiment was reported in [8] using clean fluids. Here we compare the signal characteristic one minute after stopping the flow which occurs at time T=1525 min in Figure 25 and at time T=275 min in Figure 26. The two signals are better observed in expanded view in Figure 27.

We note that with dead *E-Coli*, the signal standard deviation is 0.007 dBm whereas with live *E-Coli* the standard deviation is 0.036 dBm from minute 1 to minute 4 after stopping the flow of filtered urine. We note that 10 min after stopping the flow, a large change in output power is observed, most likely due to bacteria and debris flowing back from the microfluidic tubing of our setup and onto the sensing surface. This was previously noted as a limitation of our test setup.

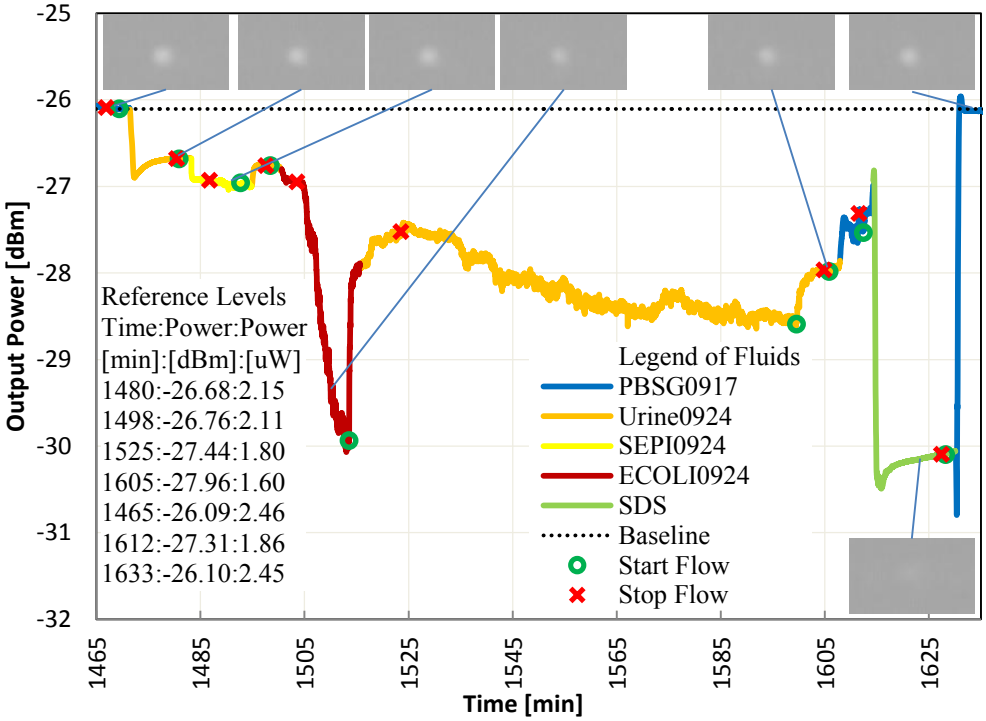

Figure 25 Live *E.coli* detection in urine, flow = 20 µl/min, laser power = 11.1 dBm, gram negative antibody surface, bacteria growth time of 4.3 hrs in LB broth.[8]

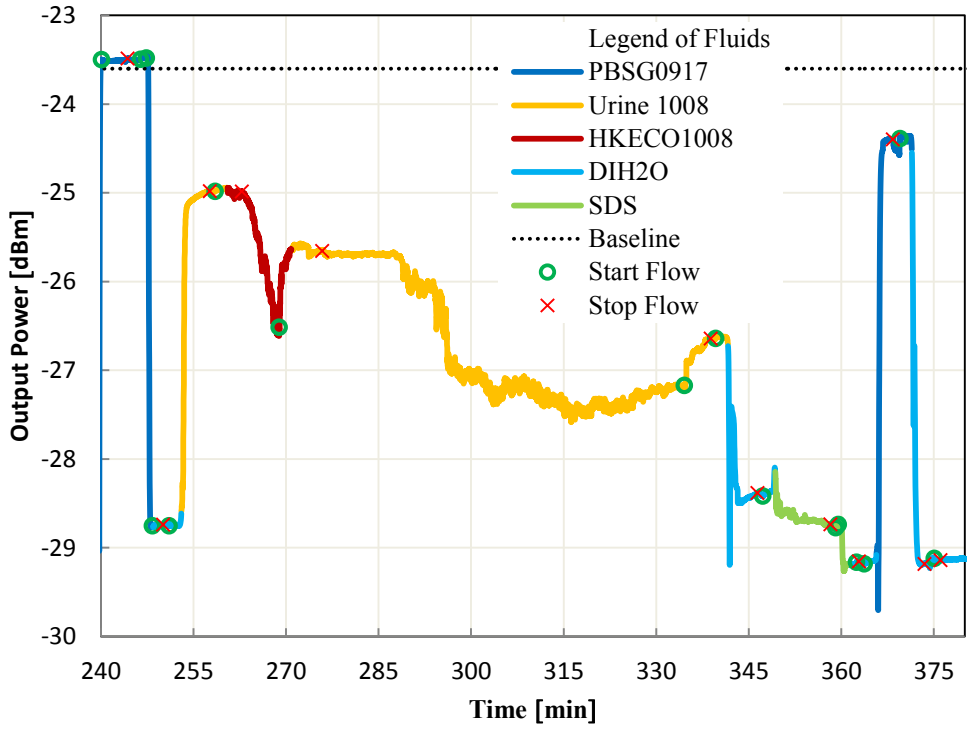

Figure 26 Dead *E.coli* detection in urine, flow = 20 µl/min, laser power = 11.1 dBm, gram negative antibody surface, Heat killed bacteria after growth time of 7 hours and transferred to urine1008

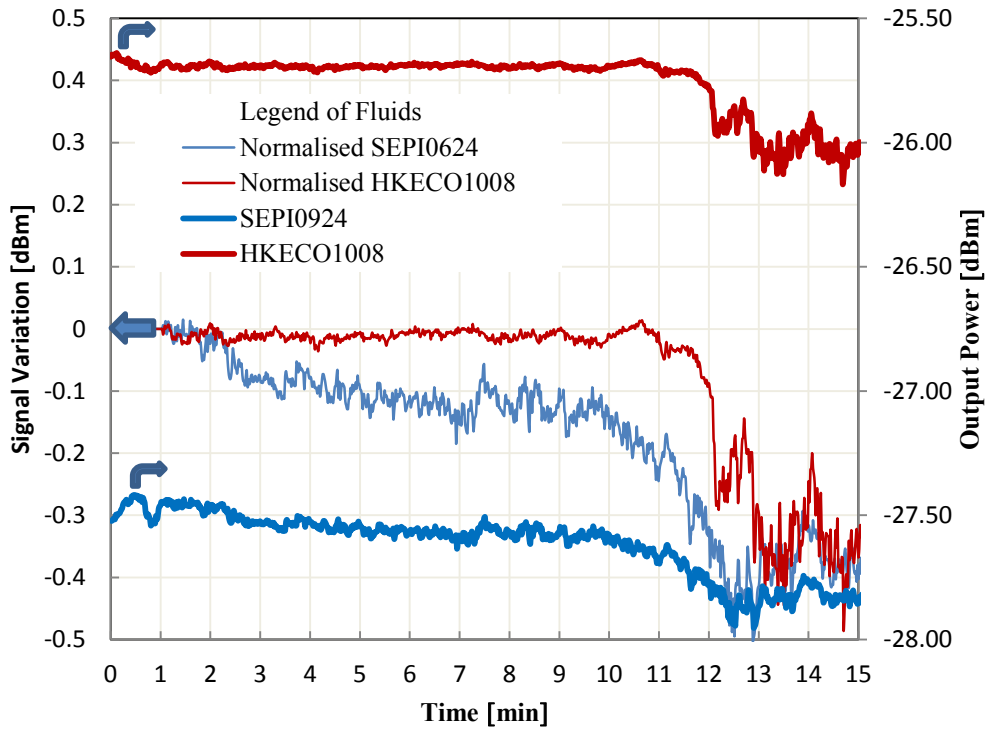

Figure 27 Comparaison of signals for live and dead *E.Coli* adsorption on a Gneg surface.

2.4.6 Detection of biofilm formation in water

The following section discusses the formation of biofilms on the surface of the biosensor. First we present a microscopic inspection of biofilm formation and then we report sensorgram measurements acquired during the formation of the biofilms. The laboratory conditions for these experiments were not controlled in that the origin of the bacteria which created the biofilm is unknown. We speculate that the filtered urine contains the microorganism responsible for the observations. Note that the urine used was centrifuged at 3000 RPM for 7 min and a 0.2 µm syringe filter was used to sterilise the urine before injecting it into the biosensor. We report here 2 different observations of a biofilm formation on a biosensor.

The die presented in Figure 28 had been injected with Gprot for 20 min and with PBS for 22 hours when we injected urine at time 1361 of Figure 29. Note that after injection of the urine, the signal becomes noisy at T= 1368. An alignment procedure was performed from time T= 1362 to T=1365. At the end of the sensorgram, the die was removed from the test jig for visual inspection. We observe that numerous biofilms had grown in the fluidic pool. The visual inspection of the die 2 months later, shown in Figure 28 c), d), e), and f) indicates that the biofilm dried out and only microorganism were left in the location of the biofilm formation.

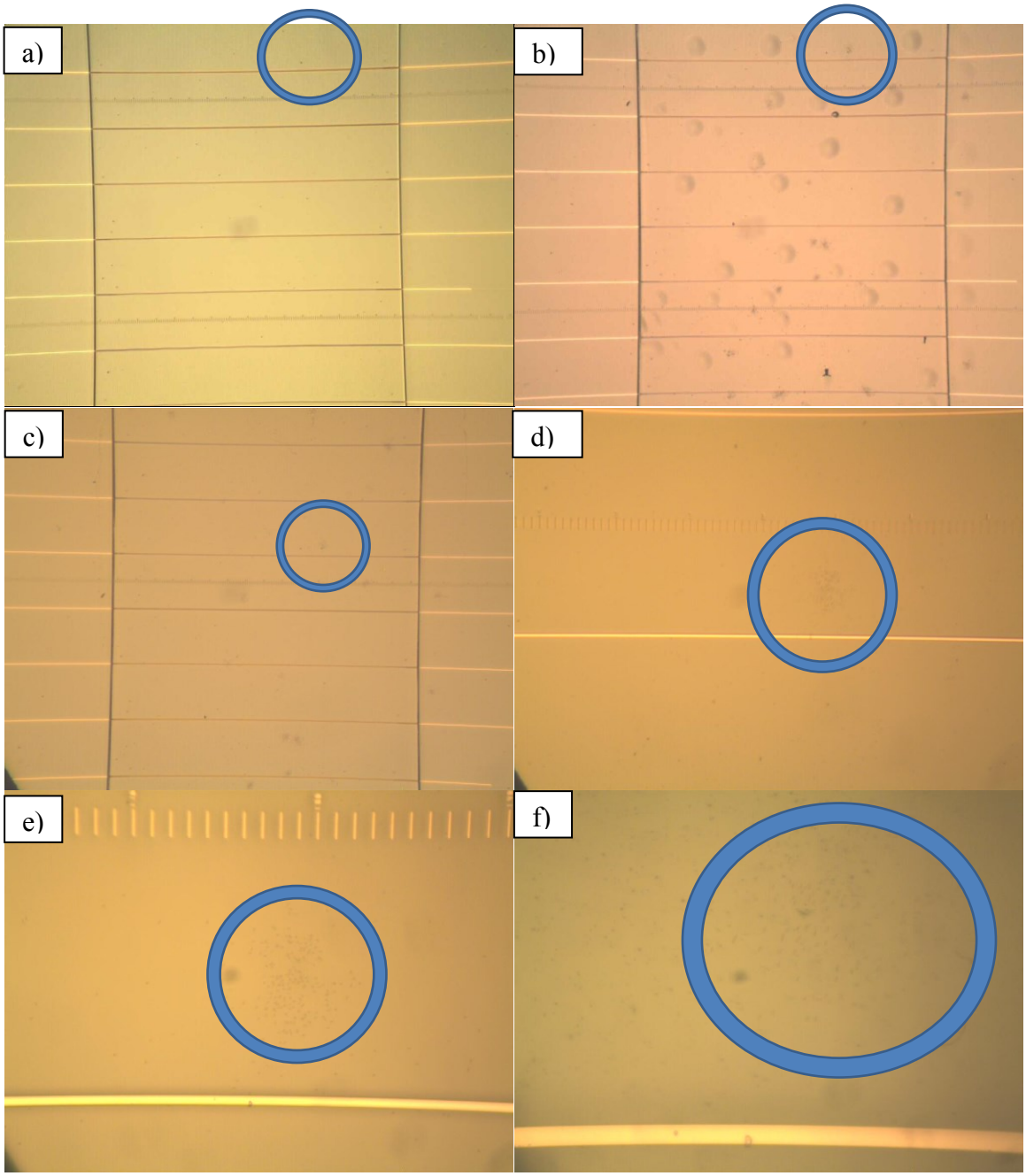

Figure 28 Microscopic inspection of biofilm formation and drying out, a) new die , 19/11/2014, 08h56, 50X, b) Biofilm 20/11/2014 11h26, 50X c) dried biofilm 26/02/2015 14h51, 50x, d) Dried biofilm 26/02/2015, 200X e) Dried biofilm 26/02/2015 500x f) Dried biofilm 26/02/2015 1000x.

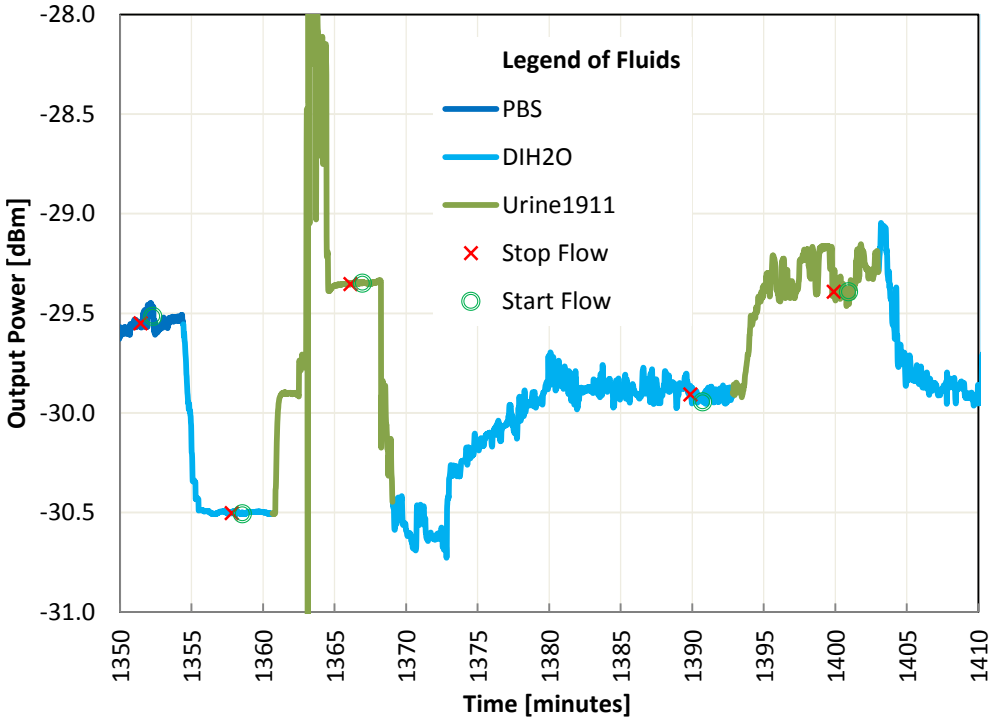

Figure 29 Sensorgram of biofilm formation in water, die functionalised with Gprot only. Time 1361 min (10h15 on 20/11/2014).

A second observation of a biofilm formation is shown in In Figure 30. A die was removed from the jig after experimentation with heat killed *E-coli* bacteria. In addition to dead E-coli from the experiment, we can observe the formation of a few biofilms in Figure 30 a) at the center of the blue circle. The biofilm is more easily observed after washing the die with IPA in Figure 30b). In Figure 30 c) we note that long exposure to SDS removed the biofilm but it didn`t dissolved the heat killed *E.Coli* nor the microorganism responsible for the biofilm formation. After one week storage of the die in DIH2O, we note that the biofilm were regenerated as shown in Figure 30 d). Subsequent drying out by storing the die in a petri dish for one day is observed in Figure 30 e) and after 126 days in Figure 30 f) where the biofilm composed at 97% of water are dried out.

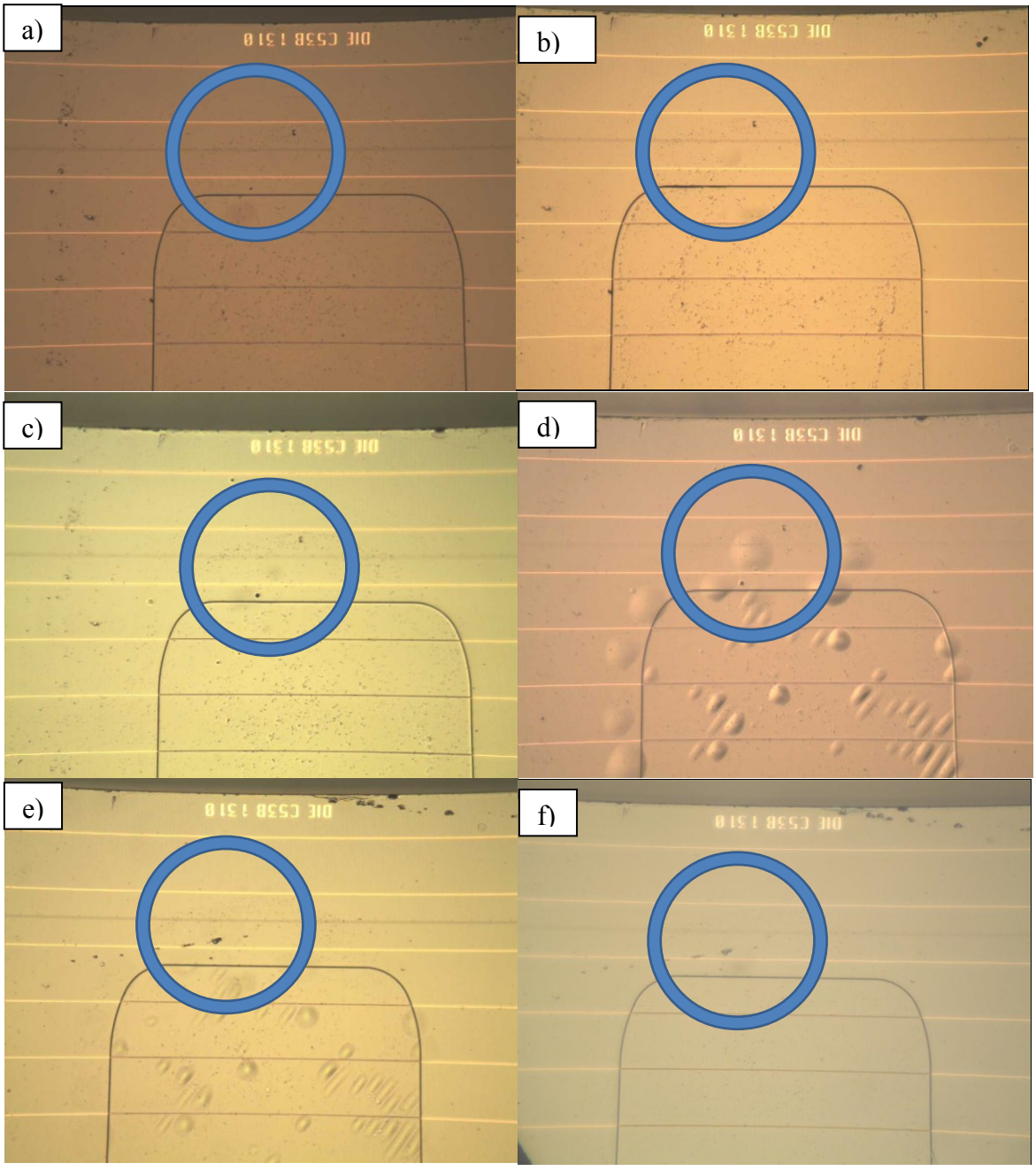

Figure 30 Evidence of biofilm formation on CYTOP magnified 50X, a) After experimentation, 9/10/2014 b) after IPA clean, 9/10/2014, c) After 7 days in SDS vial, 16/10/2014 d) after 5 days in DIH2O vial, 21/10/2014, e) after One day in petri dish (air), f) after 127 days in petri dish (air)

In addition to the microscopic observation of the creation of a biofilm, we present in Figure 31 a sensorgram detecting the biofilm formation prior to any visual inspection by microscopy. Let us describe chronological observations on this sensorgram. Before starting the data logger SDS and DIH2O were flown at 20 µl/min for 30 min to clean the HKECO1008 (Heat killed *E-Coli* in filtered urine) fluid. Then, PBSG7F08 (a specific vial of PBSG0917) as shown in Figure 31 is injection at 16h00 and produced an output power of -24.4 dBm. 17 hours later the injection of the same buffer produced an output power level of -32.5dBm. All attempts to clean the surface using SDS and DIH2O (not shown on in Figure 31) failed in recovering the output power. In Figure 32 we report imaged from the IR camera of the LRSPP waveguide mode. We note that with water we cannot distinguish the LRSPP waveguide mode from the noise in the background. Hence, the variation observed in the sensorgram with water reflects the changes in the scattering rather than the change in the LRSPP waveguide mode making it difficult to interpret the signal variation observed with water on the waveguide. All except one picture of the mode are from waveguide number 9, and the last one is from waveguide number 13 which was taken at the very end of the experimentation.

In Figure 33 we show an image at high magnification from the visual inspection previously shown in Figure 30. We observe that the surface is not smooth in addition to the large amount of debris on the guide. Four series of visual inspection were performed, first before the experiment (not reported), after the experiments, after an IPA clean, after an extended clean by storing the

die into an SDS vial for 4 days.

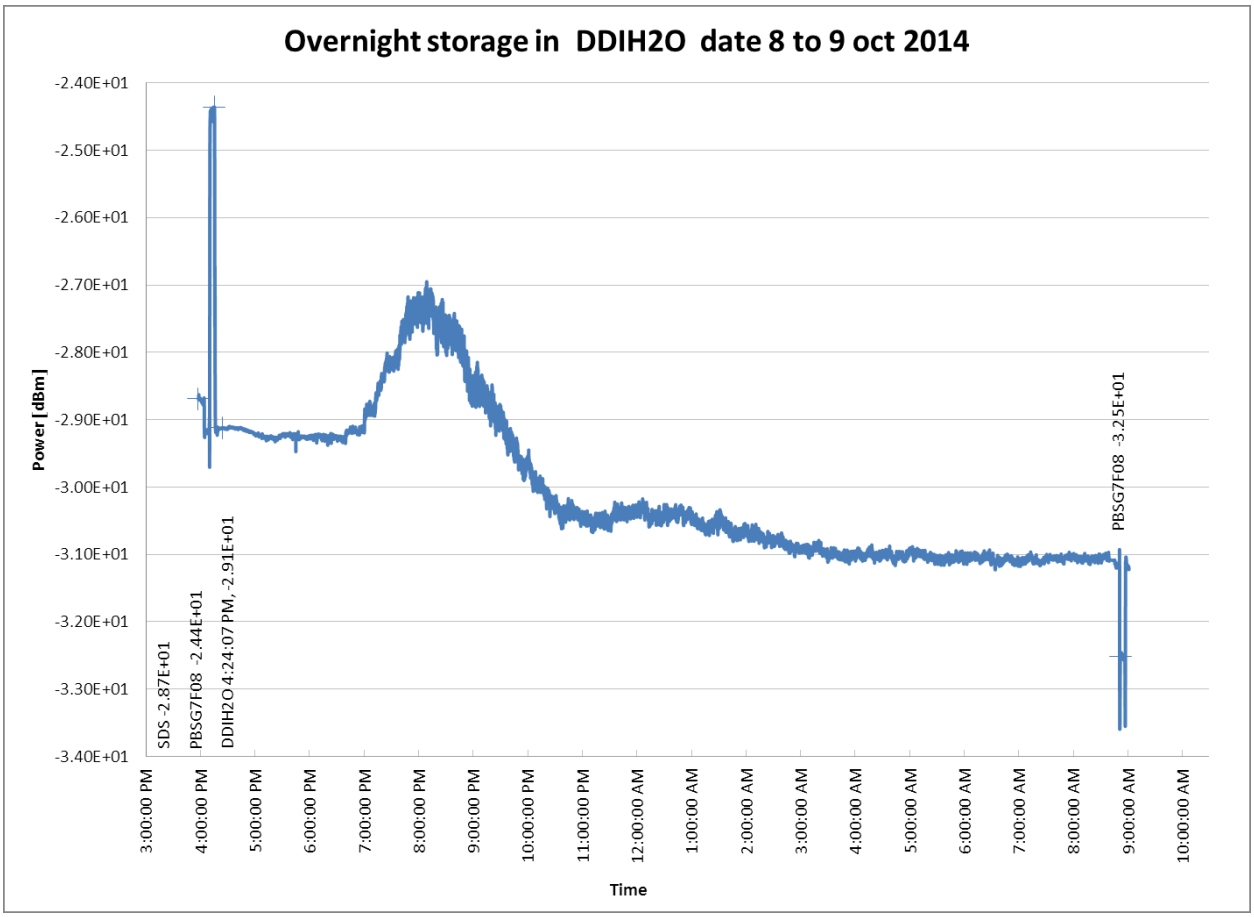

Figure 31 Biofilm formation in DIH2O.

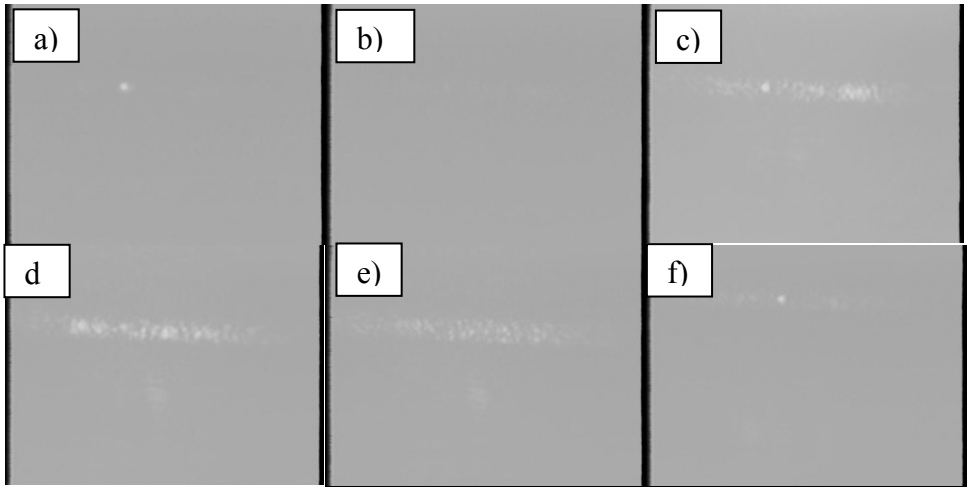

Figure 32 Picture of LRSPP waveguide mode throughout the experimentation of Figure 31 a) P= -24.4 at 16h00 on 08 oct, b) P= -32.5 at 0900 on 9 oct, c) P= -32.5 at 0900 on 9 oct Changed video attenuation to P5, P5. d) DIH2O video attenuation setting P5 P5, e) Air, f) Aligned on waveguide 13, P=-29.05 with PBSG

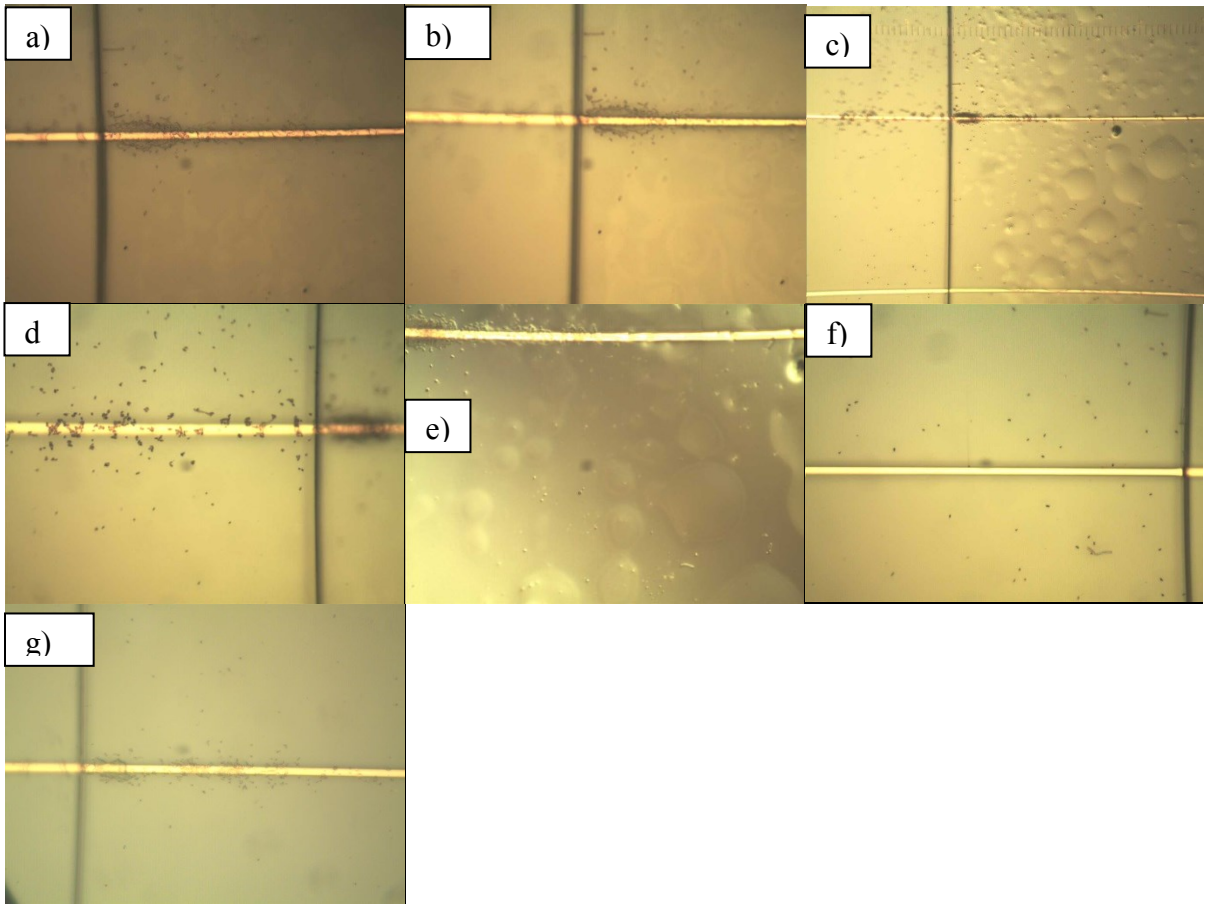

Figure 33 Visual inspection showing biofilm and dead bacteria, a) Before Cleaning, 1000X, 9/10/2014 b) after IPA cleaning, 1000X, 9/10/2014, c) Extended Cleaning, 500X, 16/10/2014 d) Extended Cleaning, 500X, 16/10/2014 , Focus on Dead E-Coli, e) Extended Cleaning, 500X, 16/10/2014 focus on Biofilm, f) Extended Cleaning, 500X, 16/10/2014 Focus on clean line output. g) After 126 days storage in petri dish 500X, 26/02/2015 focus on input of line 9.

In summary, we presented the formation of biofilms. We believe that the biofilm formation is probably due to the injection of urine inside the biosensor. Further investigation is required to understand the exact organism at origin of these biofilm formations.

2.4.7 Dead volume of fluid and removing air bubble inside the test jig.

The visual inspection shown in Figure 34 a) reveals a region close to the edge of the CYTOP pool where fluid surface tension may create a dead volume of fluid, *i.e.*, exchange of fluid in this

area does not occur when we inject air or other fluids. A short video, shown in Figure 34 b) was made after an air bubble was trapped inside the jig on top of a waveguide. In the video, we note that the size of the bubble changes when we manually apply more pressure on a syringe. Towards the end of the video, we push air which eventually clears out the air bubble. During the time that air flows through the jig, we note that fluid stays in the dead volume area on the edge of the pool. Note that the top cover of the jig has numerous scratches which results in fuzziness of the video image in certain locations.

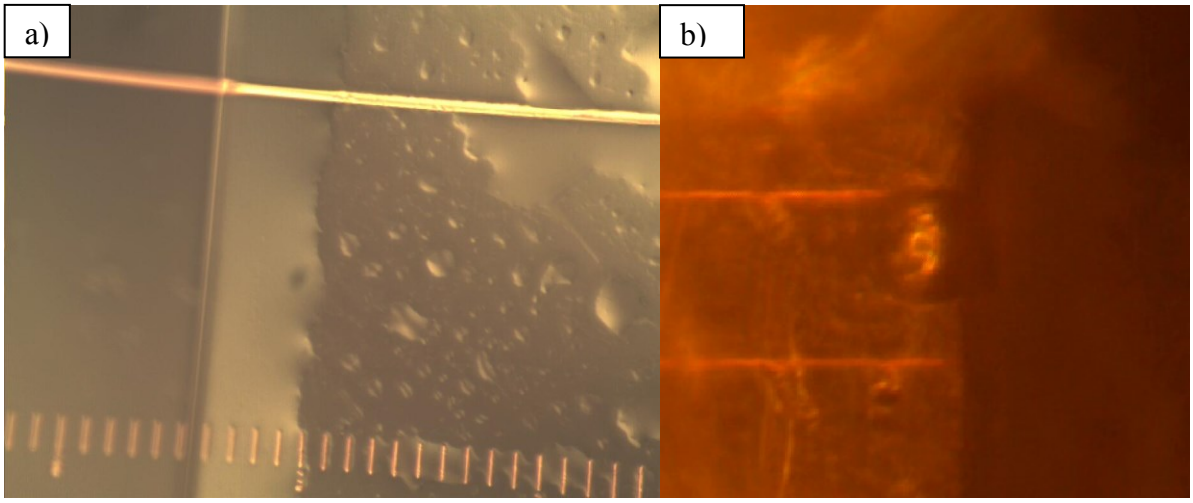

Figure 34 Visual inspection of C53B1310 Die in August, a) after removal from jig showing dead volume of water, b) video of air bubble trap in test jig over a waveguide link: (2015beland video air bubble)

2.4.8 Sensing beyond the LRSPP mode cut off.

We have previously seen that the estimated LRSPP dynamic range for an Au thickness of 30 nm was 1.4% centered about the RI of CYTOP, n =1.3346 [9]. Hence for a RI below 1.3252 (for example, the RI of water, n =1.31977) we expect that energy detected at the power detector will no longer be dominated by the LRSPP mode. We note in Figure 35 that the transition between

fluid of RI close to CYTOP (PBSG0715, n =1.33425) and water (n=1.31977) that the optical power detected transits through a minimum and maximum level at time T = 03:51 hour. The opposite transition at time T= 04:00 hour also goes through a minimum much lower than the output power with pure water. The short video of the mode during these transitions can be viewed by opening the links of the caption of Figure 35. In the first transition, we note an increase of the background noise while the LRSPP mode is attenuated. In the second transition we first note and attenuation of the background noise while the LRSPP mode intensity augments.

In Figure 36, we present the complete bulk experiment from which the snippet shown in Figure 35 was taken. Figure 35 also presents a bulk sensing sensorgram for concentrated urine and two water dilutions of the same urine, U1D1 is a 1:1 dilution (equal amount of urine and water) and U1D3 is a 1:3 dilution (1 volume of urine for 3 volumes of water). From the specific gravity table if human urine published in [10] and the dilution ratio used, we estimate the RI_{U1D1}=1.325, and RI_{U1D3}=1.322. Assuming a monotonic increase in insertion loss with increasing RI of the solutions, we would have expected the detected power for U1D1 to be higher than U1D3, and higher then DIH2O but this is not what is observed here. This suggest that beyond LRSPP mode cutoff the relation between output power and the fluid refractive index is not monotonic or simple, limiting the use of the LRSPP biosensor as a specific gravity meter in this region.

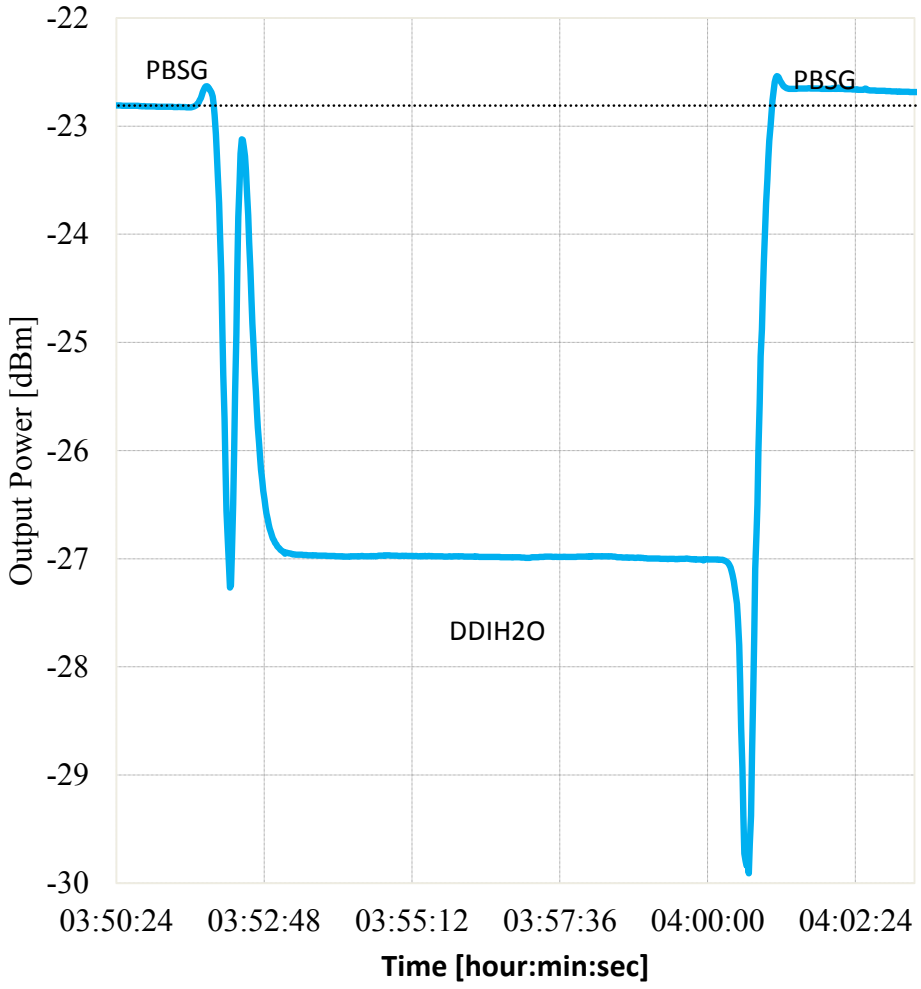

Figure 35 Bulk Transition from RI = 1.33425 (PBSG0715) to RI 1.31677 (DIH2O). Video ot PBSG0715 to DIH2O: (2015beland video PBS1507toDIH2O) Video of DIH2O to PBSG0715: (2015beland video DIH2OtoPBS1507)

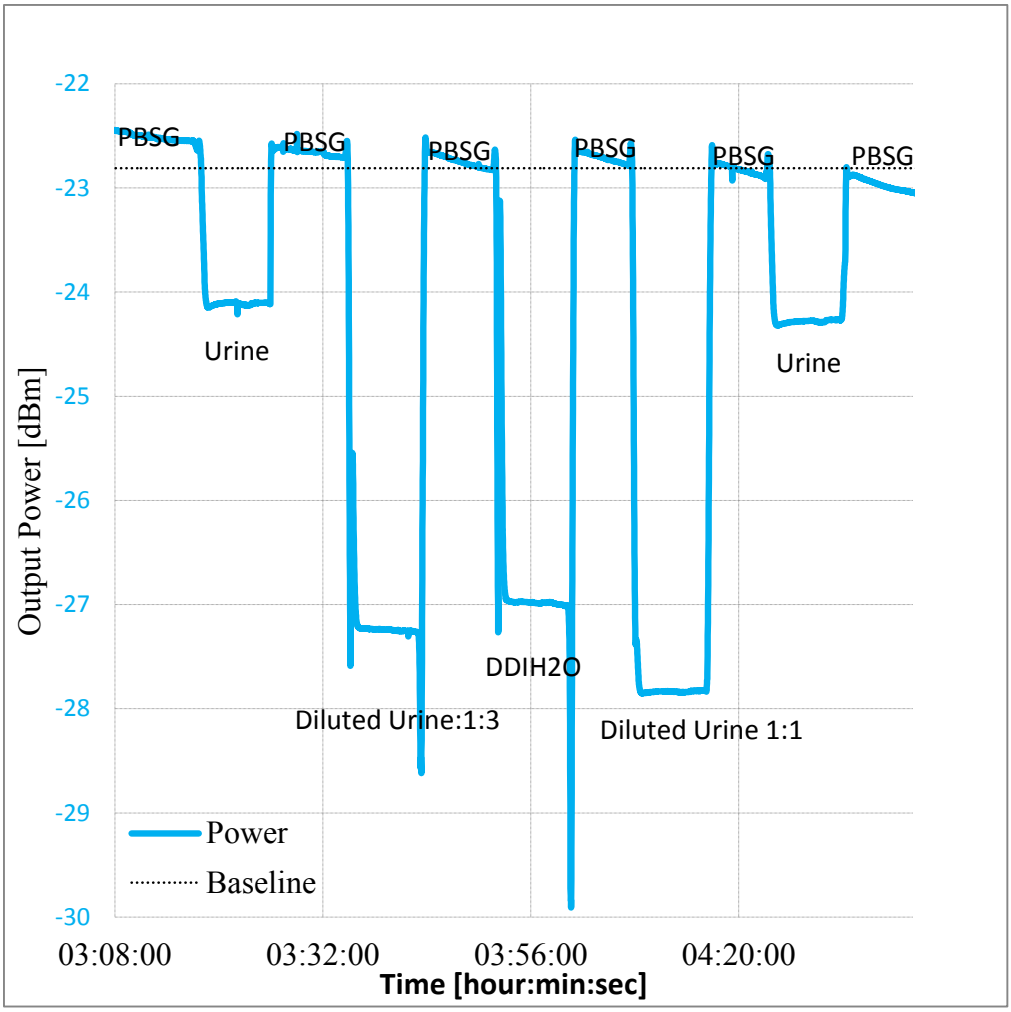

Figure 36 Bulk sensing of Urine and diluted urine

In Figure 37 we present results of a similar experiment as the one from Figure 35 but on a different die. The same behaviour is observed but to a lesser extent. We note also that the output power level for DIH2O is -31.4 dBm instead of -27 dBm as previously obtained. This denotes the large variability of the background optical energy from one biosensor to the next.

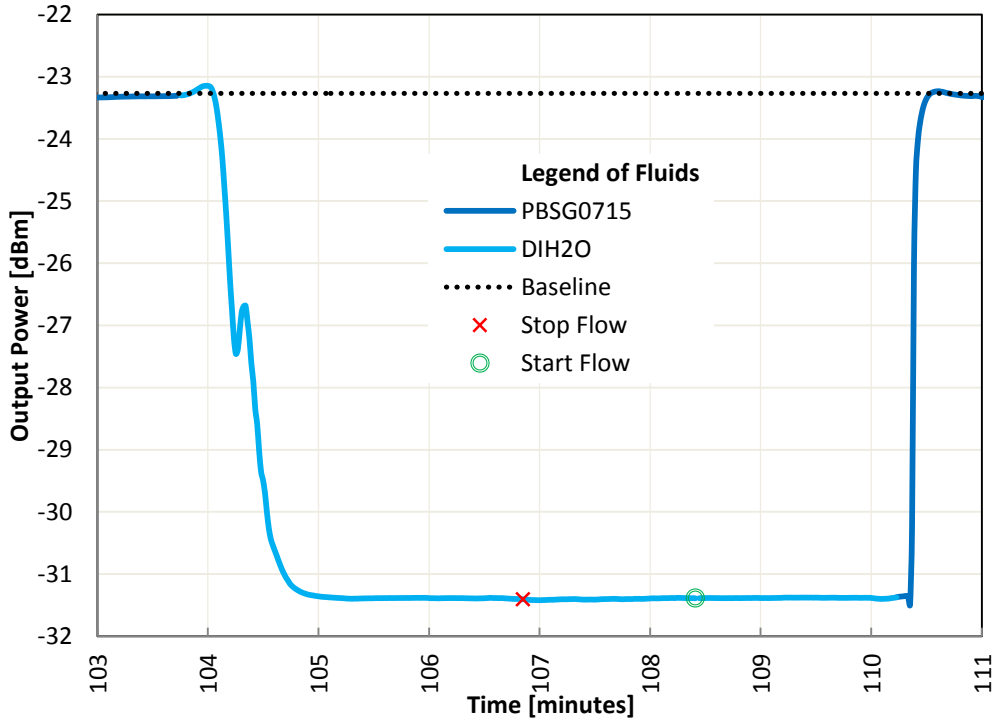

Figure 37 Details of a transition from PBSG0715 to DIH2O and DIH2O to PBSG0715. Magnified section of Figure 2 a) from [8]

2.4.9 Detection of organic material in PBSG0715

This section summarizes the discovery of an unexpected signal level change when using the PBSG0715 solution in our experimentation. In Figure 38 the measurement results when PBSG0715 solution is in the jig in static mode are presented. As can be seen the power drops at a constant rate of 0.028 dB/min, which produces a 2 dB change in 11 hours. Partial recovery of the signal was possible only after removing the die and performing a 30 min exposure to UV-Ozone. This suggest that organic material is deposited on the guide at a constant rate. A visual inspection before and after this test is presented in Figure 39 with no apparent change on the guide surface.

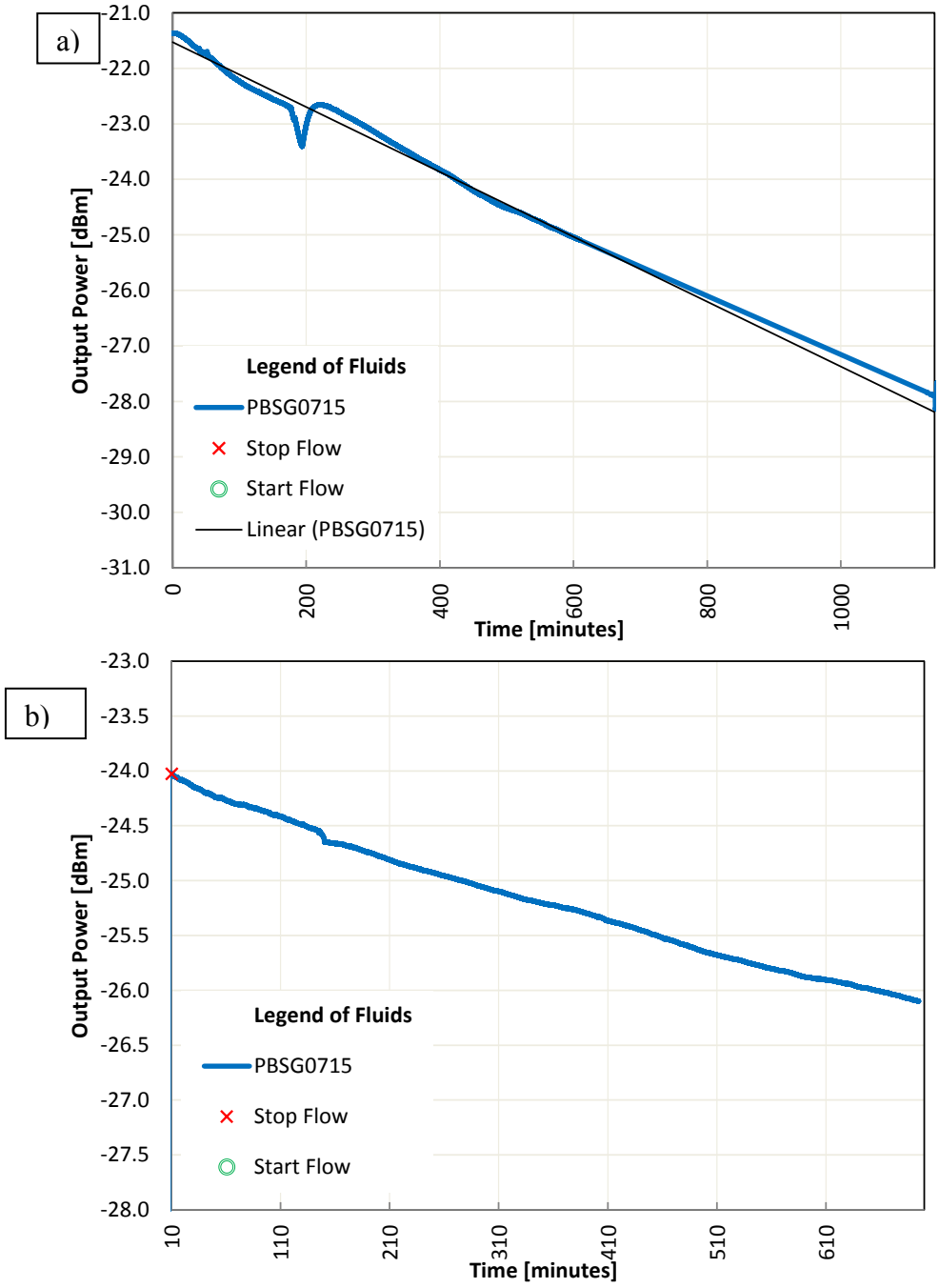

Figure 38 Change in Power with static PBSG0715 solution in the jig. a) On 9 sept 2014, with PBSG0715 vial 10, a decrease in power at a rate of 0.00572 dB/min is noted., b) On 9 sept 2014 with PBSG0715 vial 7, a decrease in power at a rate of 0.0028 dB/min is observed.

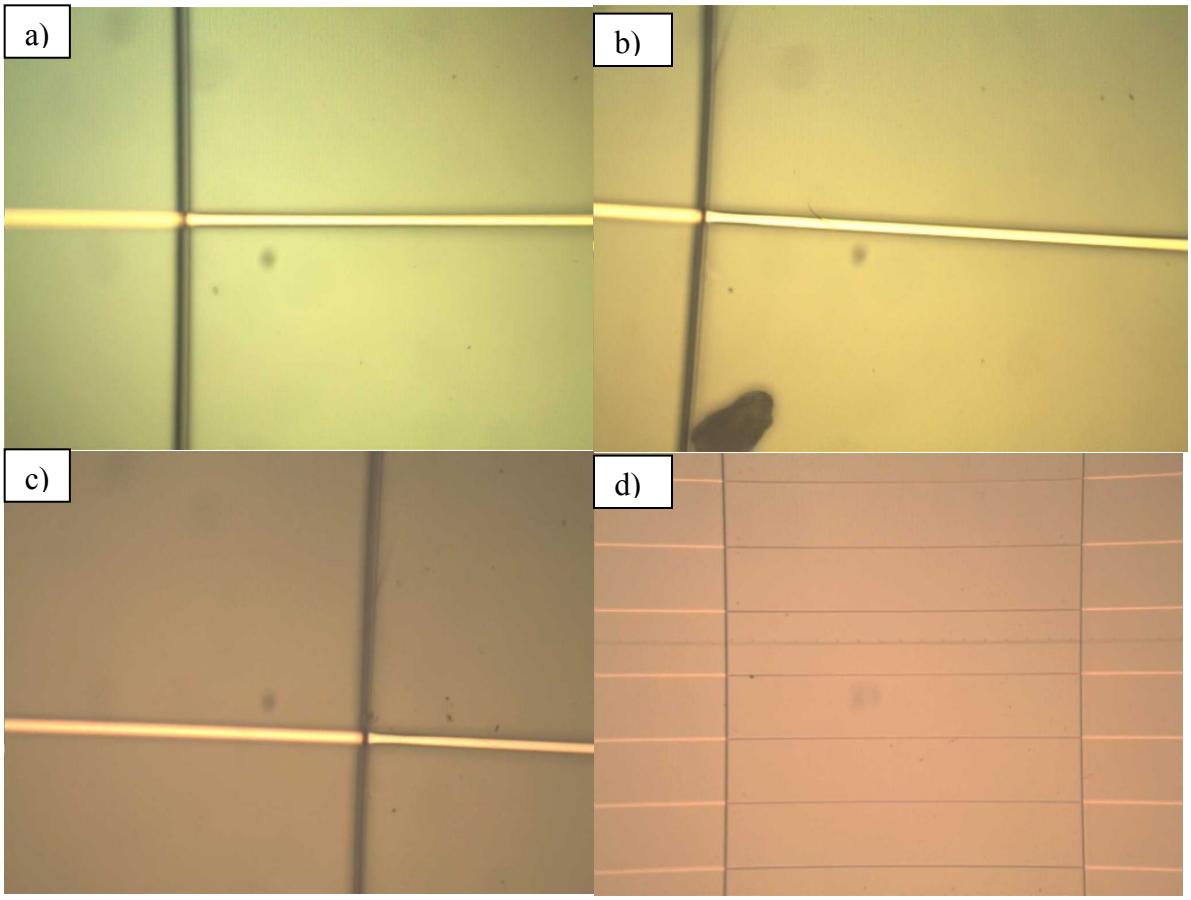

Figure 39 Visual inspection at 500x a) before, b) between, c) after the two experiments with PBSG0715 shown in Figure 38, d) 50x inspection before experimentation.

The first observation of a power decrease as a function of time with PBSG0715 was observed in the bulk measurement presented in Figure 35, Figure 36, and Figure 37. Also, the Gneg antibodies was divided in 10 aliquot using PBSG0715 and then stored in a fridge. This observation may explain the additional decrease in power as a function of time observed in Figure 40 below as compared to the one from Figure 19. This could explain the decrease in output power after Gneg functionalization instead of an increase of 0.2 dB observed in Figure 19.

In Figure 40 the sensorgram resulting from the functionalization is presented. In this case, after priming the line with DIH2O, we start the datalogger (0 minutes on graphs). For the first 120 minutes, not shown on the graph, we used the PBSG0917 solution to perform alignment of the device as well as the optical fibre. The die surface functionalization is achieved by injecting Gprot0715 for 20 minutes, PBSG0917 to provide a reference level, GNEG for 110 minutes, PBSG0917 to observe a change of level, BSA for 5 minutes to block binding site, and finally PBSG0917 as a quality control of the functionalization.

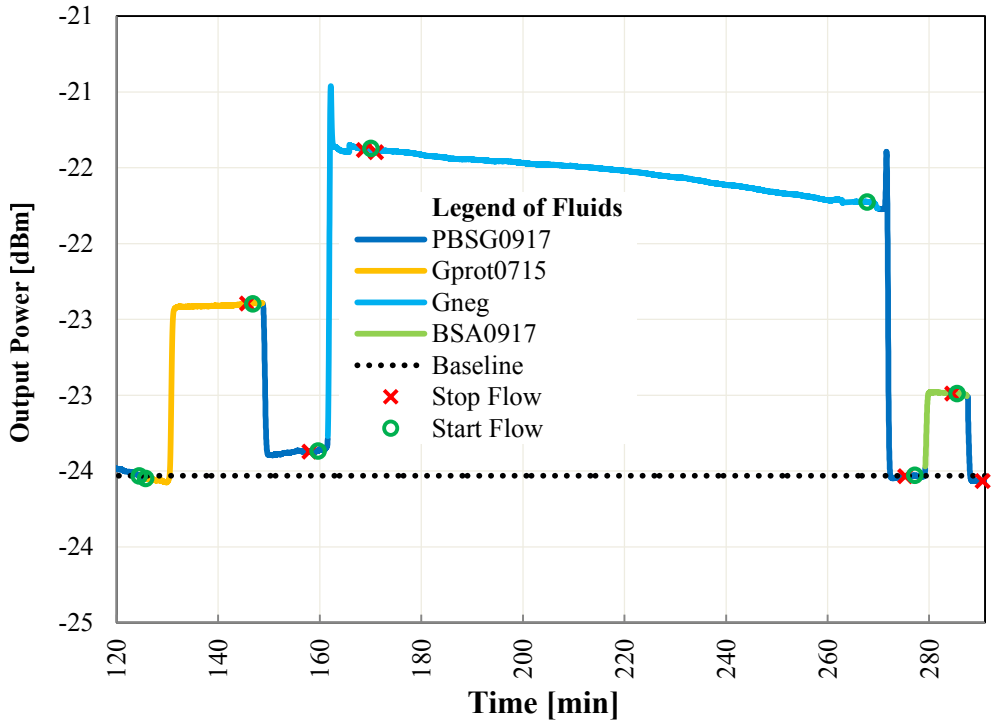

Figure 40 Functionalization of die with Protein G, Gram Negative antibody and BSA.

2.5 References

1. S. Jetté-Charbonneau, R. Charbonneau, N. Lahoud, G. Mattiussi, P. Berini, ¨Bragg gratings based on long-range surface plasmon-polariton waveguides: comparison of theory and experiment,¨ IEEE J. Quant. Electr. vol. 41, pp. 1480-1491, (2005).
2. K. Gazzaz and P. Berini¨Theoretical biosensing performance of surface plasmon polariton Bragg gratings,¨ Applied Optics, vol. 54, no. 7, (2015)

3. R. Hanif, ¨Microfabrication of Plasmonic Biosensors in CYTOP Integrating a Thin SiO2 Diffusion and Etch-barrier Layer,¨ Ottawa-Carleton Institute for Electrical and Computer Engineering, (2011) http://www.ruor.uottawa.ca/handle/10393/19880
4. Web reference: http://www.cargille.com/refractivestandards.shtml
5. W. R. Wong, O. Krupin, F. R, M. Adikan, and P. Berini, "Optimization of long-range surface plasmon waveguides for attenuation-based biosensing," J. Lightwave Technol. (in press).
6. P. Berini, ¨Long-range surface plasmon polaritons¨ Advances in Optics and Photonics, pp.484-588, (2009).
7. K. B. Laupland, T. Ross, J. D. D. Pitout, D. L. Church, and D. B. Gregson, ¨ Community on set urinary tract infections: a population-based assessment, ¨ Infection, vol. 35, no. 3, pp. 150–153, Jun. (2007).
8. P. Beland, O. Krupin, P. Berini, ¨ Selective detection of bacteria in urine with a long-range surface plasmon waveguide biosensor ¨, Biomed. Opt. Express 6(8), 2908-2922 (2015)
9. P. Berini, Charbonneau, R., Lahoud, N., Mattiussi, G. , Characterization of long-range surface plasmon polariton waveguides, Vol. 98 (1), 043109 ed. , 1-12: Journal of Applied Physics, 2005
10. CRC Handbooks of Chemistry and Physics, CRC Press Inc. 60th Edition (1980)

Chapter Three:
Conclusion

3.1 Synthesis of the long range surface plasmon waveguide as a biosensor for urinalysis

In this work, we have reviewed the clinical usefulness of urinalysis as a clinical tool for the diagnosis of disease, and more specifically for the diagnosis of UTI. Urinalysis test equipment and devices include the dipstick, the refractometer, the microscope and cytometer, the spectrophotometer, the culture of bacteria on agar plate and in liquid broth. Despite the large number of tools and expertise for urinalysis, many shortfalls remain in regards to rapid detection and identification of pathogens for the diagnosis of complicated UTI. Hence the LRSPP waveguide biosensor was studied as a candidate to fulfil those requirements.

The field of label free biosensor has emerged in the last 20 years as a dominant technique for the detection of protein, virus, health markers, and bacteria. Although a few biosensors like the pregnancy test, glucose meter, blood analysis are successful solution at the point of care, the use of label free biosensor is still constraint to the laboratory environment due to its engineering complexity and high cost of acquisition. The introduction of a new form factor device for label free biosensing (the LRSPP waveguide biosensor) promises to be easily integrated and cost efficient to provide a solution at the point of care (POC) and in particular for the rapid diagnosis of UTI.

The work presented in section 2.1 is a laboratory implementation of the LRSPP waveguide interrogation system composed of a test device, an optical interrogation system, a mechanical alignment and antivibration system, a chemical and fluidic system and a data acquisition system.

It is in the integration of all these system components that a solution for rapid diagnostic of UTI can be found. We have shown here that commercial off the shelf component exist for all the function and that a laboratory test system can be assembled in only a few months at a cost below $35 000 dollars of which the antivibration table cost and IR camera cost are the most significant. This system is used as proof of concept and only requires engineering investment to integrate its component and make it usable at the health point of care.

We have demonstrated that the direct use of urine in the detector is possible. This significantly simplifies the technical knowledge required at the POC because users can avoid laboratory handling of patient urine samples. The bulk sensing demonstration of urine and its relation to specific gravity augments the precision of tools such as the Abbe refractomer already widely used by clinicians. Refinement of the calibration and characterisation of the repeatability of the LRSPP waveguide biosensor are still required for an accurate comparison with existing tools and techniques to be performed.

The main objective of this work was summarized in section 2.2 by the paper published in the journal Biomedical Optics Express. In this report, we clearly established that the LRSPP waveguide biosensor can selectively detect the gram of bacteria in human urine at concentrations of 10^5 CFU/ml or higher. After functionalization of the test device, the worst case test time to selectively detect *E.Coli* (gram negative) or *S.EPI* (gram positive) bacteria was less than 40 min including 20 min for the negative controls, for concentrations around $2x10^6$ CFU/ml in urine with low constituent concentration. This result is not optimised and the test time could easily be reduced by reducing the time allocated for the negative control to less than 5 min and by

selecting normal urine samples instead of diluted urine. This would allow the LRSPP waveguide biosensor to operate closer the RI of CYTOP and therefore improve its sensitivity which will reduce the time required to obtain an accurate positive to negative ratio. We report below the final table of the measured positive to negative ratio presented in [8]. In conclusion, we report that LRSPP waveguide biosensors are capable of supporting the diagnosis of UTI.

Table 5. P/N ratio demonstrating selective detection of bacteria

Section, Experimental Figure; Sequence	Test Fluid	Negative Control		Detected Bacteria		P/N
	Label	Label	Growth time [hrs]	Label	Growth time [hrs]	
2.2, Fig. 3(a);1	PBSG0917	SEPI0917	4.3	ECOLI0917	4.3	13.1
2.2, Fig. 4;1	Urine0924	SEPI0924	4.3	ECOLI0924	4.3	7.5
2.2, Fig. 5(a);1	Urine1126	ECOLI1126	7.0	SEPI1126	18	3.1
2.2, Fig. 5(b);2	Urine1126	ECOLI1126	7.0	SEPI1126	18	4.8
2.2, Fig. 6(a);1	Urine1202	SEPI1203	17	Bact1202A	5.0	5.4
2.2, Fig. 6(b);2	Urine1202	SEPI1203	17	Bact1202A	5.0	1.9
2.2, Fig. 6(b);3	Urine1202	SEPI1203	17	Bact1202A	5.0	5.5
2.3, Fig. 1,1	Urine1203	SEPI1126	17	Bact1202A	5	2.5
2.3, Fig. 1,2	Urine1203	SEPI1126	17	Bact1202B	7	6.5

The LRSPP waveguide biosensor is not limited to bacteriuria, specific gravity and refractive index measurements of urine. It could also be used in support of proteinuria. Although not directly addressed in our work, many measurement results presented here reflects some of the capability of the LRSPP waveguide biosensor in this area. First, during bulk sensing experimentation with urine, adsorption of protein found in urine on a bare gold detector surface was observed with a change of power level in the order of 0.2 dB. We also routinely made use of bovine serum albumin (BSA) in our tests, a protein chemically similar to human serum albumin (HSA) which constitutes about 40% of all protein in human urine.

In the supplementary measurement section we have touched upon numerous applications of the LRSPP waveguide biosensor. We presented the functionalization of the device with protein G and gram negative as well as gram positive antibody. It was interesting to note that these functionalizations would inhibit the adsorption of bacteria of opposite gram to the functionalised antibody. We have evaluated the state of bacteria as dead or alive after adsorption by the waveguide and established a comparison criterion between dead or alive from signal characteristics taken over a time span of 10 min. We have shown measurement in excess of 10 hours detecting organic material in a PBS glycerol solution apparently clean of organic elements. We have also shown the detection of biofilm formation in DIH2O during a 12 hours growth time and confirmed it with a microscopic visual inspection.

3.2 Thesis contributions

The work presented in this thesis resulted in the following contributions to current knowledge in optical biosensing with LRSPP waveguide biosensors:

1. A demonstration of urine bulk sensing which can be used to measure the refractive index and the specific gravity of urine with a very high sensitivity.
2. A demonstration of selective detection of bacteria in clean fluid using a LRSPP waveguide biosensor. The gram negative demonstration was achieved with the *E.Coli XL1 Blue* bacteria in PBS-glycerol fluid.
3. A demonstration of selective detection of bacteria in human urine using a LRSPP waveguide biosensor. The gram negative demonstration was achieved with the *E.Coli XL1 Blue* bacteria and the gram positive demonstration was achieved with the *S.Epi ATCC 12228* bacteria.
4. A demonstration of selective detection of gram negative bacteria in urine contaminated with a gram positive bacteria using a LRSPP waveguide biosensor. This would be

typical of a patient urine sample contaminated with bacteria other than the pathogenic one.

5. A demonstration of the differentiation of dead versus live bacteria with the LRSPP waveguide biosensor.
6. Detection of biofilm formation in water on a CYTOP surface.
7. Observation of the organic contamination of a PBS-Glycerol solution.
8. An effective alignment procedure of the LRSPP waveguide built on a silicon wafer.

3.3 Suggestions for future work

In order to establish the LRSPP waveguide biosensor as a useful urinalysis tool the following work is suggested.

In the area of proteinuria and specific gravity measurements, a surface functionalization that would inhibit the nonspecific adsorption of urine constituents could be identified and its performance characterised with patient urine samples. A better surface functionalization would reduce the variability observed in the measurements due to protein adsorption by the bare gold surface. Alternatively, evaluating the variability of the thickness of the adlayer from common protein found in urine is needed to establish the accuracy of the LRSPP waveguide biosensor. Then a comparison between an Abbe refractometer and the LRSPP waveguide biosensor can establish the advantages of the LRSPP waveguide in obtaining accurate values of refractive index in the presence of cell, bacteria, and other large organic constituents. With current refractometer technologies, the type of fluid measured must be known to estimate the specific gravity from the RI measurements. With the LRSPP waveguide biosensor, it is possible to adsorb a specific protein on the LRSPP waveguide surface (using for instance antibody

recognition) which removes the uncertainty with regards to the constituents causing a change in refractive index. This characteristic may be shown to be advantageous as a diagnostic tool for proteinurea and other similar clinical applications.

In the area of bacteriurea, one needs to establish a detection threshold to distinguish low bacteria concentrations - this is required for the accurate diagnosis of UTI. In addition, clinical trials with UTI infected urine have to be performed to evaluate the effect of large urine constituents such was red blood cells, white blood cells, epithelial cells, and others on the established positive to negative selectivity parameter.

In the area of electromagnetics, a better theoretical foundation to understand the detector performance below its LRSPP waveguide mode cut-off is needed to clearly explain and predict the biosensor performance at its limits. The current investigation demonstrated that beyond cut-off the positive to negative ratio still provides accurate information on the bacteria selectivity despite the fact that the sensor is operating in a region of large signal contribution from radiative modes in addition to the LRSPP waveguide mode.